INTENSITY VARIATIONS OF LOW-FREQUENCY ELECTRODELESS DISCHARGES

by

Paul Serge Nekrasov

Thesis submitted to the Graduate Faculty of the

VIRGINIA POLYTECHNIC INSTITUTE

in candidacy for the degree of

MASTER OF SCIENCE

in

PHYSICS

APPROVED:

Director of Graduate Studies

Dean of Applied Science

APPROVED:

Head of Department

Major Professor

May 16, 1955

Blacksburg, Virginia

TABLE OF CONTENTS

ILLUSTRATIONS

Figure Page

LIST OF TABLES

Tables Page

LIST OF GRAPHS

I. INTRODUCTION

The subject of electrodeless discharges through gases deserves a great deal of attention because of the advantages they possess over the conventional discharges. The difference between the two types of discharges lies in the method of excitation employed. Both types employ sealed-off tubes or other vessels containing gas or vapor at a reduced pressure. In conventional type discharges the metallic electrodes are brought in direct contact with the gas in the tube, while in electrodeless discharges there is none.

The main advantage of the electrodeless tubes, therefore, is that they are free of the danger of contaminating the gas or vapor of the discharge investigated by sputtering or outgassing of the built-in electrodes. In spectroscopy, they are excellent light sources because the spectra obtained by means of such tubes are as pure as the substance inside the tube. Sometimes intensive discharges may liberate large quantities of heat, causing melting of the internal electrodes or cracking of the tungsten seals, if the conventional type discharge is used. Electrodeless discharges present no such dangers.

Electrodeless tubes are also most suitable for investigation of small quantities of very rare materials, result in safer handling of poisonous or radioactive substances, lend themselves to easier construction, and

serve a much longer life because of the absence of the built-in electrodes.

One may think that this type of discharge has a disadvantage in that its continuous operation is limited to that produced by sources of alternating current of high frequency and high voltage. This, however, is not a drawback. Modern electronic equipment is capable of furnishing such sources of sufficient power to maintain electrodeless discharges at a rather high intensity. The required equipment, consisting mainly of a power supply and an oscillator, can be built inexpensively and in a compact size.

II. REVIEW OF LITERATURE

Although the electrodeless discharges were discovered as long ago as 1884 by Hittorf (16), their exact nature was debatable until more recent investigators presented proofs beyond reasonable doubt. Their discoverer, as well as J. J. Thomson (23), maintained that the discharges are due to electromagnetic induction which is caused by an alternating emf induced round the periphery of the tube by the rapidly changing magnetic field through the tube (14, 24).

Townsend (25), on the other hand, developed a theory based on the assumption that the discharges were electrostatic in nature. The controversy was not clear until MacKinnon (16), who pointed out that the ring discharges investigated by Thomson are undoubtedly of electromagnetic origin, while the glow discharges are largely or entirely electrostatic. The latter type of discharges appears over a much wider range of pressures.

The discharges of electromagnetic origin are produced by bringing a tube or a sphere containing gas or vapor at a low pressure close to a coil carrying alternating current of high frequency of a magnitude up to 50 amperes.

The discharges produced in the tube with alternating emf applied to metal sleeves or terminals around the tube, which is rather far from the oscillator, are classified electrostatic.

Both types have been studied extensively. The most outstanding work on determination of the pressure-terminal voltage relationships in electrodeless discharges through various gases was done by MacKinnon (16), Smith (20), and Thomson (23). They found that generally more voltage is required to cause breakdown when pressures of the gases in the tube are increased, and that the relationship between those two quantities is approximately linear. MacKinnon also confirmed Thomson's view that the required breakdown, or firing potential is greater for tubes of greater diameters. McCallum and Klatzow (17) confirmed the above findings by means of a series of experiments done with argon. On the general appearance of the discharge column, the only record existing in modern literature was that of the investigation carried out by Banerji and Ganguli (1). Nisewanger, Holmes, and Weissler (19) interpreted the meaning of Paschen's law as applied to electrodeless discharges, namely, that the required firing potential is essentially a function of the gas pressure and the spacing between the terminals. Study of the change of the color of the discharge column with changing pressure was also made by the above investigators.

All of the investigations described above seemed to be limited to phenomena of a long-time-average character, without any attempt made to study the instantaneous variations, and to discharges excited almost exclusively

by sources of high frequencies.

Discharges investigated in this study were of electrostatic origin. This type of discharge is much easier to reproduce and observe, compared to the electromagnetic type ring discharge (16, 24). The available literature points out that in the case of electrostatic discharges, a strong electrostatic field is set up between the terminals of an electrodeless tube when the output of an alternating source of high voltage is applied. This field produces partial ionization of the gas. Electrons thus liberated move with an acceleration proportional to the field intensity. On striking the walls of the tube, these electrons will produce secondary electrons. The avalanche of free electrons produced in that manner will cause ions to be formed in the gas by collisions with the molecules of the latter, or, if the kinetic energy of the impinging electrons is insufficient, atoms in the excited state will be produced. Some of the electrons are lost to the walls, and a few by recombination. When the strength of the field applied is sufficient to form a number of electrons at least as great as the number of electrons lost, a continuous discharge is obtained.

Several modifications of the theory of the electrostatic discharges through gases in electrodeless tubes were suggested by other investigators (8, 17, 23). It is

a well-established fact that the formation of ions is largely dependent upon other factors such as the type of gas used, density of the gas, physical dimensions of the tube, distance between the terminals, etc., in addition to the strength of the field produced by the terminal voltage, as pointed out before. Another major factor is the frequency of the voltage applied. Since the frequency range used for the purposes of this study was much lower than that used by other investigators, it is not possible to make a definite statement whether any one theory suggested would fully apply to the discharges under discussion.

III. OBJECT OF THE STUDY

Electrodeless discharges, once started, are convenient and easy to control; yet, the literature reviewed gave no indication of a previous study made of the time variation of its light intensity. The object of this thesis was twofold. First, to re-examine the general properties of the electrodeless discharges with a special emphasis placed upon the instantaneous variations; second, to study the light intensity fluctuations under various conditions.

Most of the properties to be studied, including light intensity, could be revealed faithfully by means of a photomultiplier tube and an oscilloscope, provided that the frequency of the discharge did not exceed the limit of their response. The upper limit of the frequency response of the photomultiplier tube was sufficiently high, but that of the available oscilloscope was rather low.

It was decided to start with the lowest frequency available (60 cps), up to the limit of the scope, the latter being approximately one megacycle. The working range was also limited by the fact that in order to cover the whole range continuously, several oscillators would be needed. This would be rather time consuming and costly. It was therefore decided to cover all frequencies between approximately eighty kilocycles and one megacycle, in addition to 60 cps taken from the power line and 400 cps

generated by a motor-generator set. All of the above frequencies were considered low compared to those produced by the commercially available equipment such as Raytheon "Microtherm" which generates a frequency of 2450 megacycles.

Electrostatic discharges excited by using metallic sleeves, or external electrodes around the tube, were studied for two reasons: (1) to minimize pick-up by the detecting devices, and (2) to eliminate blocking of light by the inducing coil which is used to obtain electrodeless discharges of electromagnetic origin.

It was intended to study discharges in air and argon. Under some circumstances, study of the mercury discharge was also planned.

IV. DESCRIPTION OF APPARATUS

To obtain desired results, necessary equipment for initiation and maintenance of the discharges was designed and constructed. Such equipment consisted mainly of a source of stable frequency and sufficient power to produce electrodeless discharges through various gases confined at reduced pressures in tubes of different sizes. Construction of a single source of variable frequency covering the entire frequency range desired for the investigation (low audio to approximately one megacycle) would have been rather impractical and costly. For this reason three different sources were used: two of a constant frequency output of 60 and 400 cps each, and one continuously variable from 80 to 1100 kilocycles.

The following is a description of above apparatus, and other auxiliary equipment employed to provide for pressure variation of the gas in the tubes and to measure the intensity variations of the discharges.

1. Apparatus Used for Excitation of the 60-Cycle Electrodeless Discharges

Above frequency was the lowest used in this study. The advantage of the 60-cycle discharge is that the apparatus used for excitation is rather simple and inespensive, since a source of that frequency is easily available everywhere. Fig. 1 shows a diagrammatic view

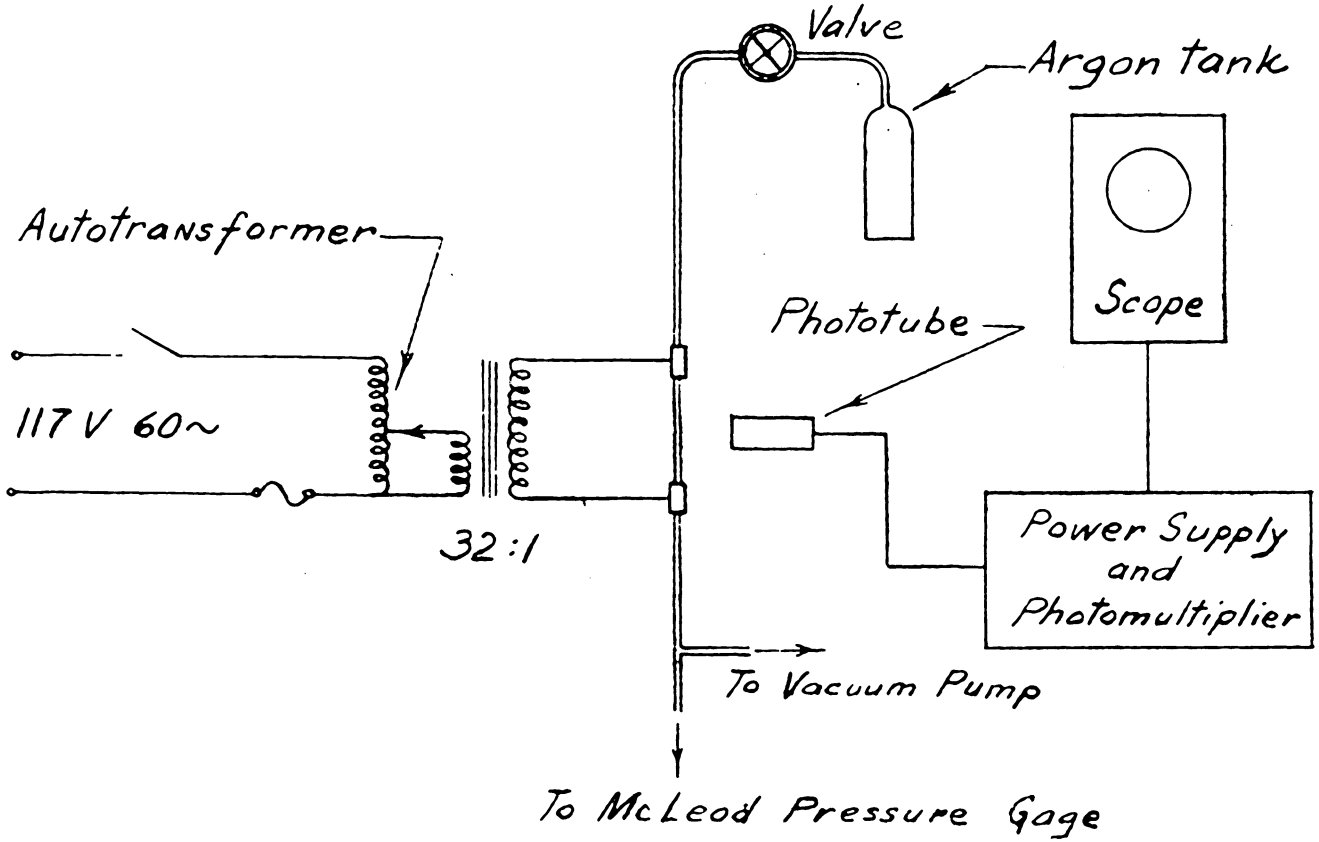

Fig. 1. Diagram of Apparatus used in connection with Discharge excited by a 60-cycle source

of such apparatus as employed for the purposes of this investigation. It consisted primarily of a variac autotransformer connected in the input circuit of a 32:1 voltage transformer. This arrangement permitted variation of the voltage across the tube terminals from zero to that equal to the line voltage multiplied by the ratio of transformation.

2. Apparatus Used for Excitation of the 400-Cycle Electrodeless Discharges

A motor-generator set was used to provide a source of voltage at 400 cps. Variation of terminal voltage was obtained by means of the transformers mentioned in the previous section.

Distorted wave shape produced by the available equipment presented a disadvantage of using this frequency for excitation of the discharges.

3. Apparatus Used for Excitation of the Electrodeless Discharges at Radio Frequencies

a. Power Supply. The power supply designed and constructed was a 1200-300-0 volt d-c supply unit. Five transformers, one variac autotransformer, two half-wave and two full-wave rectifier tubes, a voltage regulator tube, three filter circuits, and three vacuum tubes used for voltage regulation were the main components needed for construction. A detailed wiring diagram is shown on fig. 2. Figures 3 and 4 show pictorial views of the unit.

A 1200-0-1200 volt, 225 ma Stancor plate transformer (T_1) was installed to supply voltage to the RCA type 816 half-wave power rectifier tubes. A 2.86 kv-a auto-transformer (T_6) was connected in the input circuit of this transformer to provide for variation of the primary voltage. The output of the rectifiers was filtered by means of a condenser-input type filter. The smoothing filter choke (L_1) had 80 ohms internal resistance and adequate insulation for protection against high-voltage surges. To improve the output voltage regulation, a bleeder resistor (R_1) of proper dissipation rating was connected as shown on fig. 2.

A 375-0-375 volt, 160 ma Thordarsen transformer (T_2) was used in connection with the RCA type 5U4 and 6X5 full-wave vacuum tube rectifiers to provide a variable low-voltage supply and the negative bias voltage, respectively. The output of the 5U4 rectifier was filtered by means of a condenser-input type filter. Three RCA type 6L6 bean power amplifier tubes were connected in parallel in the low-voltage line to provide proper voltage regulation; their control grids were connected to the sliding contact of a potentiometer (R_2) from which the variable low voltage was taken. Negative bias voltage was obtained by connecting one side of the transformer to the cathodes of the 6X5 rectifier tube. This arrangement permitted negative voltage to be taken

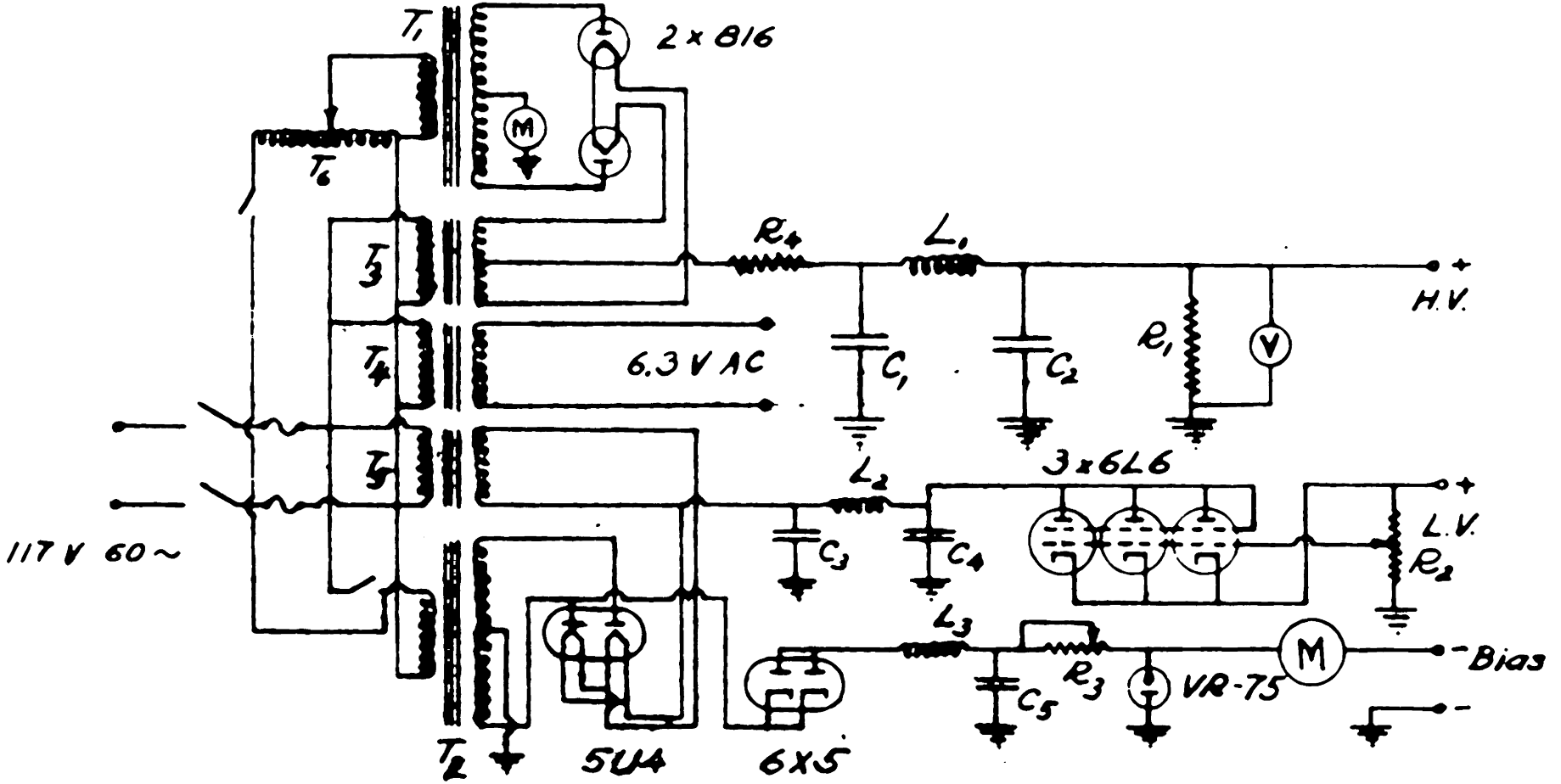

Fig. 2. Power Supply

from the plates of the 6X5. The filter used in this line was that of the choke-input type. A rheostat (R_3) and an RCA type OA3 gas diode voltage regulator were connected in the latter line to control the amount of current delivered and to regulate the output voltage at 75 volts, respectively.

The other three transformers (T_3, T_4, T_5) were used to supply filament voltage to the tubes of various ratings.

To insure safe operation, two 6-ampere fuses were installed in the 117-volt, 60-cycle input line to the unit.

b. Oscillator and Amplifier Unit. To convert the output of the power supply into the desired form of radio frequency voltage, an oscillator and amplifier unit was constructed. Diagram of connections is given on fig. 5. Figures 6 and 7 show pictorial views of the unit.

A grounded-grid oscillator was employed. Its useful range was approximately between 80 and 1100 kc. It was composed of the RCA type 6SN7 medium-mu twin triode and its circuit. When power was applied to the plate of the 6SN7, transient phenomena produced in the tube caused oscillations to be generated in the grid tank circuit (L_1C_1), their frequency being determined by the magnitude of the variable capacitance (C_1). The oscillations, once started, were maintained by the cathode follower action of

TABLE I

Meaning of Symbols Employed in Fig. 2

R_1	100-w, 100,000-ohm h-v bleeder resistor
C_1C_2	1200-volt d-c, 16-mf filter condensers
L_1	8-henry filter choke
R_2	100,000-ohm low-voltage output control
C_3C_4	500-volt d-c, 16-mf filter condensers
L_2	2-henry filter choke
R_3	25-w, 25,000-ohm rheostat
C_5	450-volt d-c, 16-mf filter condenser
L_3	10-henry filter choke
R_4	1-w, 100-ohm protective resistance
T_1	1200-0-1200 volt plate transformer
T_2	375-0-375 volt plate transformer
T_3	5-0-5 volt filament transformer
T_4	6.3-volt filament transformer
T_5	5-volt filament transformer
T_6	2.86 kv-a variac autotransformer

Fig. 3. Control panel of the power supply and the variac autotransformer.

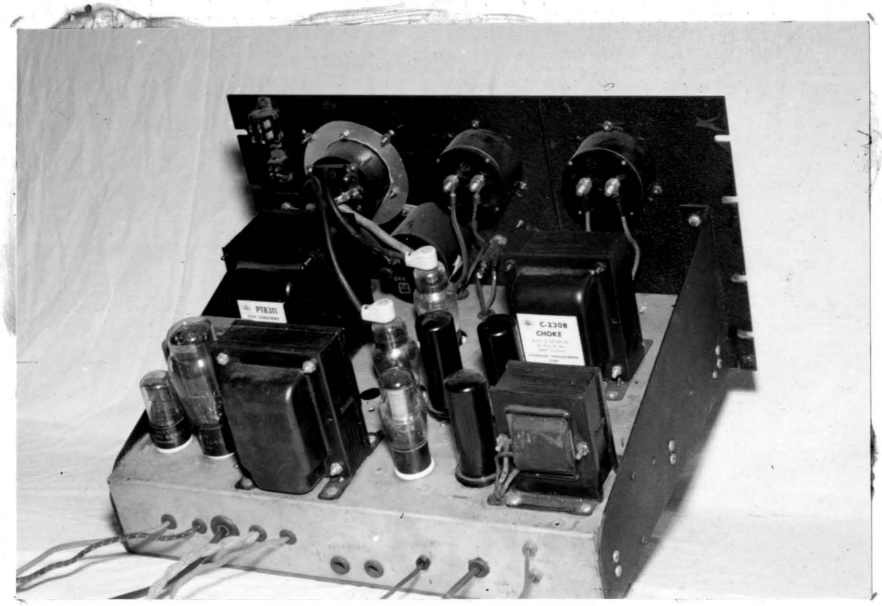

Fig. 4. Rear view of the power supply.

the tube circuit.

It was essential that the frequency generated be as nearly constant as possible over the entire range, and over time periods of various duration. It is known that any impedance that the load couples into the oscillator tank circuit always has adverse effects on the frequency stability of the oscillator (18). Such adverse effects are also produced when an electrodeless discharge tube is regarded as an electric load, because the impedance presented by the tube walls is reflected back to the source. Experiments were carried out (26) to show that an oscillator which excites electrodeless discharges undergoes variation of its frequency output due to the reaction of the discharges, unless preventive measures are taken. Production of a source of stable frequency necessitated coupling the oscillator into a buffer amplifier operated Class A_1. This class of amplifiers draws no grid current during any part of the input cycle. Hence it does not load the preceding stage, and any change in the load conditions will not affect the operation of the latter. The buffer amplifier employed in this unit consisted of a RCA type 6SJ7 sharp-cutoff pentode and its circuit.

Since the 6SJ7 was not capable of producing enough power to supply rated grid drive to the RCA type 807

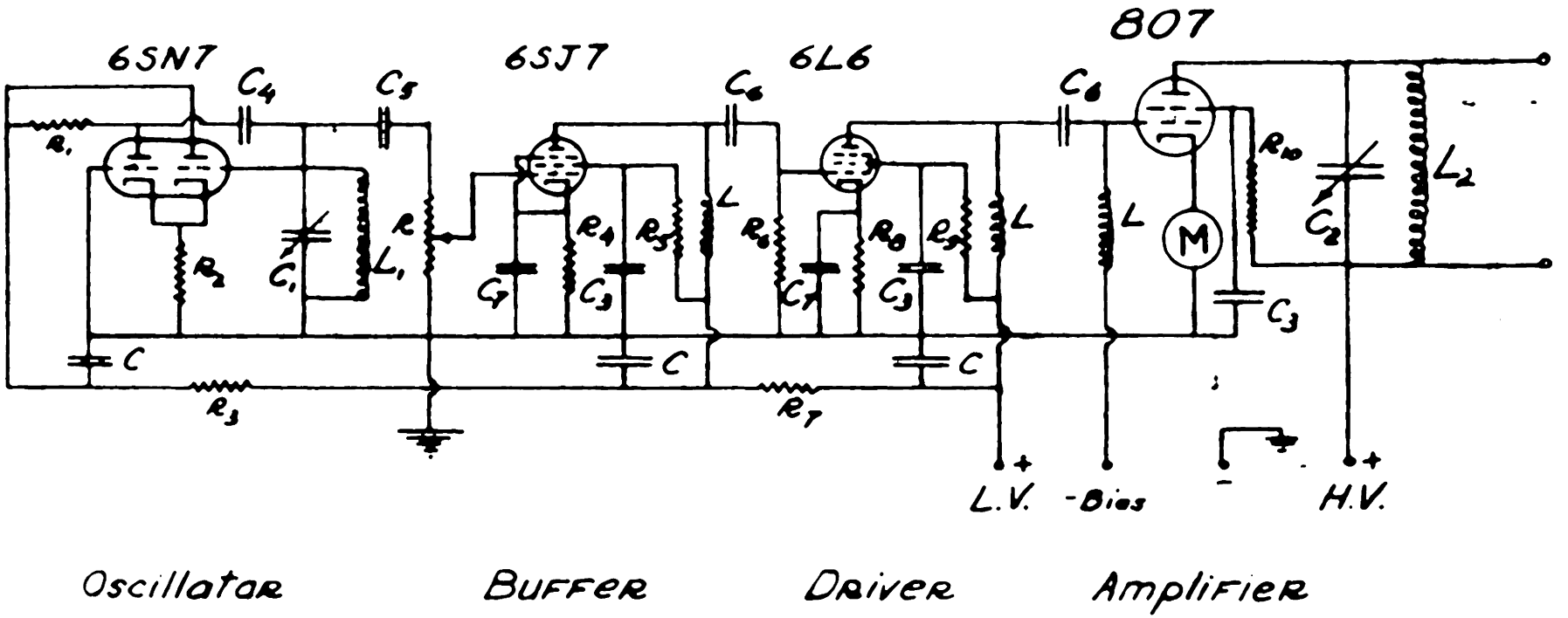

Fig. 5. Oscillator & Amplifier Circuit

TABLE II

Meaning of Symbols Employed in Fig. 5

R	.1 megohm buffer grid-input control
R_1	1-w, 68,000-ohm feedback resistance
R_2	1-w, 1500-ohm self-bias resistance
R_3	1-w, 10,000-ohm supply voltage dropping resistance
R_4	¼-w, 1000-ohm cathode bias resistance
R_5	½-w, 50,000-ohm screen grid voltage dropping resistance
R_6	1-w, 3600-ohm grid bias resistance
R_7	2-w, 22,000-ohm supply voltage dropping resistance
R_8	1-w, 1000-ohm cathode bias resistance
R_9	1-w, 22,000-ohm screen grid voltage dropping resistance
R_{10}	1-w, 50,000-ohm screen grid voltage dropping resistance
C	450-volt d-c, 16-mf a-c shorting capacitance
C_1	600-volt d-c, .00005-.006 mf variable capacitance
C_2	1200-volt d-c, 0-.006 mf variable capacitance
C_3	.1-mf by-pass capacitance

C_4	.1-mf feedback capacitance
C_5	.1-mf coupling capacitance
C_6	.001-mf coupling capacitance
C_7	25-volt d-c, 10-mf cathode by-pass capacitance
L	.0025-henry r-f choke
L_1	.001-henry oscillator tank circuit coil
L_2	.001-henry 807 plate tank circuit coil

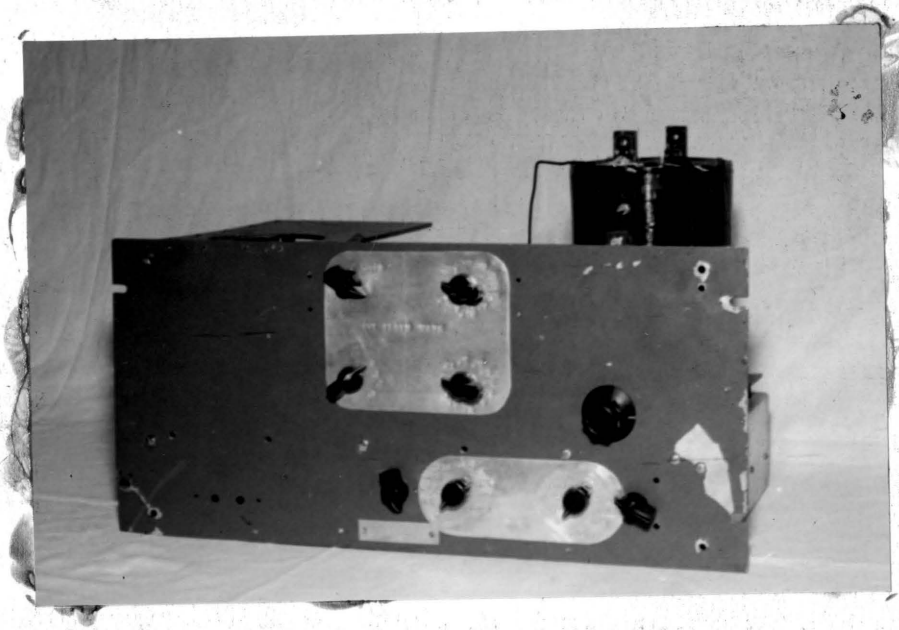

Fig. 6. Control panel of the oscillator and amplifier unit.

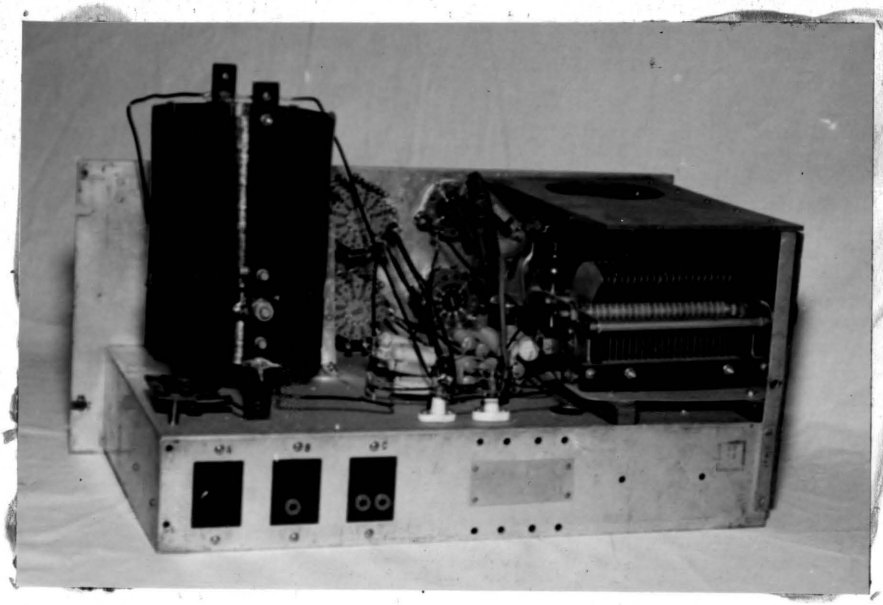

Fig. 7. Exterior view of the oscillator and amplifier unit.

power amplifier employed in the final stage, the output of the former was fed into the driver stage consisting of a RCA type 6L6 beam power tube operated Class AB. The driver stage developed the necessary amount of power to be fed to the grid of the Class C amplifier stage comprised of the 807 and its circuit. Maximum voltage was developed across the load when the 807 plate tank (L_2C_2) was tuned to the output frequency of the oscillator by means of the variable capacitance (C_2).

4. Evacuating System

A vacuum system consisting of a motor-driven Cenco Magnavac vacuum pump, a three-stage oil diffusion pump, and an expansion tank was used to provide means of lowering the pressure of the gas in the discharge tube to the desired magnitude. Fig. 8 shows a block diagram of the system.

Two McLeod vacuum gauges were employed to measure the pressure. One was a standard 0-250 micron gauge, while the other (fig. 9) was especially designed for the project. The latter permitted readings to be taken from any one of the three scales, depending on the magnitude of the pressure measured. The lowest scale, 0-6000 microns, was exponential. It was used at very low pressures, being most accurate in the 0-1000 micron range. The other two scales (0-7 mm. and 0-10 cm.) were linear.

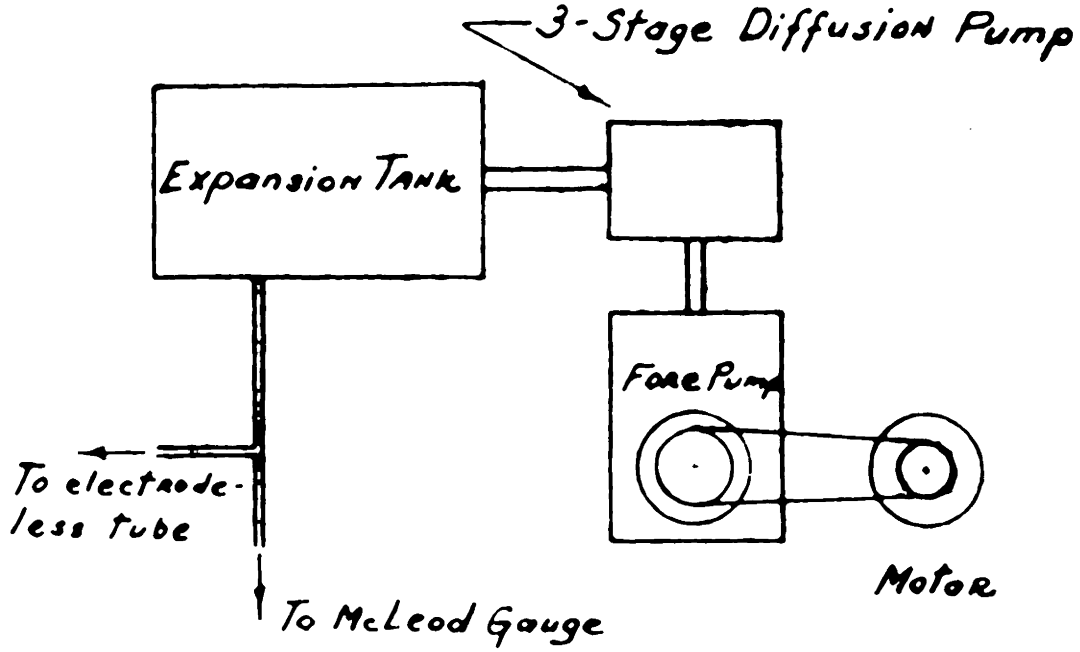

Fig. 8. Block Diagram of the Evacuating System

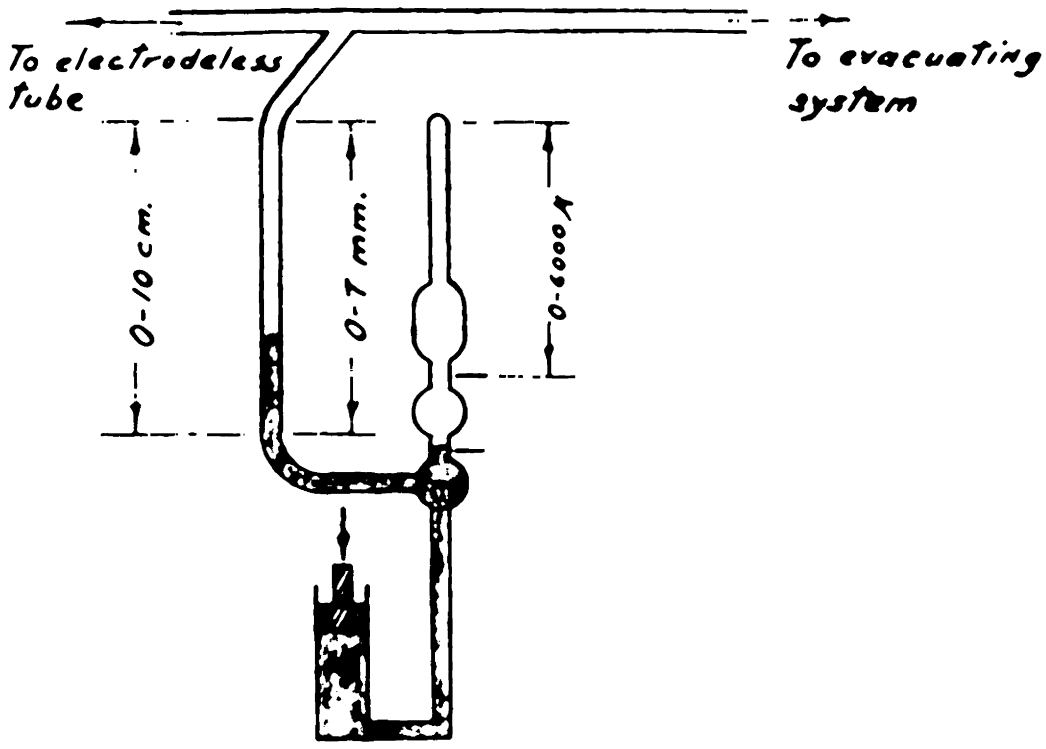

Fig. 9. Three-Scale McLeod Mercury Vacuum Gauge

5. Photomultiplier and Photocurrent Measuring Circuits

For light intensity measurements of the discharge, the RCA type 931-A multiplier vacuum phototube was used. In this type of phototube, maximum sensitivity occurs at 4000 ± 500 Angstrom units, that is, in the blue and violet spectrum region.

To provide rated anode-supply voltage for the phototube, a power supply originally designed and built by P. K. Cheo (4) was employed. It supplied a smooth and steady direct current of 1000 volts. As seen in fig. 10, its main parts were: one plate transformer, two filament transformers, two RCA type 2X2/879 half-wave rectifier tubes comprising a voltage doubler circuit, and a two-stage choke-input type filter. Eight voltage regulator tubes (RCA type VR-150), a protective 25,000-ohm resistor, and a switching circuit were embodied in the same unit. Pictorial view of the unit is shown in fig. 11.

A cable capable of carrying high voltage was constructed to conduct rated voltage to the phototube. Since the phototube was operated in the vicinity of strong electromagnetic fields, the cable was shielded to minimize pick-up. The tube itself was placed in a housing provided with a double-deck parallel slit for light passage to insure adequate light shielding. The housing contained ten 39,000-ohm ½-watt multiplier resistors in

series to provide rated voltage (100 volts d-c) for each phototube dynode. The positive high-voltage terminal was grounded, rather than negative. Grounding the positive terminal placed the photocathode at a high negative potential, making the dangerous high voltage less accessible to the human body. Finally, the housing was rigidly attached to a sliding vernier scale, so that the light intensity measurements could be taken anywhere along the luminous column of the discharge. Figure 12 shows the phototube, the cable, and the housing assembly mounted on the scale.

The switching arrangement shown in fig. 10 permitted photocurrent measurements to be taken from either the microammeters or the oscilloscope. The latter *) was used because of the sensitivity of its response and the adaptability for operation in conjunction with a photomultiplier tube (6). The output of the photomultiplier was fed into a high resistance placed in parallel with the proper terminals of the oscilloscope. This resistor was a part of the RC network which constituted the time constant of the circuit. Proper value of the time constant RC depended upon the maximum frequency that the circuit was called upon to handle. It could be varied

*) Cathode-Ray Oscillograph type 208, Allen B. Du Mont Laboratories, Inc., Passaic, New Jersey.

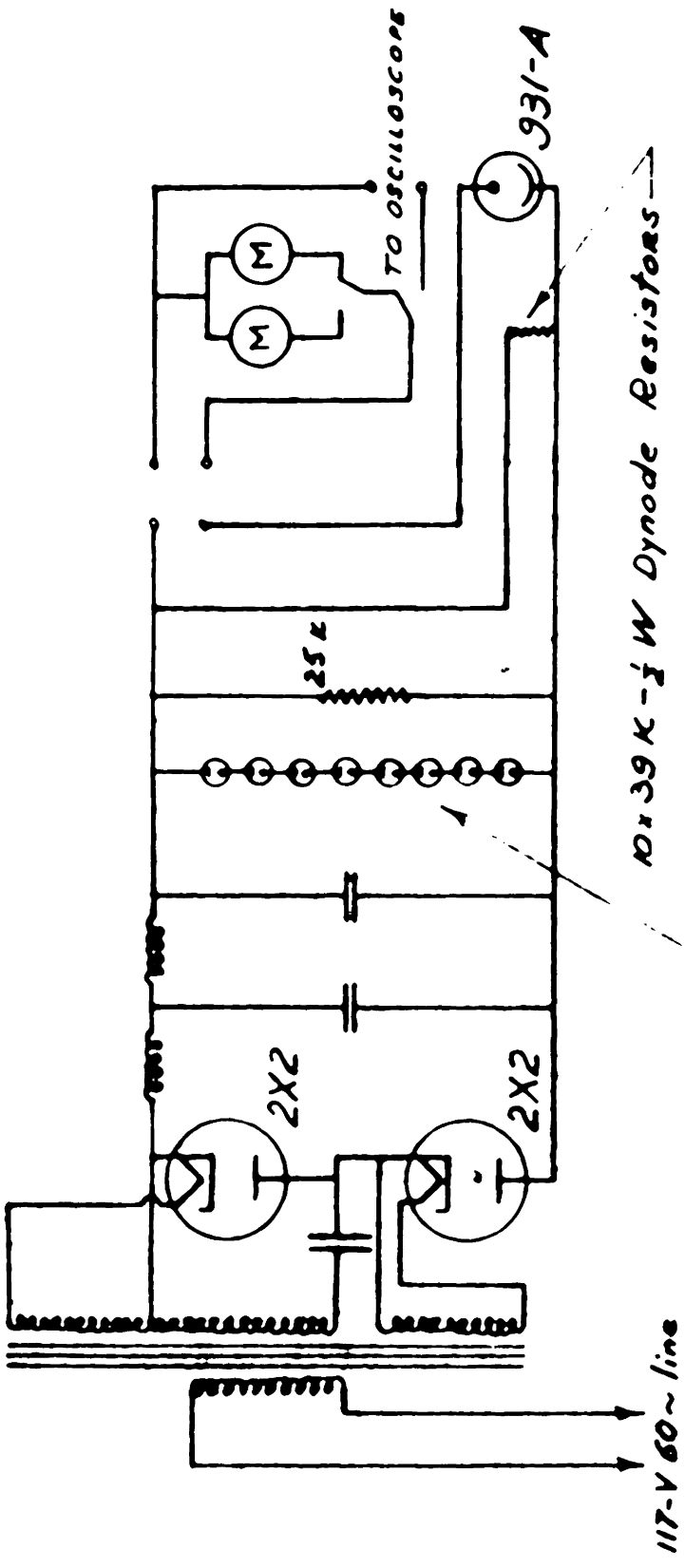

Fig. 10. Power Supply, Photomultipliers & Switching Circuits

Fig. 11. Front view of the power supply for the photomultiplier unit.

Fig. 12. Phototube, shielded cable, and housing assembly.

by placing resistors of different ohmic values in the circuit. During the course of preliminary study, a 100,000-ohm ½-watt resistor seemed to give most satisfactory results. Potential drop across this resistor determined the magnitude of the maximum deflection on the scope screen.

6. Accessory Equipment

For maximum source-to-load power transfer, external load-matching capacitive impedances were connected in the output circuit of the 807 amplifier, as seen in fig. 14.

Certain parts of this study necessitated a visual comparison of the output voltage and the load current wave shapes. This was accomplished by means of an oscilloscope. The voltage developed across the 807 plate tank circuit, however, was much too high to be applied directly to the oscilloscope terminals. A resistive divider network shown in figures 13 and 15 was built, so that only a safe portion of the total load voltage was utilized. Method of measuring current on the scope, as seen in fig. 13, consisted of tapping the potential off the network across a 3000-ohm resistor in series with the load.

7. Summary

The apparatus described in above sections was considered as satisfactory for studying the initiation and maintenance, as well as the light intensity variations of the electrodeless discharges under various conditions.

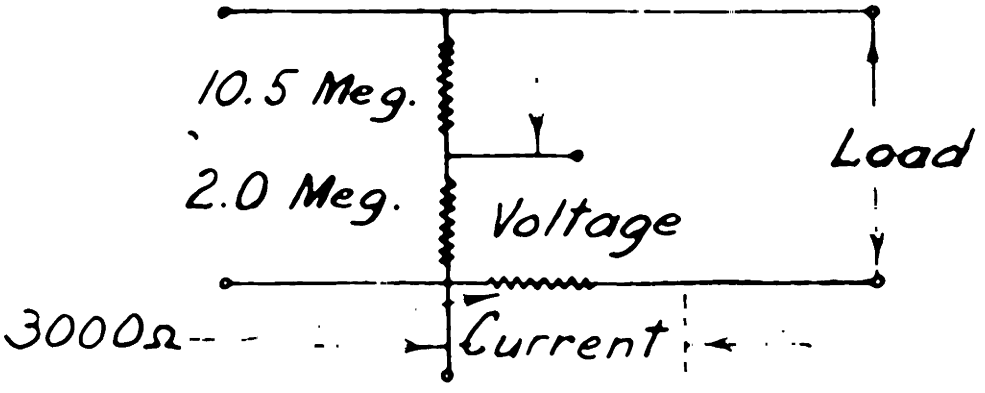

Fig. 13. Divider Network for Voltage and Current Measurements

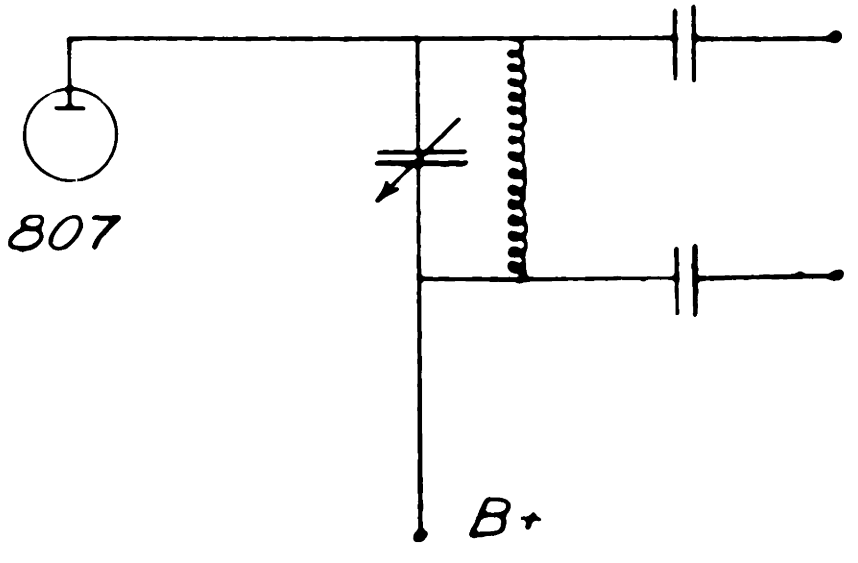

Fig. 14. Impedance Matching

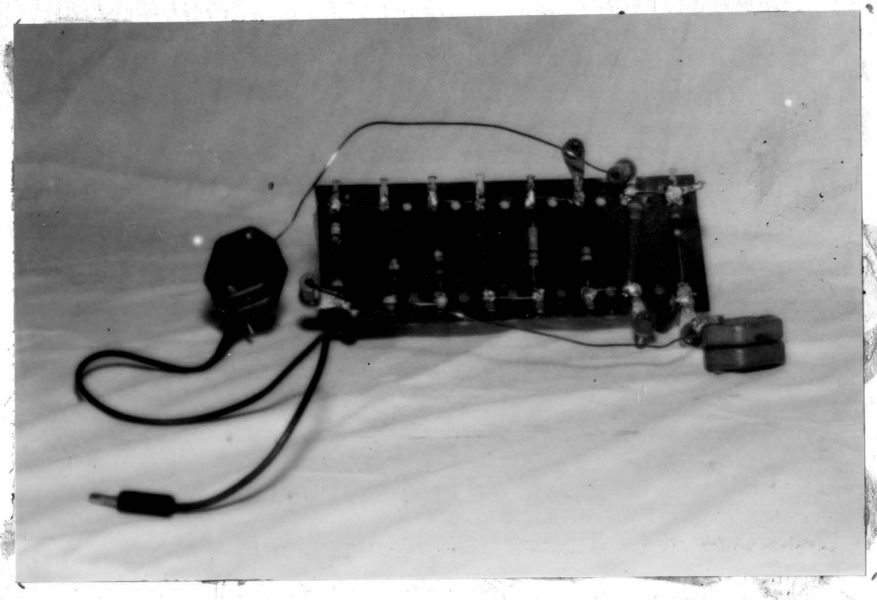

Fig. 15. Pictorial view of the divider network and impedance matching condensers.

Fig. 16. Loading coil employed for impedance matching.

V. PROCEDURE

To obtain discharges at a certain frequency, pressure of the gas in the tube was first reduced by turning on the electric motor connected to the vacuum pump, with the exception of the mercury discharge tube, where the evacuating system was not used. The magnitude of the pressure at any time was read on the McLeod gauges.

When the pressure was reduced to the desired value, the motor was turned off, and voltage of the required grequency was applied to the terminals of the tube to produce a discharge. Operating procedure of either the 60-cycle or the 400-cycle source was relatively simple. It merely required applying line voltage or the output of the 400 cps generator to the primary of the 32:1 voltage transformer and connecting the secondary directly to the tube terminals. In either case, the secondary voltage could be varied by means of the autotransformer connected in the primary. Operation of the source of radio frequency was much more complicated, as it required a number of adjustments to be made before discharges could be produced. The following is the summary of the operating procedure to be used in normal operation of the apparatus for excitation of electrodeless discharges at frequencies ranging from approximately 80 to 1100 kilocycles:

1. Turn on the switch marked "117 V Line" located

on the power supply control panel (fig. 3) to supply 60-cycle a-c to the power supply unit.

2. After a warm-up period of at least ten seconds, apply plate voltage to the 5U4 rectifier tube by turning on a switch marked "LV Transformer" on the power supply panel.
3. Make sure the knob of the variac autotransformer (figures 2 and 3) is turned all the way counter-clockwise for zero voltage input to the high-voltage transformer.
4. Turn on the high voltage switch located on the power supply panel.
5. Adjust the variac for proper high voltage output read on the meter located at the right on the power supply panel. This may not exceed rated d-c plate voltage of the 807 amplifier tube (700 volts).
6. Tune the oscillator for the desired frequency output by placing the capacitance selector switches located on the oscillator-amplifier panel (fig. 6) in proper positions. Make fine adjustment by means of the air-core condenser in parallel with the oscillator tank coil.
7. Adjust the control switch marked "Buffer Grid Input" for proper drive. This switch is located

on the oscillator-amplifier panel. Amount of drive is indicated on the milliammeter located at the left on the power supply panel. Reading of that meter should not exceed rated grid drive of the 807 amplifier (8 ma d-c).

8. Tune the 807 tank for resonance by varying the plate tank capacitance selector switches until a marked "dip" of the needle is observed on the milliammeter located near the middle of the power supply panel. Current at the "dip" should not exceed rated d-c plate current of the 807 amplifier tube (50 ma d-c). Capacitance selector switches are located on the oscillator-amplifier panel. Make fine adjustment for resonance with the air-core condenser in parallel with the 807 tank circuit.
9. Vary the amount of drive until a discharge is produced.

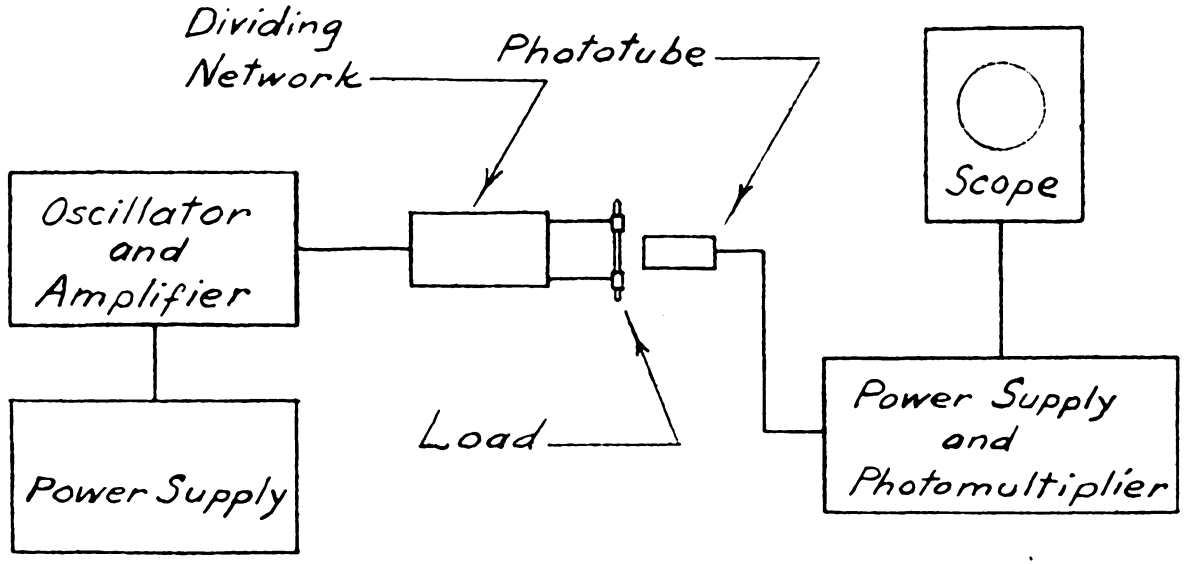

Fig. 17. Block Diagram of Apparatus used in Connection with Mercury Discharge

VI. PRELIMINARY WORK

Prior to construction of the final oscillator and amplifier set shown in figures 5, 6, and 7, a similar unit shown diagrammatically in fig. 18 was constructed on experimental basis. Testing the experimental unit revealed the necessity of using a buffer stage, aided in selection of proper circuit constants for the final unit, and presented a means for comparison of various methods of load matching.

Method of load matching shown in fig. 14 proved to be most efficient. Other methods studied included using only one condenser connected between the positive end of the 807 tank circuit and the load and grounding the negative end of the load; also, using a tuned 5.84-mh loading coil (L_3) shown in figures 16 and 18. The latter was coupled inductively to the 807 plate tank coil (L_2) by means of a movable link (M) inside the latter. This method of load matching was effective but laborious, as it required another adjustment to be made in addition to those described in the preceding section.

High-frequency parasitic oscillations in the final amplifier stage developed into a major problem. They seemed to have been transient in nature, occurring near the resonance point, or when the drive was too high. The above condition made the adjustment of the apparatus for proper operation very critical, if not altogether

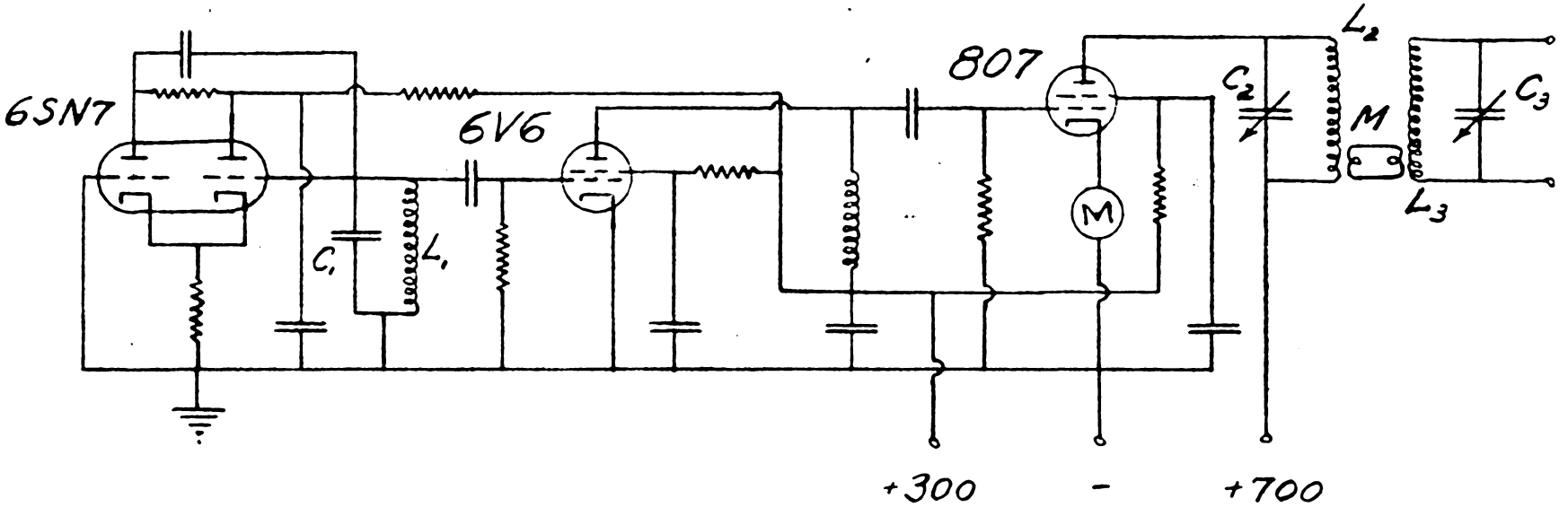

Fig. 18. Expeeimental Oscillator & Amplifier

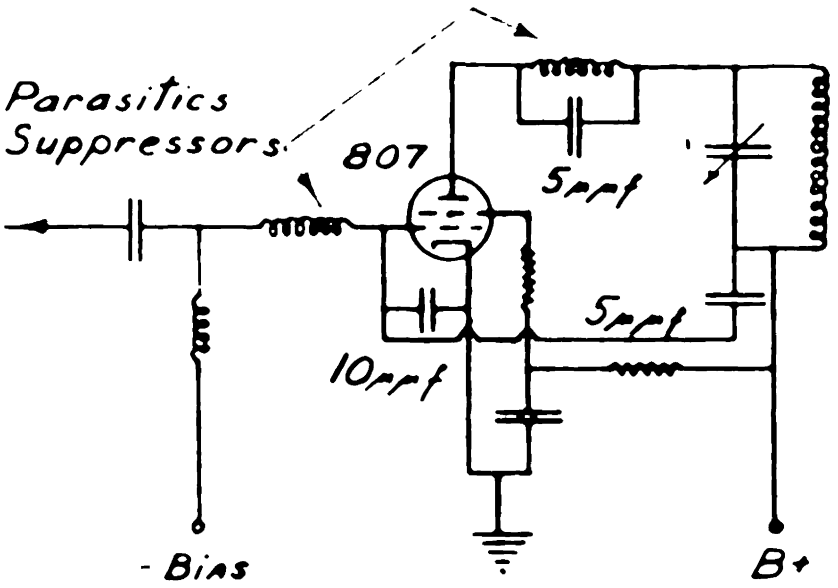

Fig. 19. Method of Neutralization of Parasitic Oscillations

impossible. To eliminate the effects of the offending circuit that caused parasitics, a method of neutralization shown in fig. 19 was successfully employed.

Improper filtering of the high voltage in the power supply was evidenced by the 60-cycle modulation envelope that appeared on the oscilloscope screen. To remedy this, the choke-input type filter originally used in the high-voltage line was replaced by a condenser-input type by using two condensers of greater capacitance.

To limit the peak current drawn by the 816 rectifiers, a 100-ohm protective resistor (R_4) was installed in the high-voltage line as shown in fig. 2. The above measure insured adequate protection of the tubes and other equipment in the high-voltage line.

As a safety precaution, masonite guards were erected to prevent physical contact with the high-voltage components of the oscillator-amplifier unit.

A peculiar set of conditions was observed when the output of the source of r-f appeared to be modulated by a low-frequency modulation envelope. Though the origin of this low frequency, or modulation frequency, was not determined, it is most reasonable to assume that it was a parasitic oscillation produced in the circuit of the final amplifier stage. It appeared near the resonance point, and disappeared completely when the 807 tank

circuit was properly tuned.

Nothing was done to eliminate that low frequency, since the ability of the source to exhibit that unaccounted-for phenomenon was not harmful to obtaining results with sine wave output voltage variation. It was rather unstable, decreasing from about fifty down to one kilocycle as the load was increased by increasing the drive. Some rather interesting results obtained by applying "modulated" voltage to the terminals of the discharge tube are discussed in the next chapter.

VII. DISCUSSION OF RESULTS

A study of electrodeless discharges through mercury vapor, air, and argon was made under various conditions at frequencies ranging from 60 cps to approximately one megacycle.

For studying mercury discharges, a vertically mounted 1.57 ± .01 cm outside diameter tube (fig. 20) containing a drop of mercury at an unknown reduced pressure was used. No provisions were made to vary the vapor pressure inside the tube. The terminals used were aluminum foil caps fitted around the ends of the tube and spaced approximately ten cm. apart. Mercury discharge was investigated only at frequencies of 80 kc. or higher.

For all other work, glass tubes of various diameters and approximately fifty cm. long were used. Parts of work requiring no comparison of results obtained in tubes of various diameters were accomplished by means of a single tube. Effects of varying physical dimensions of the discharge tubes were studied by means of three tubes of various diameters, fused together in parallel as shown in fig. 21, so that a simultaneous observation of the light intensity variation produced under various conditions could be accomplished. Inside and outside diameters of the tubes shown in fig. 21 were, respectively:

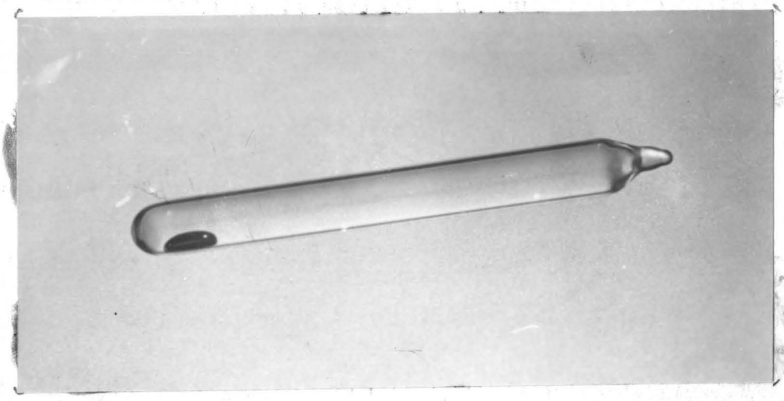

Fig. 20. Electrodeless tube used for studying discharges in mercury vapor.

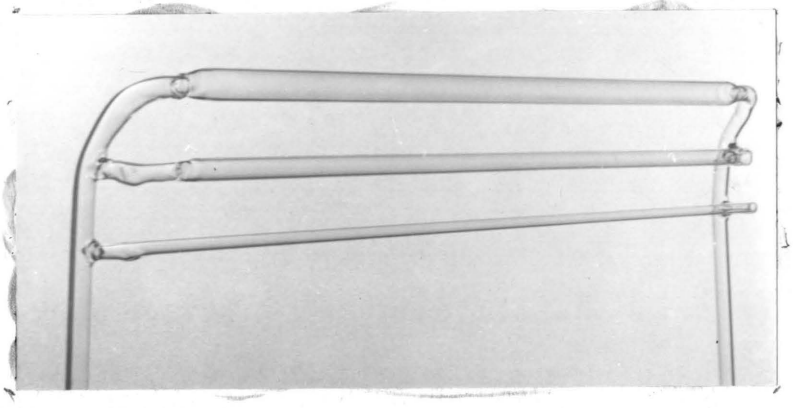

Fig. 21. Electrodeless tubes of various diameters.

.555 cm. and .762 cm.; .951 cm. and 1.192 cm.; and 1.508 cm. and 1.779 cm.

A review of characteristics studied and results obtained to date are given below.

1. General Appearance of the Discharges

It was mentioned before that no direct means were employed to vary the pressure of the mercury vapor in the discharge tube employed. Heating the tube with a Bunsen burner, however, produced an increase in intensity and a change in color of the discharge column from uniform light-blue to bright greenish-blue. It is not known whether this change in color was a direct temperature effect or an effect due to increase of the density of the vapor by heating, although some change in color of the discharge with density, and therefore with pressure, was observed by Nisewanger, Holmes, and Weissler (19).

Generally, the color of the mercury discharge immediately after its initiation was bluish-white, similar to that of the air discharge discussed in a latter part of this section. A short period of time thereafter it turned to color characteristic of the mercury discharge. If it is permissible to assume that the bluish-white color was due to air discharge which produced initial heating of the mercury, then it is obvious that the change in color was due to the increase of the density of the

mercury vapor in the tube. Once the discharge was started, it could be easily re-started again. A "cold tube" was difficult to start since the density of the mercury vapor was low. Thus it is seen that mercury discharges were easier to start than air discharges. Experiments carried out in the past support that conclusion (12).

At the input frequency of 60 cycles, it was determined by visual observation that the intensity of the luminous column in both air and argon discharges was rather uniform throughout its entire length. Color of the air discharge at that frequency was bluish-white, possibly somewhat more "faded" in appearance compared to that observed at radio frequencies. In argon, the color observed was faint purple. At 400 cycles, the air discharge column remained bluish-white, while argon resembled sky-blue in color.

Characteristic color of the discharge column in argon was light-purple when radio frequencies were applied.

For sinusoidal r-f voltage and current variation, various shapes of the luminous column were observed in both air and argon, when pressures were gradually increased from the lowest obtainable with the available apparatus up to approximately two mm. Hg. At the input frequency of 724 kc. and a constant distance of 9 cm.

between the terminals, a typical variation of the general appearance of the discharge column with pressure in air discharge is shown in figures 22-30.

At the lowest pressure used for this test (100 microns) the discharge was very weak, with a bright region in the vicinity of each terminal, as seen in fig. 22. At a pressure of 180 microns these regions became brighter (figure 23), until the discharge column suddenly appeared in form of four bright regions separated by dark spaces, as seen in fig. 24. When the pressure was raised to 280 microns, the shape of the discharge again changed sharply. Figure 25 shows the shape at that pressure: bright regions reappeared near the terminals, the luminous column thinning out into a distinct bright spot half-way between the terminals. The above condition was very critical and a very slight increase in pressure made the discharge column appear in the shape shown in fig. 26, namely, a more or less even pattern with two dark spaces close together. The picture shown in fig. 26 was taken at a gas pressure of 300 microns. As the pressure increased to 355 microns, the discharge column became brighter (fig. 27), and at a still higher pressure (920 microns) the dark spaces began moving away from each other and closer to the terminals. See fig. 28. Figure 29 shows the discharge column at a pressure of

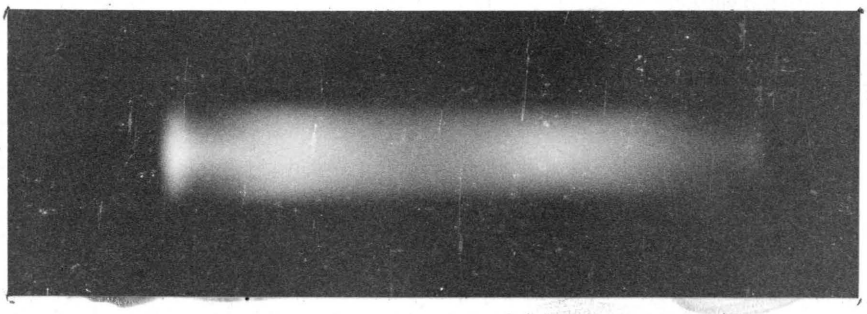

Fig. 22. General appearance of the discharge column in air at 100 microns.

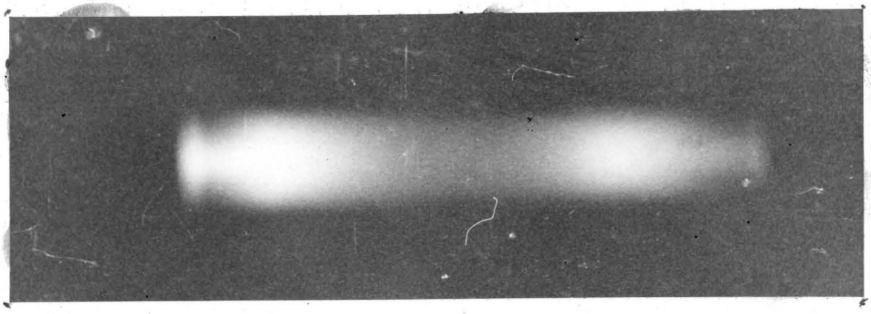

Fig. 23. General appearance of the discharge column in air at 180 microns.

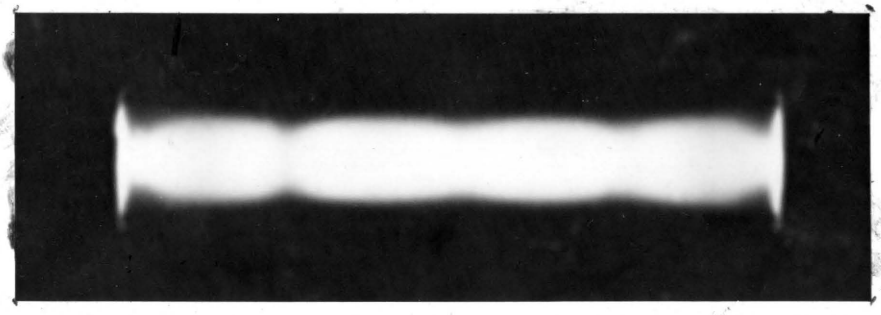

Fig. 24. General appearance of the discharge column in air at 210 microns.

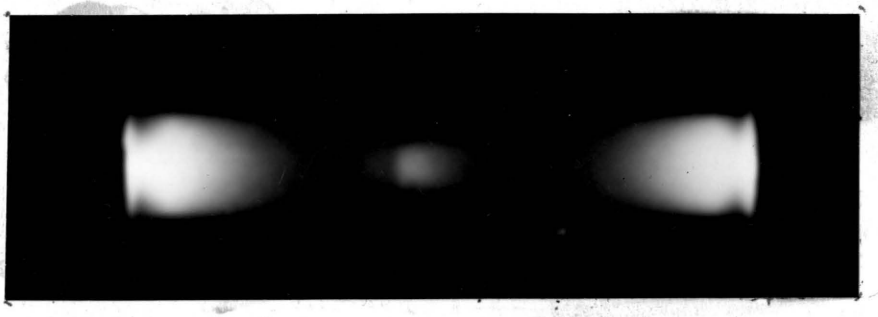

Fig. 25. General appearance of the discharge column in air at 280 microns.

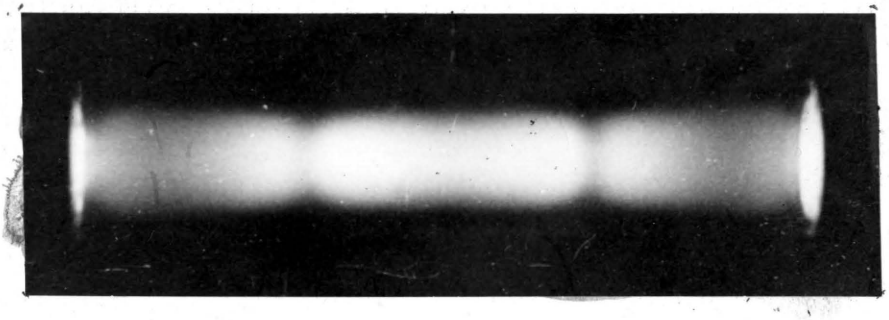

Fig. 26. General appearance of the discharge column in air at 300 microns.

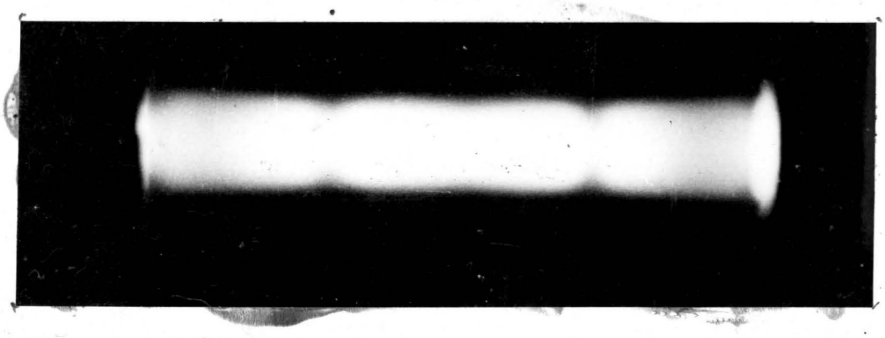

Fig. 27. General appearance of the discharge column in air at 355 microns.

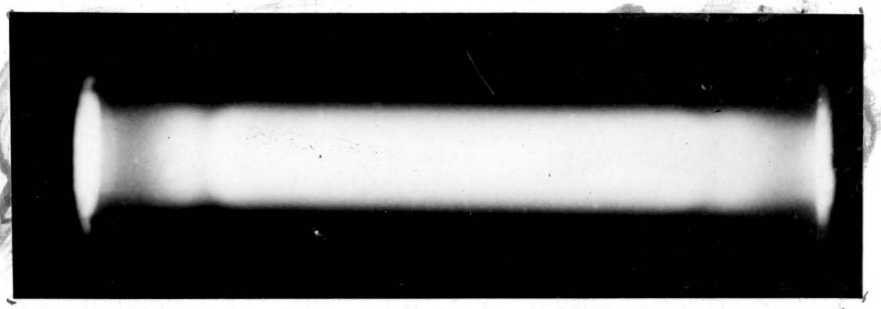

Fig. 28. General appearance of the discharge column in air at 920 microns.

Fig. 29. General appearance of the discharge column in air at 1300 microns.

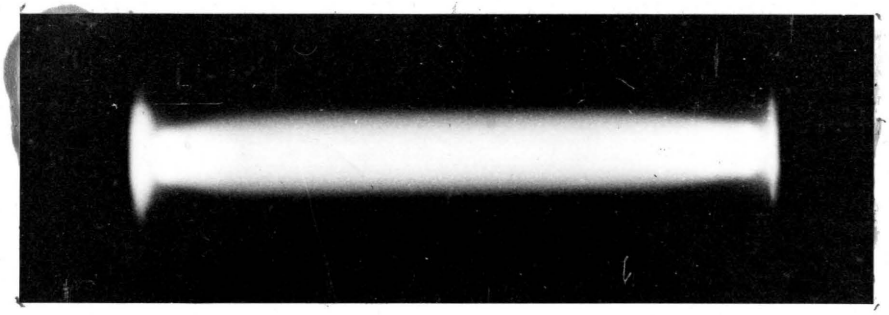

Fig. 30. General appearance of the discharge column in air at 2300 microns.

1300 microns. It is seen that at this pressure the dark spaces moved even further away from each other and closer to the terminals as before. The last picture taken (fig. 30) was that of the luminous column at 2300 microns. The column appeared to be very uniform along the tube, the dark spaces being at a maximum distance from each other. A further increase in pressure caused the discharge to discontinue.

Such a periodicity of the variation in appearance of the luminous column was observed at all frequencies within range of the available source of r-f.

Other factors remaining constant, changing diameter of the discharge tubes produced a definite variation of the general appearance of the discharge column. A test upon argon discharge was made at a frequency of 343 kc. and a constant distance of 9 cm. between the terminals. Results shown in figures 31-38 show that as the diameter of the tube decreased, the dark spaces moved away from each other and closer to the terminals, as when the pressure was increased in the vicinity of one mm. Hg in the previous test made on a single tube of constant diameter. At a pressure of 600 microns a very well defined "dark space" was observed in the largest tube, as seen in fig. 34. A similar, though less defined shape was observed in the medium tube (fig. 35), while in the small tube such

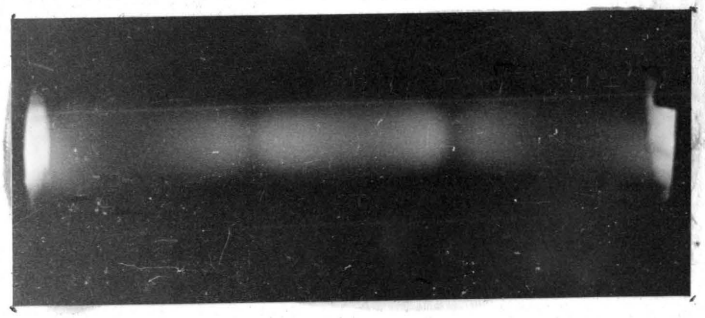

Fig. 31. General appearance of the discharge column in argon in the large tube at 320 microns.

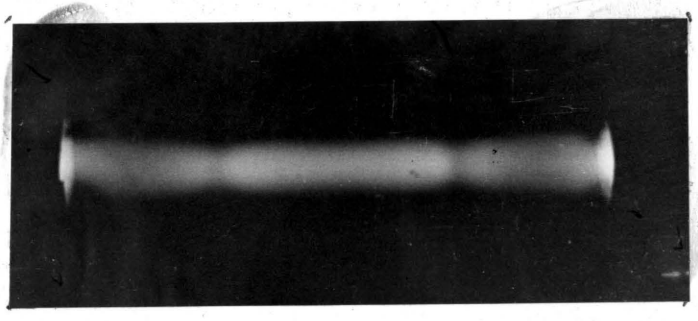

Fig. 32. General appearance of the discharge column in argon in the medium tube at 320 microns.

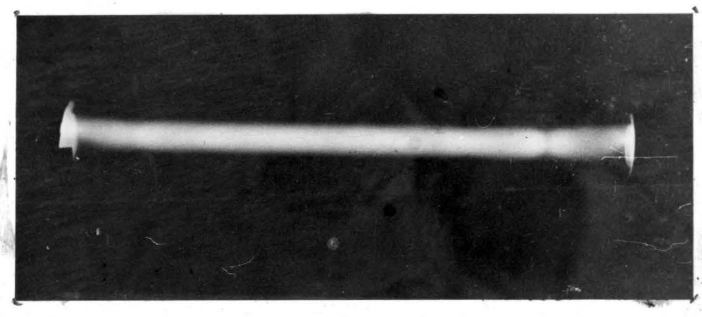

Fig. 33. General appearance of the discharge column in argon in the small tube at 320 microns.

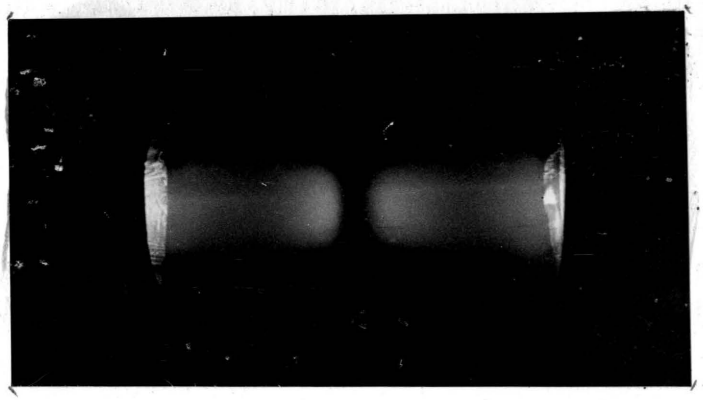

Fig. 34. General appearance of the discharge column in argon in the large tube at 600 microns.

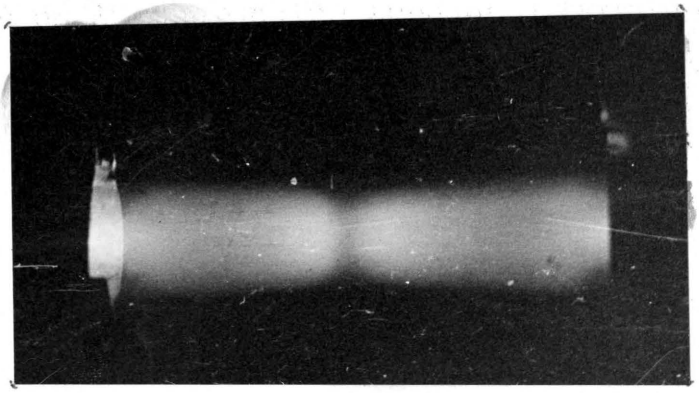

Fig. 35. General appearance of the discharge column in argon in the medium tube at 600 microns.

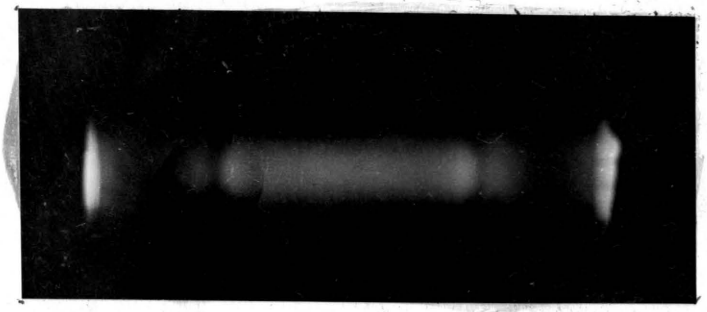

Fig. 36. General appearance of the discharge column in argon in the large tube at 1000 microns.

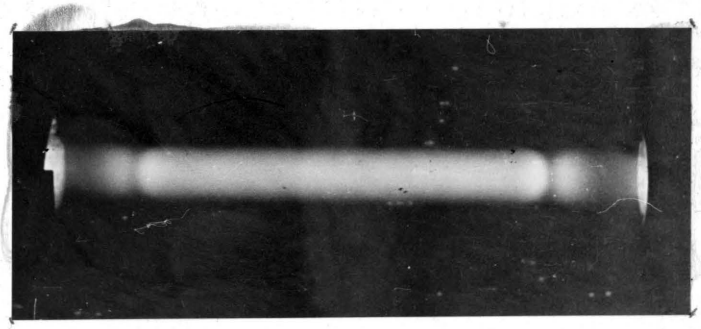

Fig. 37. General appearance of the discharge column in argon in the medium tube at 1000 microns.

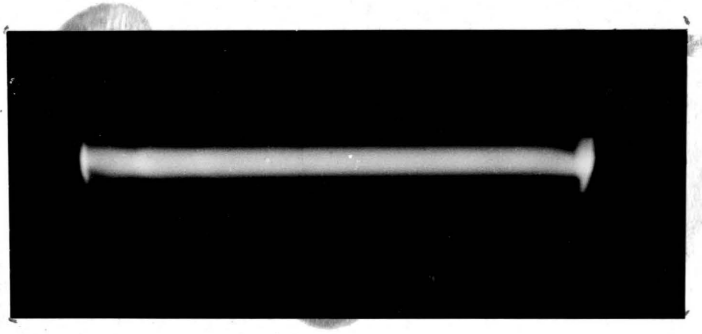

Fig. 38. General appearance of the discharge column in argon in the small tube at 1000 microns.

shape could not be produced, the luminous column showing no apparent variation.

Shapes almost identical with those shown in figures 22, 27, and 34 were obtained by Banerji and Ganguli (1) in hydrogen discharge with mercury vapor introduced as impurity, at a frequency of approximately three megacycles and at pressures ranging from .02 to 1 mm. Hg. According to the same investigators, the observed dark spaces are due to a diminution of electronic concentration in those regions caused by a sudden drop of potential between the edge and the center of the dark space, resulting in a higher degree of ionization away from those regions. Increased electric field caused by the potential drop forces electrons away, producing a visible "dark space".

2. Firing and Extinction Potentials

By varying the terminal voltage and the pressure from above eighty mm. Hg down to approximately one mm. Hg, minimum potentials required to initiate the discharges at various gas pressures were found. Once the discharge was initiated, a gradual reduction of the terminal voltage permitted establishment of points of the lowest potential required to maintain the discharge at each pressure. The former was called the firing potential, the latter - extinction potential.

Firing and extinction potentials were found in air

and argon discharges at frequencies of 60 and 400 cps only, since the available source of r-f was not equipped with means of measurable terminal voltage variation. Results plotted on graphs I-VIII are based on experimental values given in tables III-VIII.

Several common characteristics were found for both gases investigated at each frequency. The firing potential was somewhat higher than the extinction potential in all cases, the slope of the firing curve being somewhat steeper than that of the extinction curve at the lowest pressures. Increasing gas pressures generally resulted in an increase of both potentials.

General shapes of the curves obtained are very similar to those obtained by McCallum and Klatzow for high-frequency argon discharges (17). They have found that the bending-over of the curves may be attributed to the heating of the gas in the tube caused by the currents in the discharge column at pressures higher than 30 mm. Hg. Values of pressure given by the McLeod gauge indicate only approximately the amount of the gas in the tube because of the heating effects of the currents, the true values being somewhat less than those indicated.

Comparison of the curves obtained for air and argon reveals that in argon much lower potentials were required to initiate and maintain the discharges compared to those

required for air.

Results obtained with argon discharge shown on graphs I and II illustrate the effect of the amount of impurities present in the gas on the firing and extinction potential variation. Other experiments (17) revealed that as much as .1% nitrogen introduced as impurity will change the variation of firing potential very considerably. The curve shown on graph I is a result of work done upon argon without any attempts made to purify the gas. It is seen that at higher pressures the required firing potential deviates sharply from the nearly linear variation characteristic of other curves, increasing greatly and apparently tending to approach the characteristic variation in air plotted on the same graph. The above results were checked by using argon with a much smaller percentage of impurity content and employing a very careful procedure in obtaining readings of terminal voltage at each pressure tested. Results of this test are plotted on graph II. It is seen that, contrary to McCallum and Klatzow (17), decreasing the amount of impurities in argon brought about a general increase of the magnitude of the required potentials. This apparent discrepancy may be due to the fact that the frequency used in this study was much lower, and that the variation of firing and extinction potential with

Variation of Firing and Extinction Potential with Pressure at 60 cps.

GRAPH I

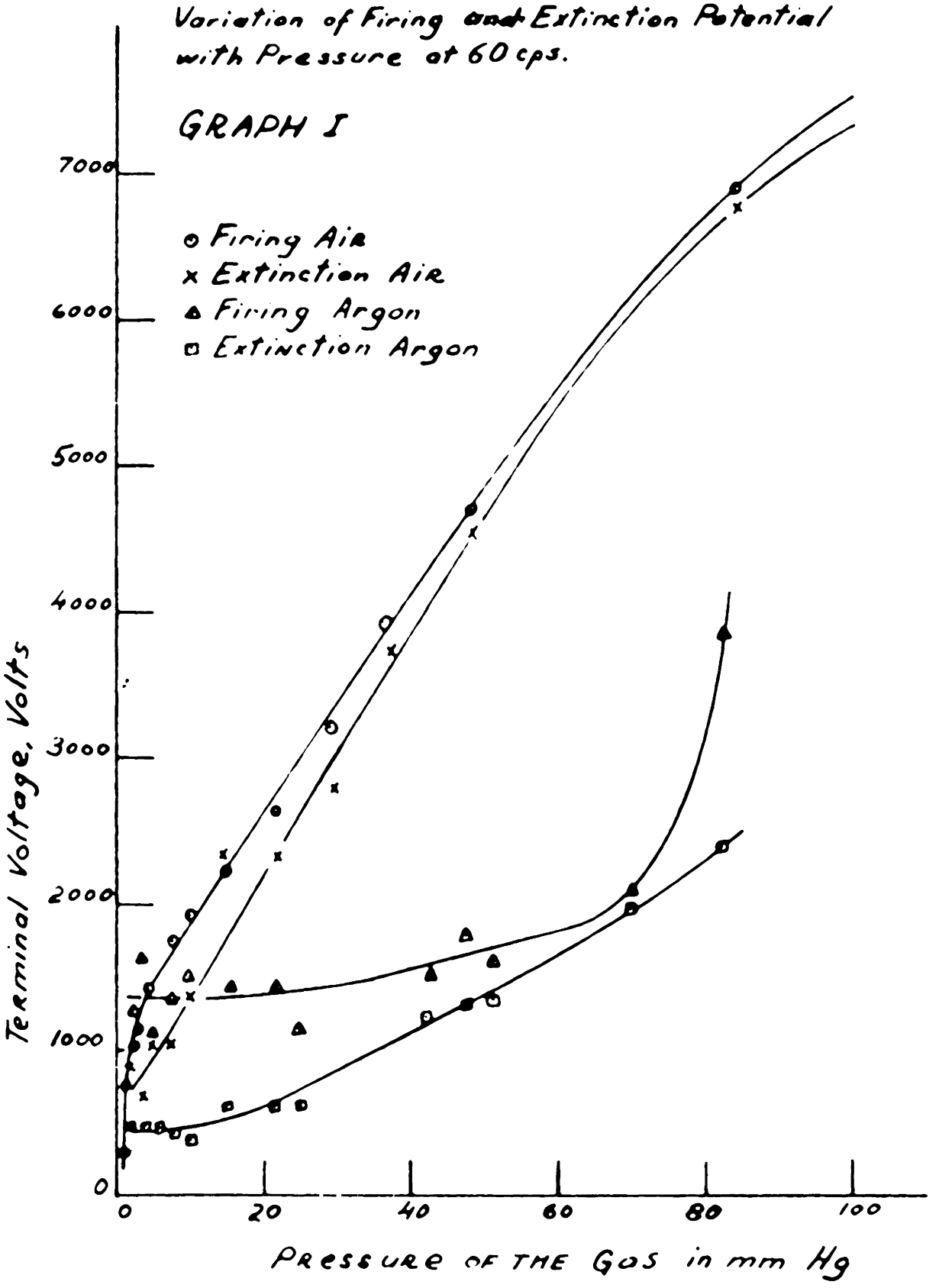

TABLE III (Graph I)

Firing and Extinction Test for Air Discharge

Material of the tube tested: glass

Terminals: wound, 30 turns per terminal, width 1.4 cm.

Distance between the terminals: 3.75 cm.

Frequency applied: 60 cps.

Pressure mm. Hg	Average Firing Potential, Volts	Average Extinction Potential, Volts
84.0	6940	6800
48.0	4670	4525
36.5	3955	3752
29.0	3220	2865
21.5	2556	2340
15.0	2265	2360
10.0	1922	1330
7.8	1734	1000
5.8	1438	1036
2.8	1212	634
1.2	1100	877

TABLE IV (Graph I)

Firing and Extinction Test for Argon Discharge

Material of the tube tested: glass

Terminals: wound, 30 turns per terminal, width 1.4 cm.

Distance between the terminals: 3.75 cm.

Frequency applied: 60 cps.

Pressure mm. Hg	Average Firing Potential, Volts	Average Extinction Potential, Volts
82.0	3791	2370
70.0	2092	1978
55.5	1623	1370
47.3	1790	1324
42.2	1559	1220
24.8	1221	606
21.5	1419	606
15.5	1419	597
10.0	1501	411
7.4	1333	457
4.9	1158	485
3.8	1604	485
2.9	870	466
1.2	774	298

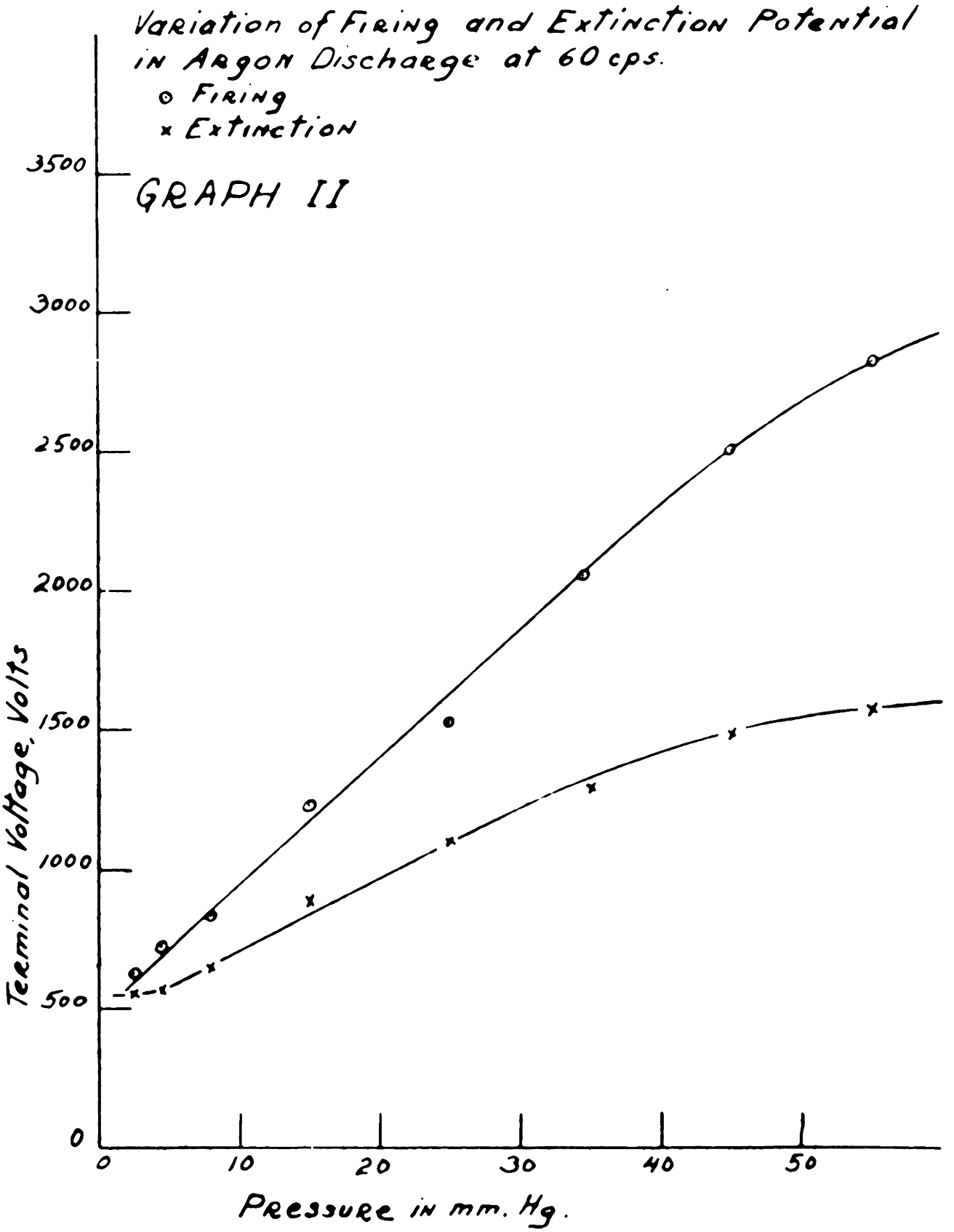
Variation of Firing and Extinction Potential
in Argon Discharge at 60 cps.
o Firing
x Extinction
GRAPH II
3500
3000
2500
2000
1500
1000
500
0
Terminal Voltage, Volts
0
10
20
30
40
50
Pressure in mm. Hg.

TABLE V (Graph II)

Firing and Extinction Test for Discharge in Purified Argon

Tube tested: inside diameter .951 cm.

outside diameter 1.192 cm.

Material of the tube: glass

Terminals: aluminum foil sleeves 2.5 cm. wide

Distance between the terminals: 3.75 cm.

Frequency applied: 60 cps.

Pressure mm. Hg	Average Firing Potential, Volts	Average Extinction Potential, Volts
55.0	2805	1569
45.0	2500	1495
34.5	2050	1280
25.0	1515	1100
15.0	1210	880
7.8	826	646
4.5	720	563
2.5	611	550

percent impurity in argon may not be linear, other things remaining constant.

To illustrate the effect of changing diameter of the tubes upon firing and extinction potential variation, tests were made using the three tubes shown in fig. 21. Results are given on graphs III, IV, and V for 60 cps, and on graphs VI, VII, and VIII for 400 cps. Experimental values are given in tables VI, VII, and VIII. It is seen that at larger pressures somewhat more voltage was required to initiate and maintain the discharges at the lower frequency. The characteristic bending-over of the curves was more pronounced at lower pressures in the 400-cycle discharge. At the latter frequency, the difference in magnitudes of the firing and extinction potentials at any pressure within range was much greater. A characteristic common to discharges in air and argon at both frequencies was that the slope of the curves was somewhat steeper for larger tubes, which indicates that more voltage was required to produce discharges in tubes of larger diameters.

The values of firing and extinction potential, particularly at higher pressures, varied considerably, sometimes as much as 16%. Both potentials seemed to depend upon many factors such as "past history" of the discharge, time interval between initiations of the

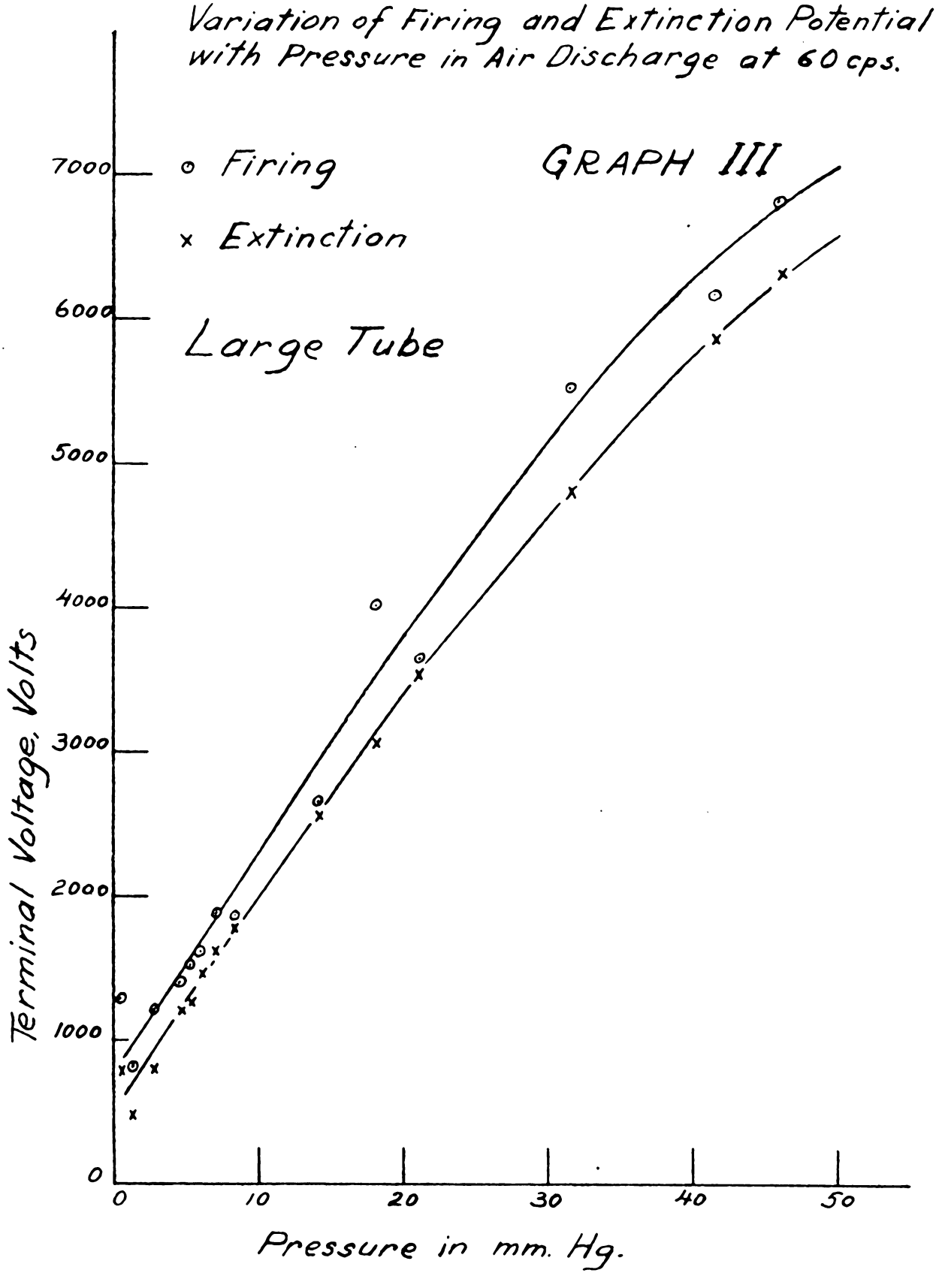
Variation of Firing and Extinction Potential with Pressure in Air Discharge at 60 cps.
GRAPH III
o Firing
x Extinction
Large Tube
7000
6000
5000
4000
3000
2000
1000
0
Terminal Voltage, Volts
0
10
20
30
40
50
Pressure in mm. Hg.

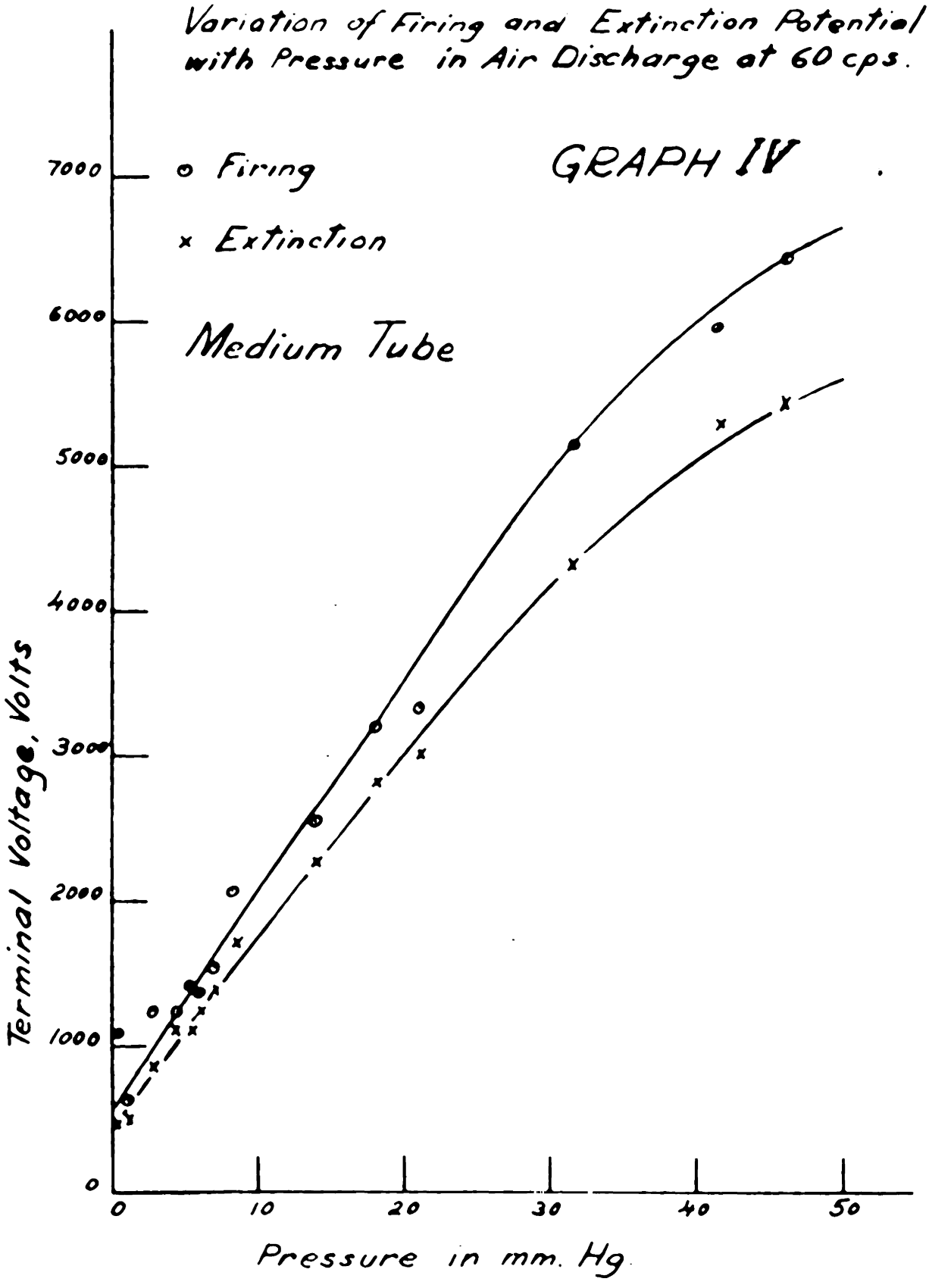
Variation of Firing and Extinction Potential with Pressure in Air Discharge at 60 cps.
GRAPH IV
o Firing
x Extinction
Medium Tube
Terminal Voltage, Volts
Pressure in mm. Hg
0
1000
2000
3000
4000
5000
6000
7000
0
10
20
30
40
50

Variation of Firing and Extinction Potential with Pressure in Air Discharge at 60 cps.

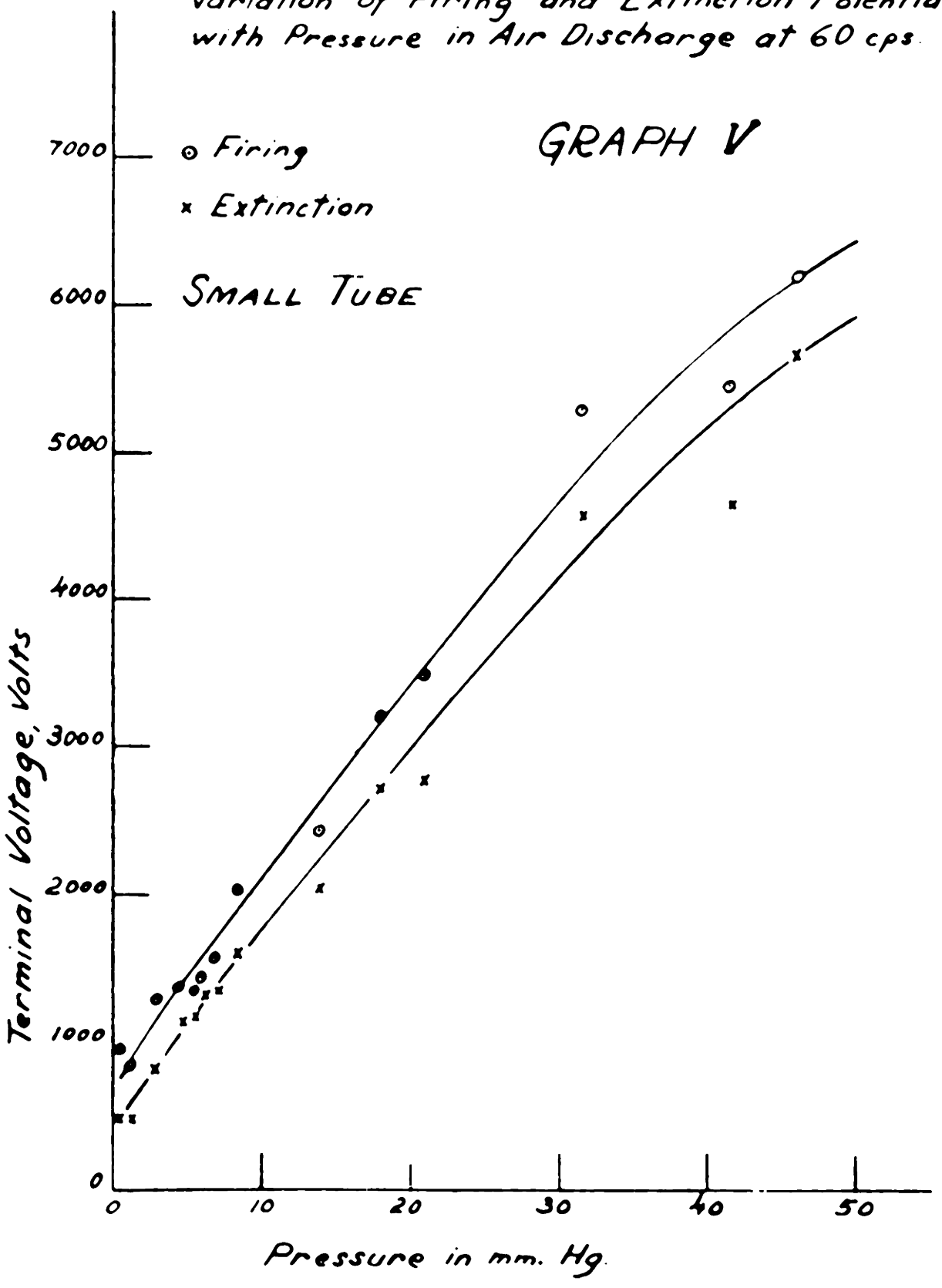

TABLE VI (Graphs III, IV, and V)

Firing and Extinction Tests in Air Discharges for Tubes of Various Diameters *)

Inside and outside diameters, respectively, of the tubes used: small tube, .555 cm. and .762 cm.
medium tube, .951 cm. and 1.192 cm.
large tube, 1.508 cm. and 1.779 cm.

Material of the tubes: glass

Terminals: aluminum foil sleeves 2.5 cm. wide

Distance between the terminals: 9 cm.

Frequency applied: 60 cps.

Pressure mm. Hg	Small Tube F. P.	Small Tube E. P.	Medium Tube F. P.	Medium Tube E. P.	Large Tube F. P.	Large Tube E. P.
.3	960	480	1088	448	1280	800
1.1	830	480	640	480	800	480
2.8	1272	800	1280	864	1216	800
4.6	1336	1120	1215	1122	1376	1189
5.3	1336	1157	1408	1122	1505	1248
6.0	1463	1343	1375	1259	1600	1472
7.0	1590	1375	1534	1410	1889	1600
8.5	2008	1600	2045	1730	1856	1792
14.0	2420	2015	2655	2275	2686	2539
18.0	3200	2720	3200	2820	4000	3075
21.0	3485	2757	3330	3015	3650	3520
31.5	5280	4580	5150	4320	5510	4800
41.5	5440	4670	5950	5280	6270	5890
46.0	6175	5650	6430	5440	6820	6305

Note: Average firing and extinction potentials abbreviated F. P. and E. P., respectively, and tabulated in volts.

*) See fig. 21

Variation of Firing and Extinction Potential with Pressure in Air and Argon Discharge at 400 cps.

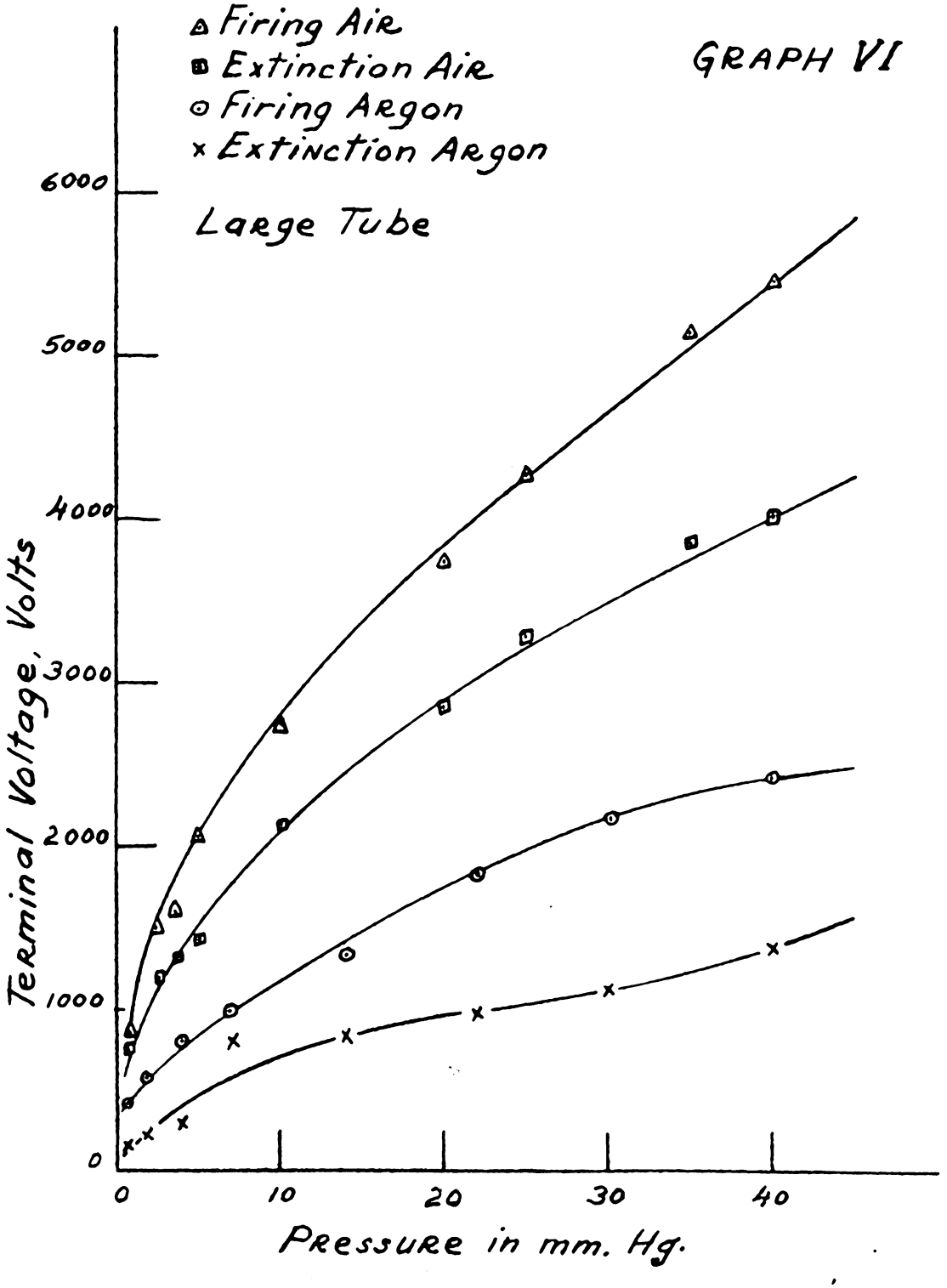

Variation of Firing and Extinction Potential with Pressure in Air and Argon Discharge at 400 cps.

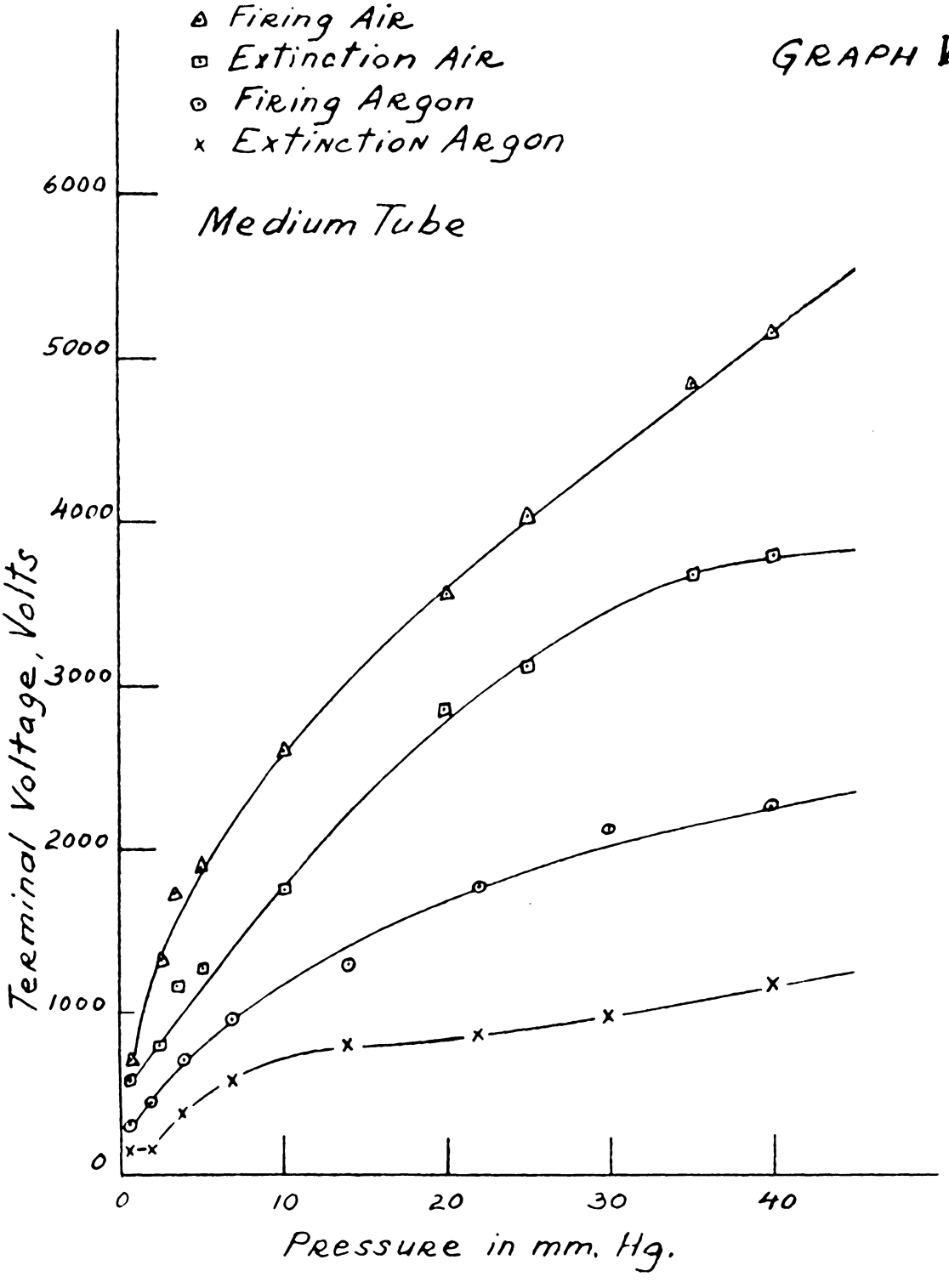

Variation of Firing and Extinction Potential with Pressure in Air and Argon Discharge at 400 cps.

GRAPH VIII

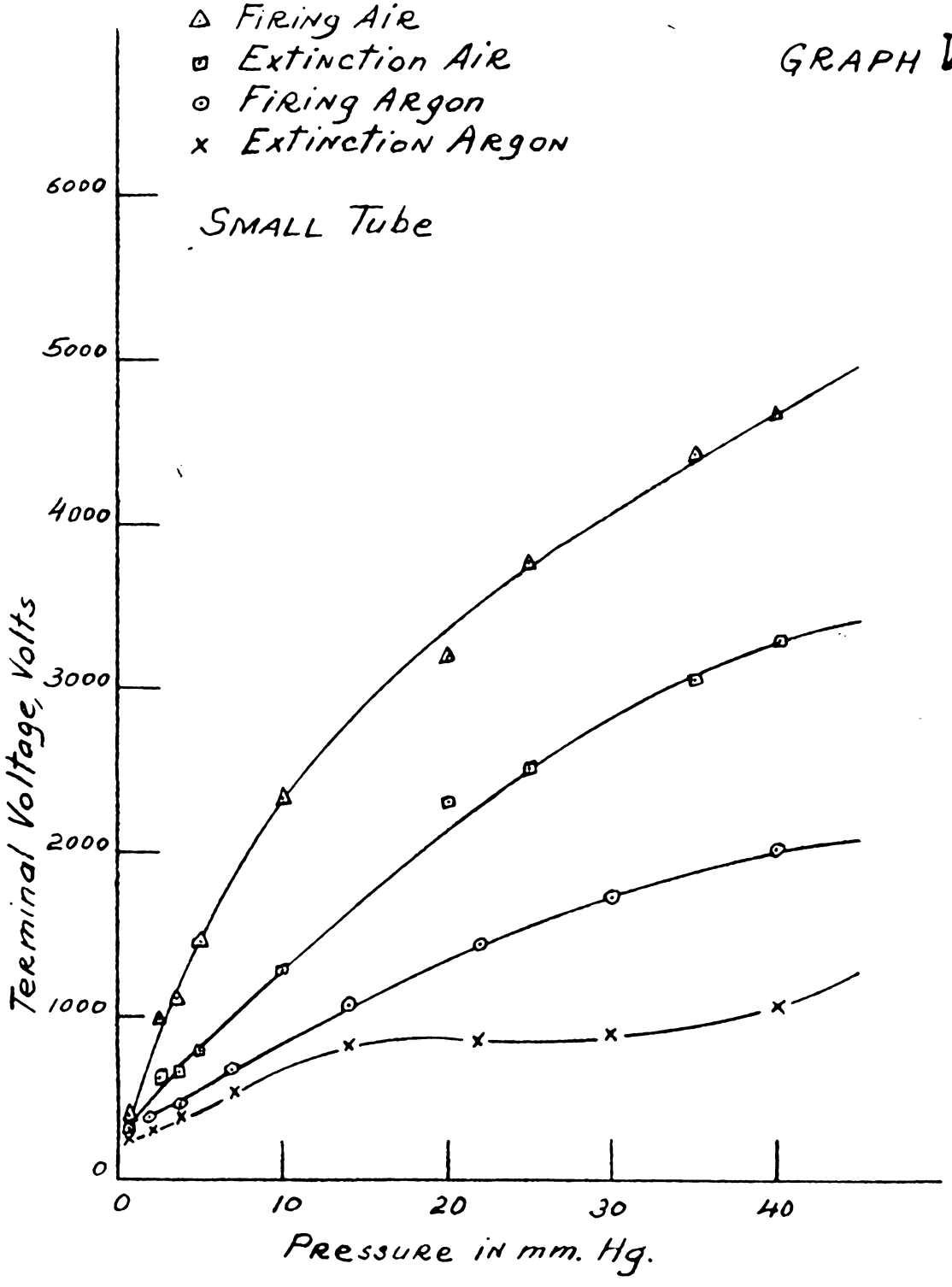

TABLE VII (Graphs VI, VII, and VIII)

Firing and Extinction Tests in Air Discharges for Tubes of Various Diameters

Inside and outside diameters, respectively, of the tubes used: small tube, .555 cm. and .762 cm.
medium tube, .951 cm. and 1.192 cm.
large tube, 1.508 cm. and 1.779 cm.

Material of the tubes: glass

Terminals: aluminum foil sleeves 2.5 cm. wide

Distance between the terminals: 5 cm.

Frequency applied: 400 cps.

Pressure mm. Hg	Small Tube F. P.	Small Tube E. P.	Medium Tube F. P.	Medium Tube E. P.	Large Tube F. P.	Large Tube E. P.
.7	840	750	700	580	425	300
2.5	1500	1200	1320	800	965	605
3.5	1600	1310	1730	1150	1060	655
5.0	2050	1420	1870	1250	1450	795
10.0	2740	2120	2605	1755	2310	1260
20.0	3730	2853	3540	2850	3160	2300
25.0	4272	3260	4030	3120	3760	2500
35.0	5155	3856	4840	3670	4320	3040
40.0	5440	4000	5160	3785	4640	3265

TABLE VIII (Graphs VI, VII, and VIII)

Firing and Extinction Tests in Argon Discharges for Tubes of Various Diameters

Inside and outside diameters, respectively, of the tubes used: small tube, .555 cm. and .762 cm.
Medium tube, .951 cm. and 1.192 cm.
large tube, 1.508 cm. and 1.779 cm.

Material of the tubes: glass

Terminals: aluminum foil sleeves 2.5 cm. wide

Distance between the terminals: 5 cm.

Frequency applied: 400 cps.

Pressure mm. Hg	Small Tube F. P.	Small Tube E. P.	Medium Tube F. P.	Medium Tube E. P.	Large Tube F. P.	Large Tube E. P.
.5	300	230	320	145	416	176
1.7	360	290	450	160	560	224
4.0	450	370	700	360	800	256
6.9	655	505	960	567	992	800
14.0	1050	810	1296	800	1310	832
22.0	1420	810	1760	864	1822	990
30.0	2000	1040	2250	1150	2420	1370
40.0	2390	1110	2450	1200	2590	1365

discharges, temperature, stray radiation from outside, and possibly others. The data given in the tables III, IV, VI, VII, and VIII are based on the averages of at least four observations at each pressure. In one case, for pure argon (table V), at least twenty readings were taken at equal intervals of time.

Despite the difficulties encountered in determining the firing and extinction potentials, the results obtained show that Paschen's law holds at least approximately at very low frequencies, as it does for electrodeless discharges at high frequencies (19, 23).

During the course of the investigation some indication was obtained that as the pressure was lowered continuously, the firing and extinction potential would increase sharply after passing a minimum value. At such low pressures the discharges were so faint that it was difficult to determine whether the point of extinction has been reached or not, even with the aid of the photo-tube. This and the fact that the exact values of the potentials were difficult to find, as explained before, prevented further investigation of this phenomenon.

3. Distance Between the Terminals

Several experiments were carried out to determine the maximum distances between the terminals sufficient to maintain the discharges at a given set of conditions.

Table IX shows results of tests performed in attempt to establish the relationship between those distances and the magnitude of the terminal voltage and pressure at the input frequency of 60 cycles. It is seen that a higher pressure or a lower terminal voltage necessitated sliding the terminals closer together to cause firing. For example, at a pressure of 26 mm. Hg a terminal voltage of 3200 volts was sufficient to start firing when the terminals were 4.7 cm. apart along the tube. When the pressure was increased to 50 mm. Hg, the same terminal voltage produced firing when the distance between the terminals was only one cm.

Effects of variation of tube diameter upon the maximum permissible distance between the terminals were investigated in connection with discharges excited by means of the 400-cycle source. As seen in table X, changing the diameter of the tube produced no observable effect on the maximum distance between the terminals. Comparison of the values given in same table for air and argon discharges reveals that at a constant terminal voltage and pressure, the terminals in argon discharges could be left much further apart without the danger of extinguishing the luminous column.

Table XI is a summary of the results obtained at a frequency of 545 kc. This table, as well as tables IX and X, shows that the lower the pressure, the greater the

TABLE IX

Variation of Firing Potential with Pressure for Various Distances Between the Terminals in Air Discharge

Material of the tube tested: glass

Terminals: wound, 30 turns per terminal, width 1.4 cm.

Frequency applied: 60 cps.

Pressure mm. Hg	Distance Between the Terminals, cm.	Firing Voltage
26.0	.9	1600
26.0	2.9	2400
26.0	4.7	3200
30.0	1.2	2400
30.0	2.9	3200
30.0	3.8	4000
44.0	.7	2400
44.0	1.2	3200
44.0	2.5	4000
50.0	1.0	3200
50.0	1.9	4000
50.0	3.7	4800

TABLE X

Variation of Maximum Distance Between the Terminals with Pressure for Air and Argon Discharges in Tubes of Various Diameters

Inside and outside diameters, respectively, of the tubes used: small tube, .555 cm. and .762 cm.
medium tube, .951 cm. and 1.192 cm.
large tube, 1.508 cm. and 1.779 cm.

Material of the tubes: glass

Terminals: aluminum foil sleeves 2.5 cm. wide

Terminal voltage: 1745 volts

Frequency applied: 400 cps.

(1) Air Discharge

Pressure mm. Hg	Distance Between the Terminals, cm. small tube	medium tube	large tube
20.0	1.5	1.5	1.5
15.3	2.0	2.5	2.8
7.9	8.2	9.3	7.8
2.8	15.3	15.3	15.2
(2) Argon Discharge			
30.0	.9	.9	.9
26.0	4.7	4.7	4.7
22.0	9.9	10.1	10.1
19.0	16.8	16.5	16.0

TABLE XI

Variation of Pressure with Maximum Distance Between the Terminals Required for Firing in Air and Argon Discharges

Material of the tube tested: glass

Terminals: aluminum foil sleeves 2.5 cm. wide

Frequency applied: 545 kc.

(1) Air Discharge

Pressure mm. Hg	Distance Between the Terminals, cm.
.23	47.0
.60	12.5
1.00	7.3
2.50	4.0
5.30	1.9

(2) Argon Discharge

.55	46.0
.60	21.0
1.70	17.0
3.00	8.5
7.00	1.9

maximum permissible distance between the terminals. It also shows that argon discharges could be initiated at higher pressures and with the terminals further apart, compared to air discharges, which is in accord with the results obtained with the 400-cycle discharges.

4. Magnitude of the Load Current

By means of a 0-20 ma r-f milliammeter connected in series with the tube it was possible to determine the dependence of the magnitude of the load current upon the pressure of the gas, distance between the terminals, and physical size of the discharge tubes. Tubes used in this part of the study are shown in fig. 21.

Load current showed a marked decrease as the distance between the terminals increased. Table XII shows results obtained for air discharge at 370 kc. and 1035 kc., and for argon discharge at 370 kc. Inspection of the curves plotted on graphs IX and X reveals that the load current seemed to increase slightly with frequency, but after it was corrected for "cold current" it remained practically the same at both frequencies tested.

Discharges in larger tubes drew more current than those in the smaller ones, pressure and distance between the terminals remaining the same. This is evidenced by the curves plotted on the graphs IX, X, and XI. It is

also seen that tubes of larger diameters maintained the discharge at greater distances between the terminals, which is contrary to the results obtained with the 400-cycle discharge and described in the previous section. Table XII shows that the largest one of three tubes maintained the discharge at a distance of as much as 24 cm. between the terminals, while that for the medium and the small tubes was 20 and 14 cm., respectively, other factors remaining constant.

Comparison of the curves on graphs IX and XI shows that for the same distance between the terminals the load current drawn by air discharges was larger than that drawn by argon discharges.

The broken lines shown on graphs under discussion indicate the amount of current indicated by the r-f milliammeter when the load was disconnected. This "cold current" was caused by the stray capacitance of the measuring circuit, its magnitude depending on the frequency applied. At 1035 kc. it was equal to 14.0 ma., and at 370 kc. 13.6 ma., the net current drawn by the discharge at both frequencies remaining approximately the same.

To determine the characteristic variation of the load current with pressure, the gas pressure in the medium tube was varied and the corresponding changes of the load

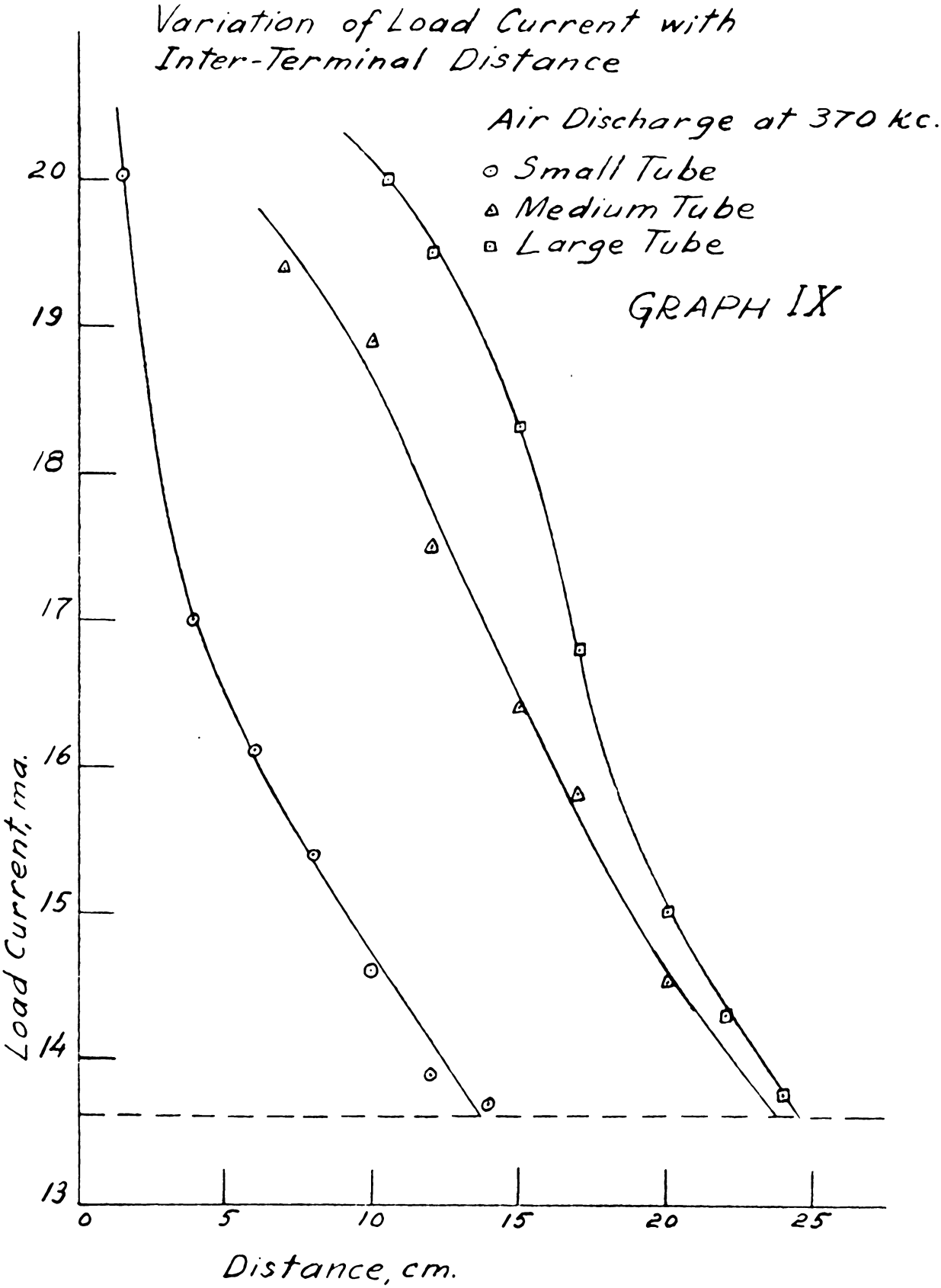
Variation of Load Current with Inter-Terminal Distance
Air Discharge at 370 kc.
o Small Tube
Δ Medium Tube
□ Large Tube
GRAPH IX
20
19
18
17
16
15
14
13
Load Current, ma.
0
5
10
15
20
25
Distance, cm.

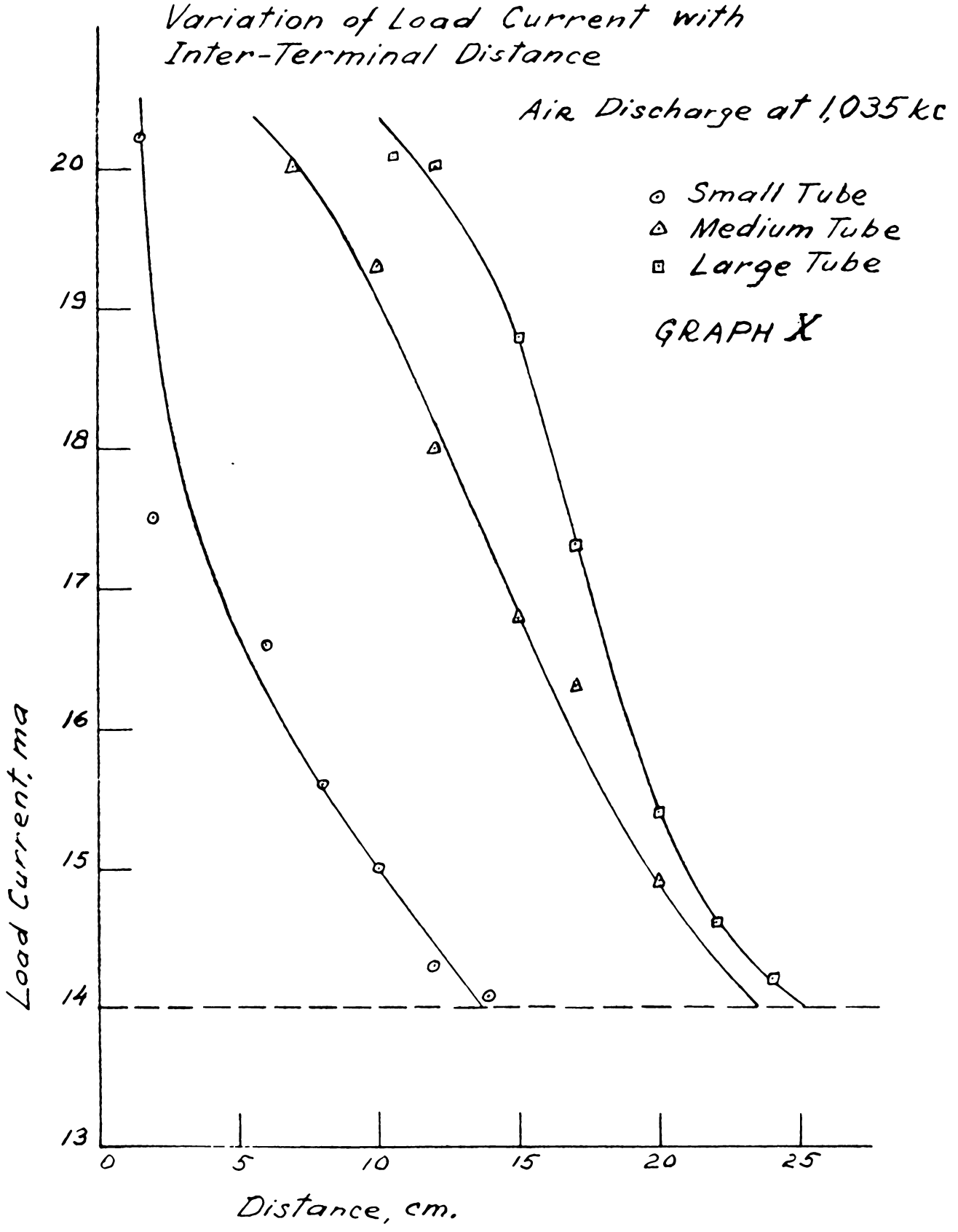
Variation of Load Current with Inter-Terminal Distance
Air Discharge at 1,035 kc
Small Tube
Medium Tube
Large Tube
GRAPH X
Load Current, ma
20
19
18
17
16
15
14
13
0
5
10
15
20
25
Distance, cm.

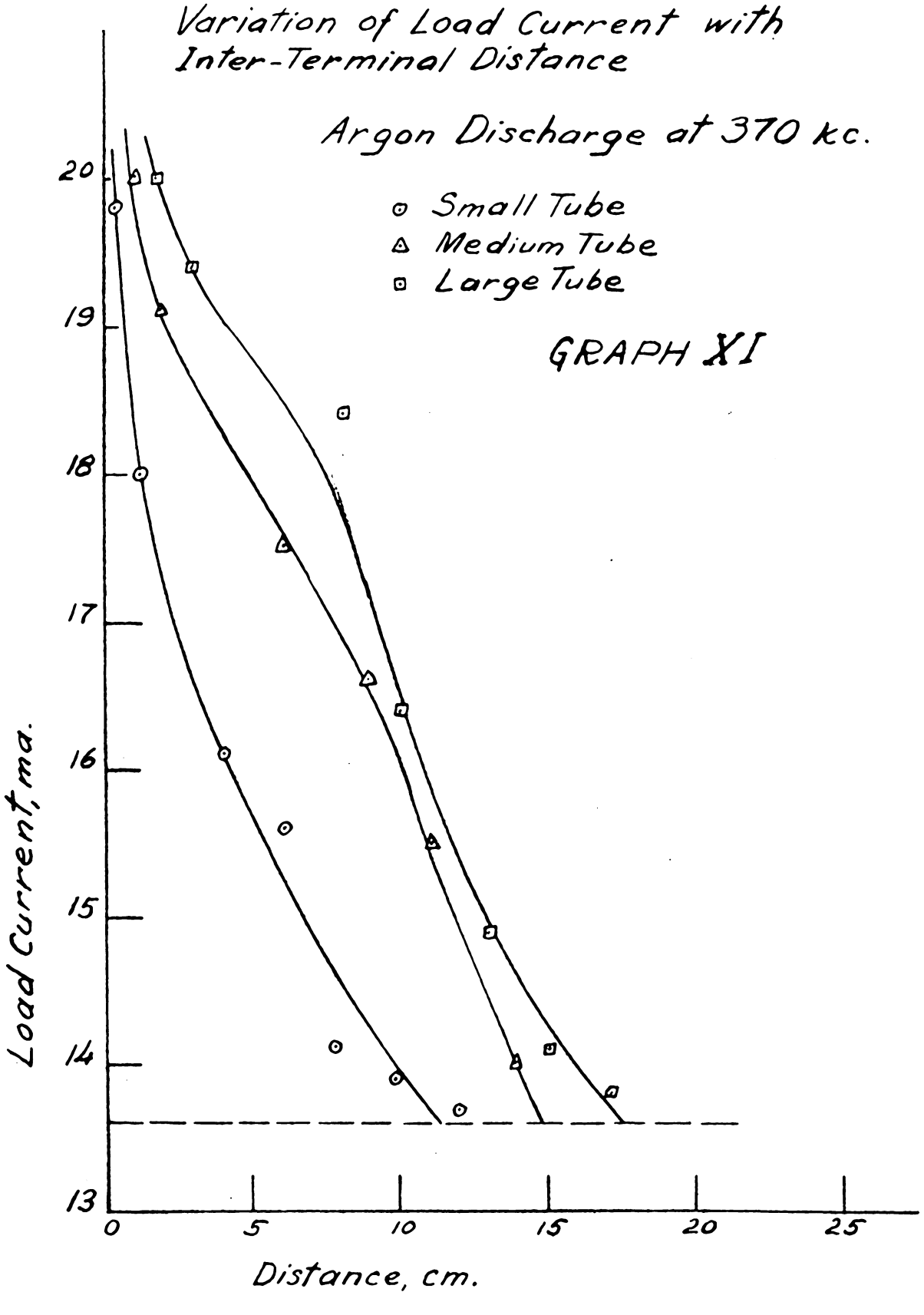
Variation of Load Current with Inter-Terminal Distance
Argon Discharge at 370 kc.
Small Tube
Medium Tube
Large Tube
GRAPH XI
Load Current, ma.
20
19
18
17
16
15
14
13
0
5
10
15
20
25
Distance, cm.

TABLE XII (Graphs IX, X, and XI)

Variation of Load Current with the Distance Between the Terminals in Air and Argon Discharges in Tubes of Various Diameters

Inside and outside diameters, respectively, of the tubes used: small tube, .555 cm. and .762 cm.
medium tube, .951 cm. and 1.192 cm.
large tube, 1.508 cm. and 1.779 cm.

Material of the tubes: glass

Terminals: aluminum foil sleeves 2.5 cm. wide

Pressure of the gas: .3 mm. Hg.

(1) Air discharge, frequency = 370 kc.

a. Small tube

Distance Between the terminals, cm.	Load Current, ma.
1.5	20.0
4.0	17.0
6.0	16.1
8.0	15.4
10.0	14.6
12.0	13.9
14.0	13.7
-	13.6

b. Medium tube

Distance Between the Terminals, cm.	Load Current, ma.
7.0	19.4
10.0	18.9
12.0	17.5
15.0	16.5
17.0	15.8
20.0	14.5
-	13.6

c. Large tube

Distance Between the Terminals, cm.	Load Current, ma.
10.5	20.0
12.0	19.5
15.0	18.3
17.0	16.8
20.0	15.0
22.0	14.3
24.0	13.8
-	13.6

(2) Argon discharge, frequency = 370 kc.

a. Small tube

Distance Between the Terminals, cm.	Load Current, ma.
.3	19.8
1.2	18.0
4.0	16.1
6.2	15.6
7.9	14.1
9.8	13.9
12.0	13.7
-	13.6

b. Medium tube

Distance Between the Terminals, cm.	Load Current, ma.
1.0	20.0
3.9	19.1
6.0	17.5
8.8	16.6
11.0	15.5
13.9	14.0
-	13.6

c. Large tube

Distance Between the Terminals, cm.	Load Current, ma.
3.3	20.0
5.7	19.4
8.0	18.4
10.0	16.4
12.8	14.9
15.0	14.1
17.2	13.8
-	13.6

(3) Air discharge, frequency = 1035 kc.

a. Small tube

Distance Between the terminals, cm.	Load Current, ma.
1.5	21.0
4.0	17.5
6.0	16.6
8.0	15.6
10.0	15.0
12.0	14.3
14.0	14.1
-	14.0

b. Medium tube

Distance Between the Terminals, cm.	Load Current, ma.
7.0	20.0
10.0	19.3
12.0	18.0
15.0	16.8
17.0	16.3
20.0	14.9
-	14.0

c. Large tube

Distance Between the Terminals, cm.	Load Current, ma.
10.5	20.8
12.0	20.0
15.0	18.8
17.0	17.3
20.0	15.4
22.0	14.6
24.0	14.2
-	14.0

Variation of Load Current with Pressure in Air and Argon Discharge at 370 kc.

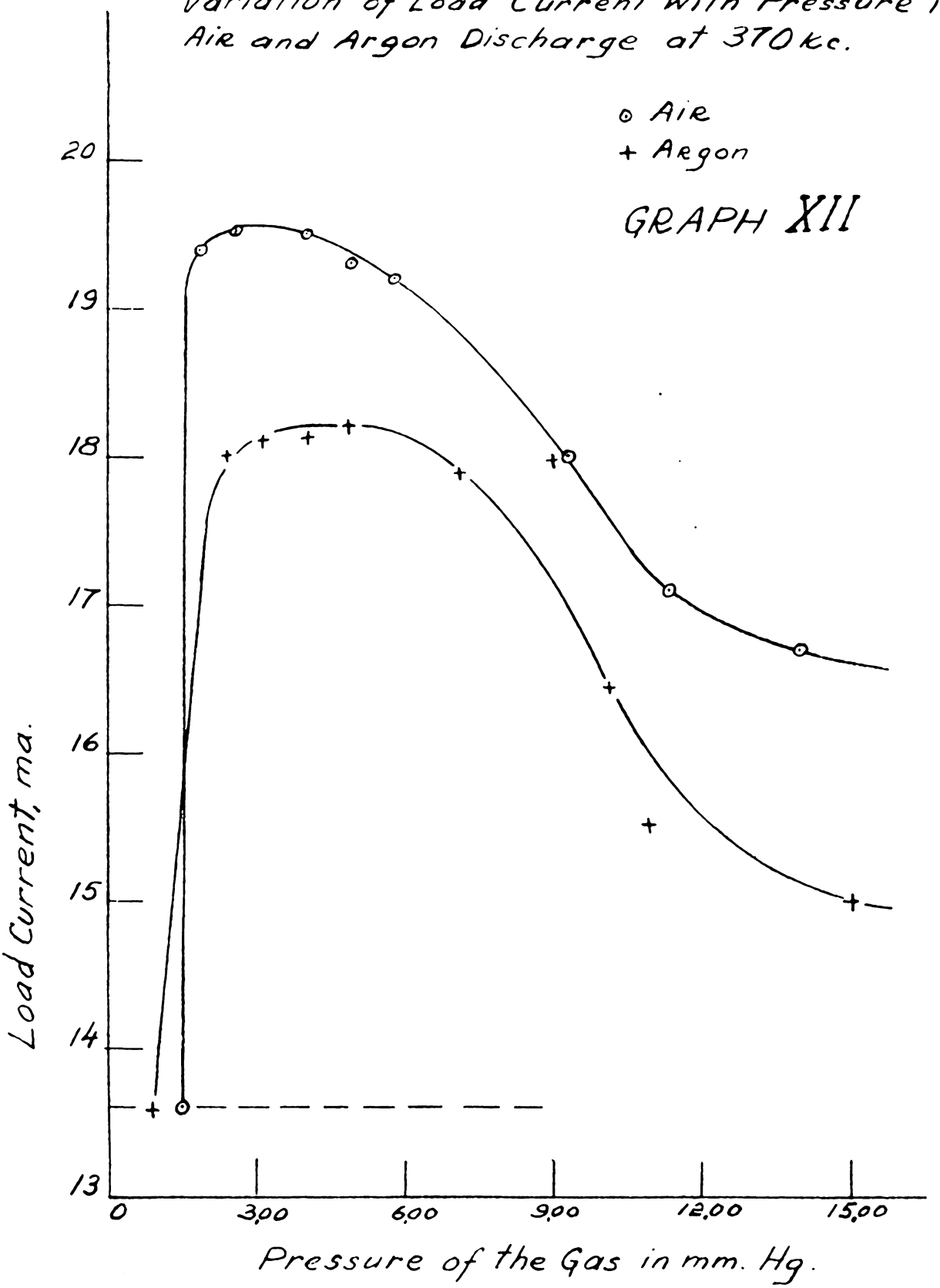

Variation of Load Current with Pressure in Air Discharge at 1,035 kc.

GRAPH XIII

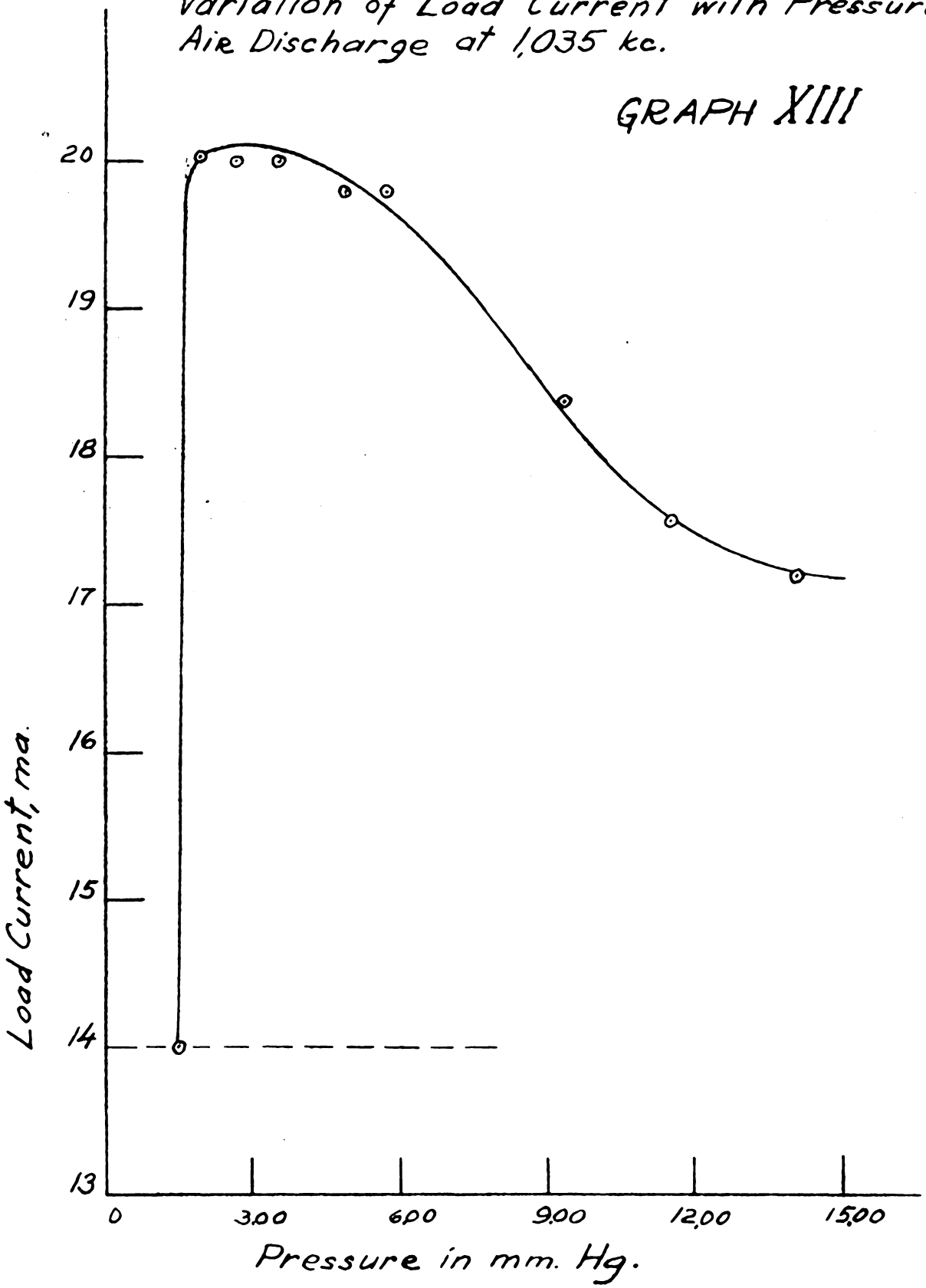

TABLE XIII (Graphs XII and XIII)

Variation of Load Current with Pressure in Air and Argon Discharges

Material of the tube tested: glass

Terminals: aluminum foil sleeves 2.5 cm. wide

Distance between the terminals: 7.0 cm.

(1) Air discharge, frequency = 370 kc.

Pressure mm. Hg	Load Current, ma.
14.0	16.7
11.5	17.1
9.3	18.0
5.8	19.2
5.0	19.3
3.9	19.5
2.6	19.5
2.0	19.4
1.5	13.6

(2) Argon discharge, frequency = 370 kc.

Pressure mm. Hg	Load Current, ma.
15.0	15.0
11.0	15.5
10.0	16.4
9.0	18.0
7.0	17.9
5.0	18.2
4.0	18.1
3.1	18.1
2.5	18.0
1.2	13.6

(3) Air discharge, frequency = 1035 kc.

Pressure mm. Hg	Load Current, ma.
14.0	17.2
11.5	17.6
9.3	18.4
5.8	19.8
5.0	19.8
3.9	20.0
2.6	20.0
2.0	20.2
1.5	14.0

current were observed in air and argon discharges at frequencies same as those applied for variation of the distance between the terminals. Results obtained are shown in table XIII, and the characteristic curves are plotted on graphs XII and XIII. The curves show that the current increased as the pressure was decreased, the rate of increase of the current being greater at lower pressures. When the pressure was decreased down to a certain critical value, the current dropped off down to its "cold" value shown by a broken line, at which time the discharge was discontinued.

The above variation also seemed to be independent of frequency. Graph XII shows that argon discharges drew less current at any given pressure as compared to air discharges, which is in agreement with results described before. Values of the "cold current" were the same as those indicated on graphs IX, X, and XI for the same frequencies applied, the net value of the current drawn by the discharge being practically independent of frequency.

5. Light Intensity Variation

The instantaneous variation of light intensity was studied under varying conditions of pressure, terminal voltage, drive, distance between the terminals, frequency, load matching, and physical size and shape of the

electrodeless tubes and terminals. Results obtained with mercury, air, and argon discharges are shown in the form of oscillogramms in figures 39-115.

a. With Pressure and Frequency. Definite variation of the wave shape of the light output at 60 cycles was observed as the pressure of the gas was changed. In the case of both air and argon discharges it was in the shape of a series of peaks in groups of one or more, each group corresponding to one-half cycle. At the lowest pressure, the number of peaks per group was a maximum and their height a minimum. Increase in pressure resulted in a decrease of the number of peaks per group and an increase of their height. When the pressure was high enough for the discharge to be almost at the point of extinction, the number of peaks per group went down to one.

While the terminal voltage variation of the 60-cycle discharges followed a sine wave variation at all times (fig. 39), the load current variation changed considerably as the pressure was changed. It was also in form of a series of grouped peaks whose number per group corresponded apparently to that observed in the light intensity variation at the same pressure. The oscillogramms shown in figures 40-53 represent load current variation and a corresponding variation of the light intensity of argon discharge as the pressure was increased

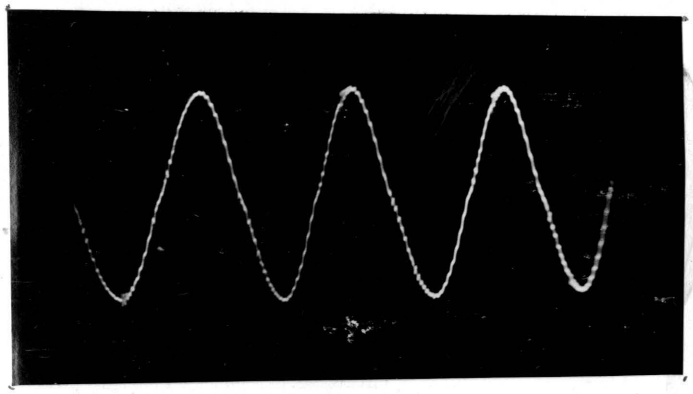

Fig. 39. 60-cycle terminal voltage variation.

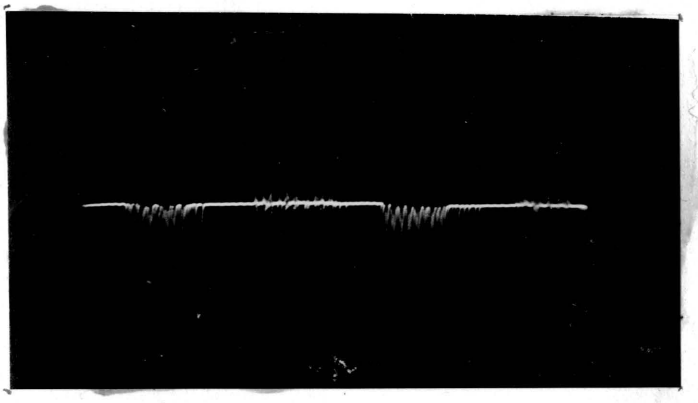

Fig. 40. Load current variation of argon discharge (60 cps) at .04 mm. Hg. V. A. 100 *)

Fig. 41. Light intensity variation of argon discharge (60 cps) at .04 mm. Hg. V. A. 100

*) Vertical amplification of the oscilloscope.

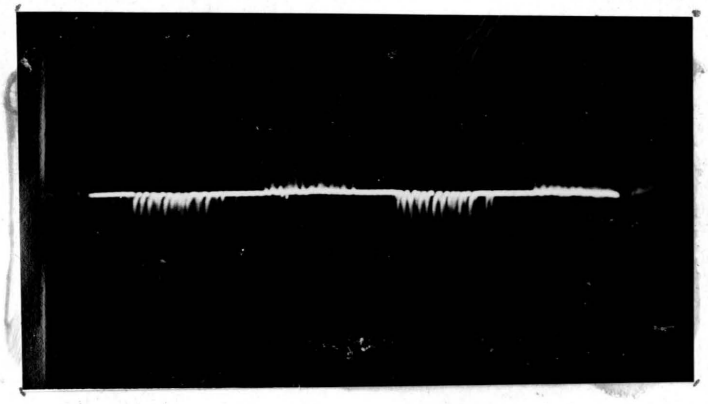

Fig. 42. Load current variation of argon discharge (60 cps) at 1.05 mm. Hg. V. A. 60

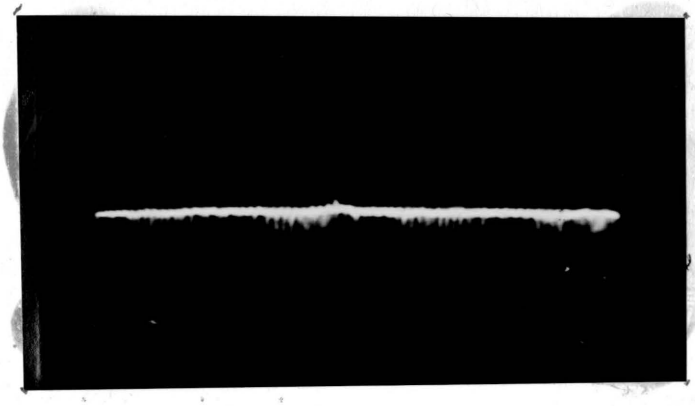

Fig. 43. Light intensity variation of argon discharge (60 cps) at 1.05 mm. Hg. V. A. 100

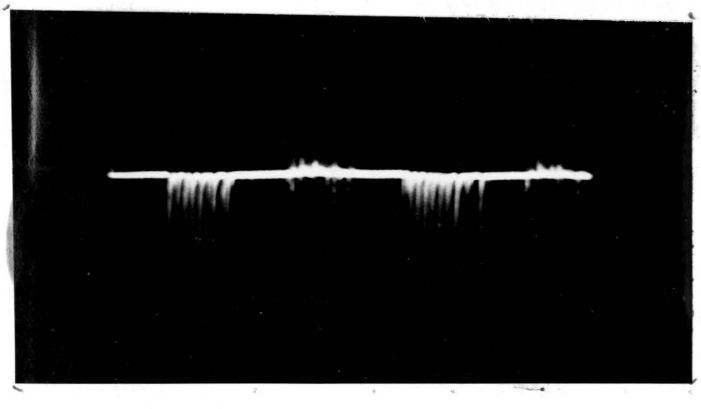

Fig. 44. Load current variation of argon discharge (60 cps) at 4.95 mm. Hg. V. A. 50

Fig. 45. Light intensity variation of argon discharge (60 cps) at 4.95 mm. Hg. V. A. 100

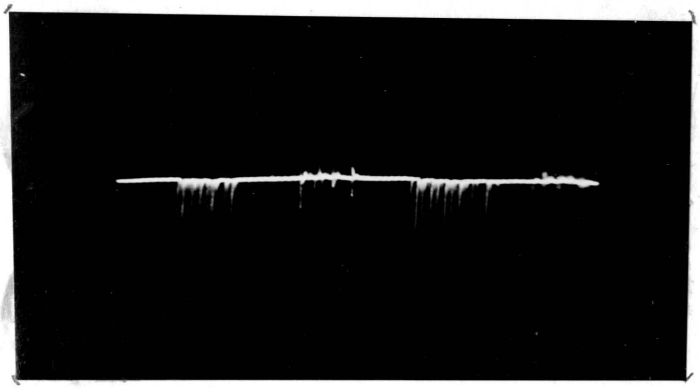

Fig. 46. Load current variation of argon discharge (60 cps) at 5.7 mm. Hg. V. A. 44

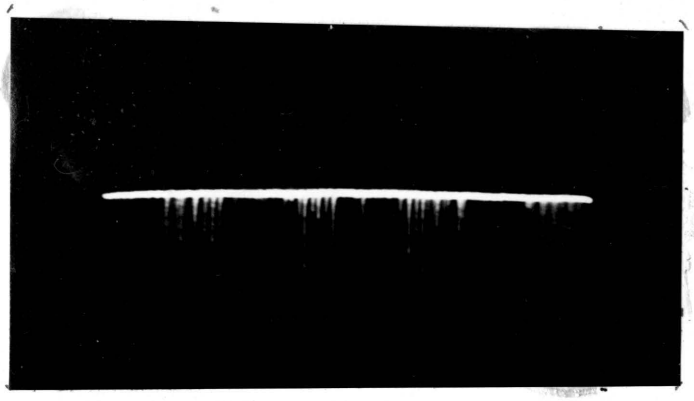

Fig. 47. Light intensity variation of argon discharge (60 cps) at 5.7 mm. Hg. V. A. 80

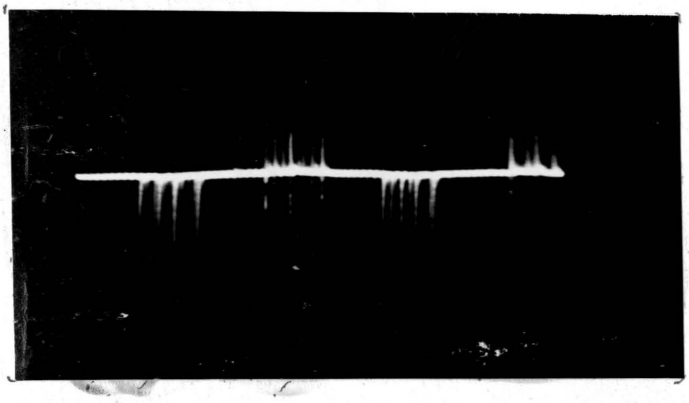

Fig. 48. Load current variation of argon discharge (60 cps) at 7.5 mm. Hg. V. A. 30

Fig. 49. Light intensity variation of argon discharge (60 cps) at 7.5 mm. Hg. V. A. 100

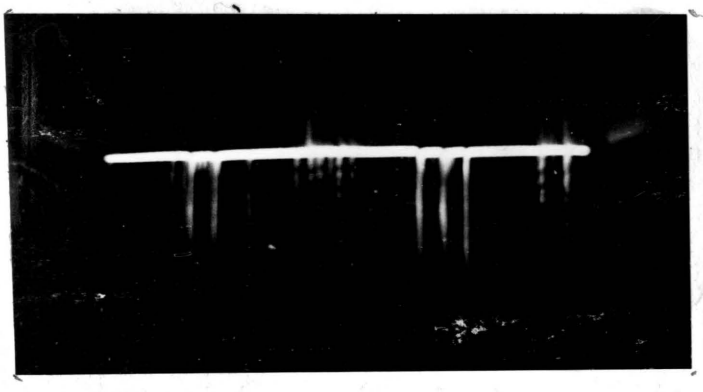

Fig. 50. Load current variation of argon discharge (60 cps) at 10 mm. Hg. V. A. 18

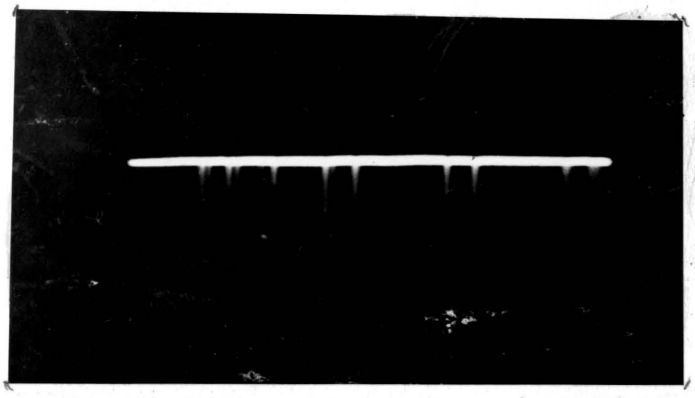

Fig. 51. Light intensity variation of argon discharge (60 cps) at 10 mm. Hg. V. A. 30

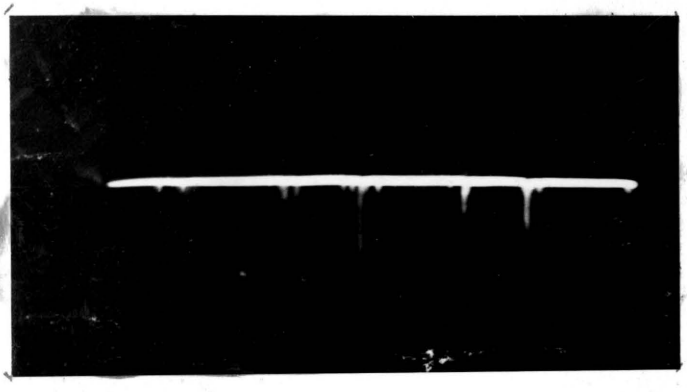

Fig. 52. Load current variation of argon discharge (60 cps) at 30 mm. Hg. V. A. 12

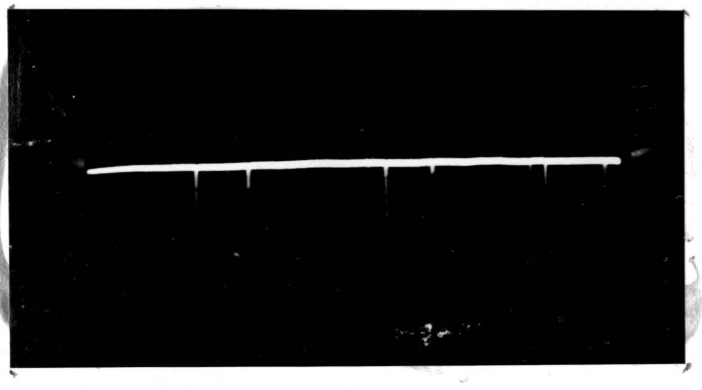

Fig. 53. Light intensity variation of argon discharge (60 cps) at 30 mm. Hg. V. A. 20

from .04 to 30 mm. Hg at a constant terminal voltage of 3520 volts. Distance between the terminals was kept at 5 cm. A somewhat uneven shape of voltage variation shown in fig. 39 was due to the discharges produced at that frequency.

To compare the heights of peaks at various pressures, each oscillogram of the light intensity variation is provided with a number corresponding to the vertical amplifier setting of the oscilloscope at the time the picture was taken, a larger number indicating that a correspondingly larger amplification was needed to show peaks of smaller height.

Variation of the light intensity of the 400-cycle discharge was almost identical with that at 60 cycles at the highest pressures used. Figures 65 and 67 show such variation at 6.5 and 14.0 mm. Hg, respectively. As the pressure was decreased, the peaks became higher as before, but their number per group was not as well defined as in the case of the 60-cycle discharge. At some pressures the wave shape was very unstable, at others it closely resembled 60-cycle variation.

Instantaneous load current variation also changed with pressure, the wave shape changing considerably at lower pressures, as seen in figures 55, 57, and 59. At pressures of approximately one mm. Hg and higher the

current wave shape remained relatively constant (figures 62 and 66), which is not in agreement with results obtained with the 60-cycle discharge, where a constant variation of the current wave shape with pressure was observed.

Figures 55-67 show results obtained with the 400-cycle discharge. The pictures at that frequency were taken for argon discharge. Terminals were kept apart at a constant distance of 6 cm. The magnitude of the terminal voltage was 1745 volts. Very similar results were obtained with air discharges, when other variables remained the same.

While it is entirely reasonable to assume that the 400-cycle discharge should have a specific light intensity and load current variation different from that obtained at 60 cycles, it is possible that major differences were caused by the distorted terminal voltage variation (fig. 54) produced by the available source of that frequency.

A characteristic common to discharges at both frequencies was the increase of the height of the peaks produced in the light intensity variation as the pressure of the gas was increased.

The variation of light intensity of electrodeless discharges through mercury, air, and argon at radio frequencies was entirely different from that at 60 or

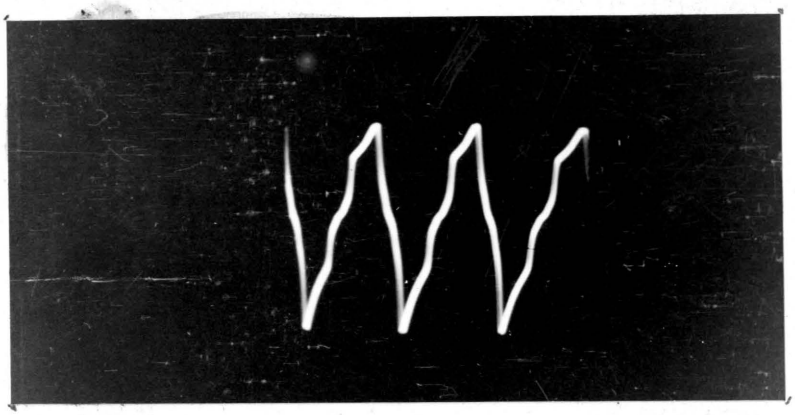

Fig. 54. 400-cycle terminal voltage variation.

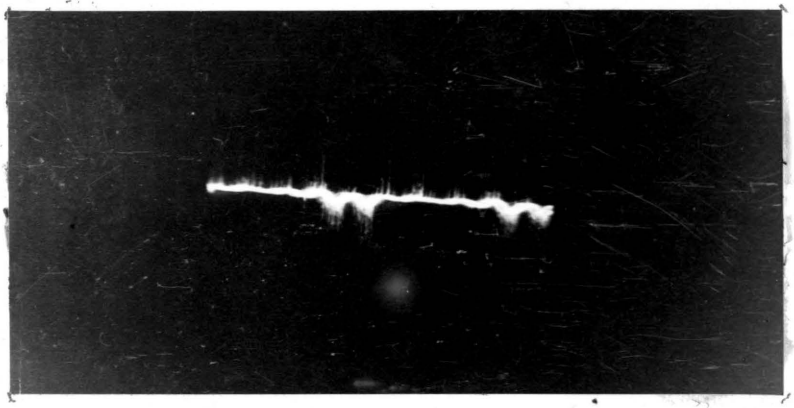

Fig. 55. Load current variation of argon discharge (400 cps) at .1 mm. Hg. V. A. 90

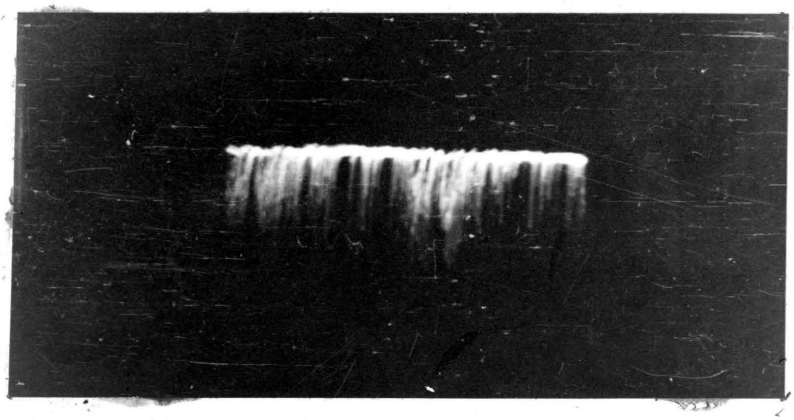

Fig. 56. Light intensity variation of argon discharge (400 cps) at .1 mm. Hg. V. A. 100

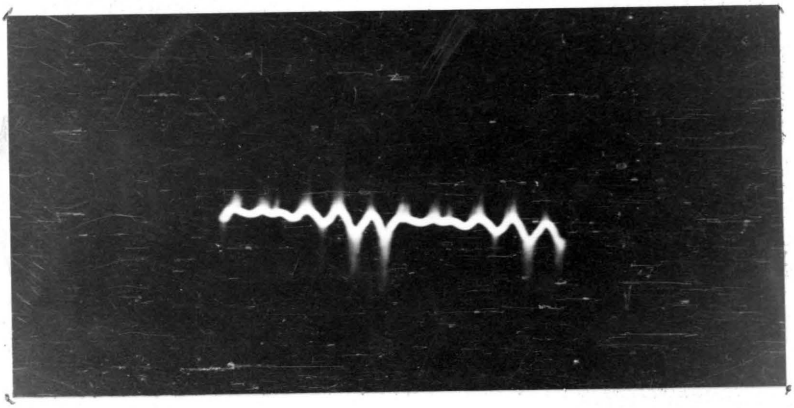

Fig. 57. Load current variation of argon discharge (400 cps) at .2 mm. Hg. V. A. 100

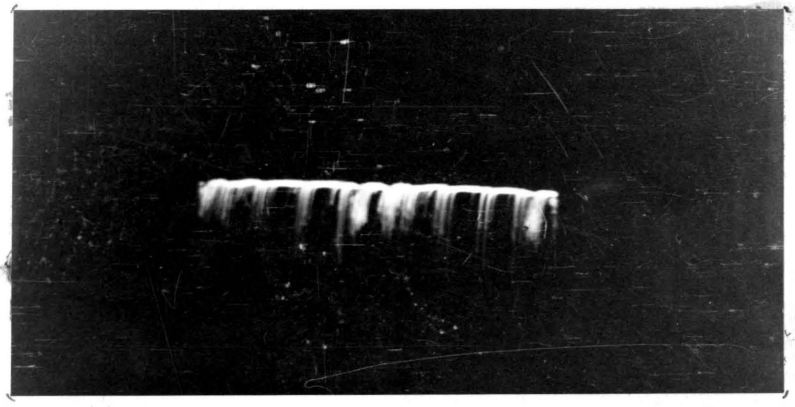

Fig. 58. Light intensity variation of argon discharge (400 cps) at .2 mm. Hg. V. A. 100

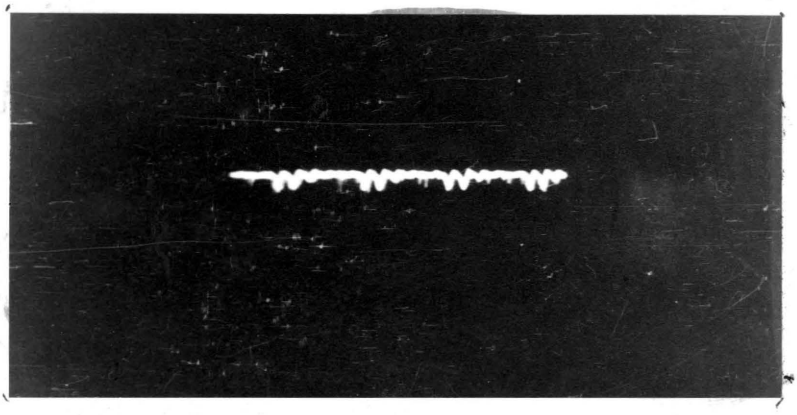

Fig. 59. Load current variation of argon discharge (400 cps) at .5 mm. Hg. V. A. 40

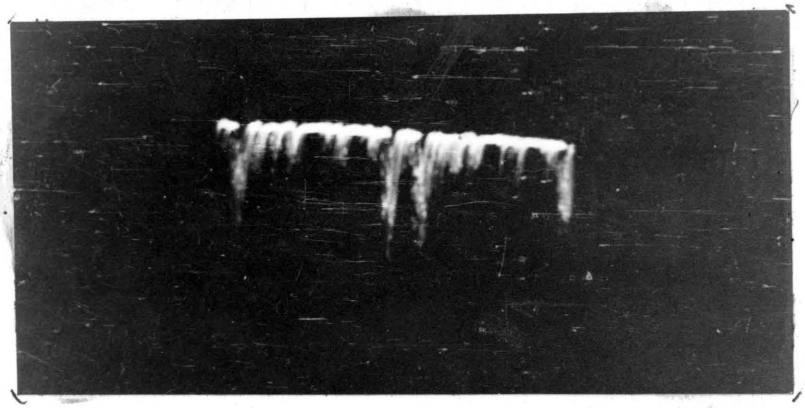

Fig. 60. Light intensity variation of argon discharge (400 cps) at .5 mm. Hg. V. A. 76

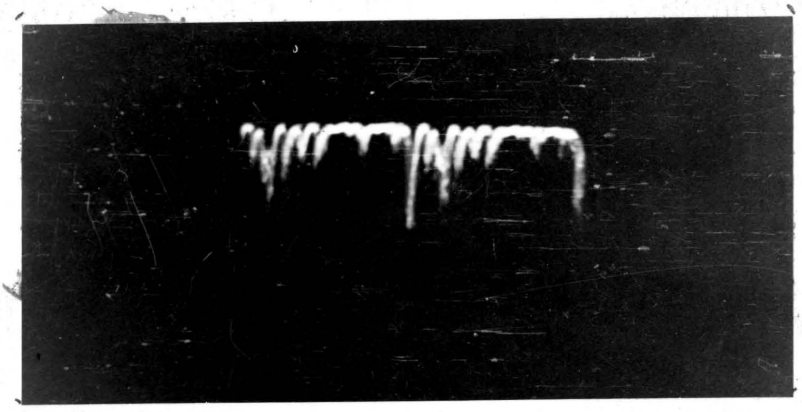

Fig. 61. Light intensity variation of argon discharge (400 cps) at 1.0 mm. Hg. V. A. 63

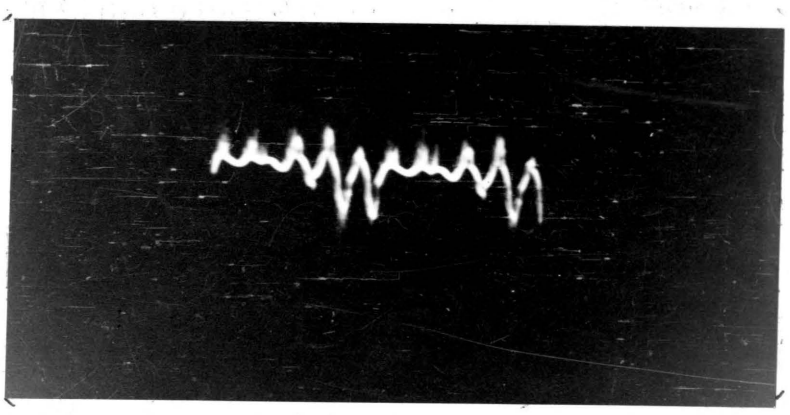

Fig. 62. Load current variation of argon discharge (400 cps) at 2 mm. Hg. V. A. 40

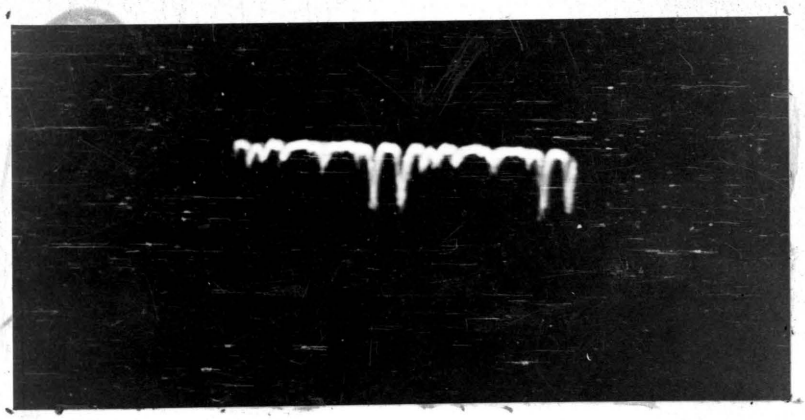

Fig. 63. Light intensity variation of argon discharge (400 cps) at 2 mm. Hg. V. A. 63

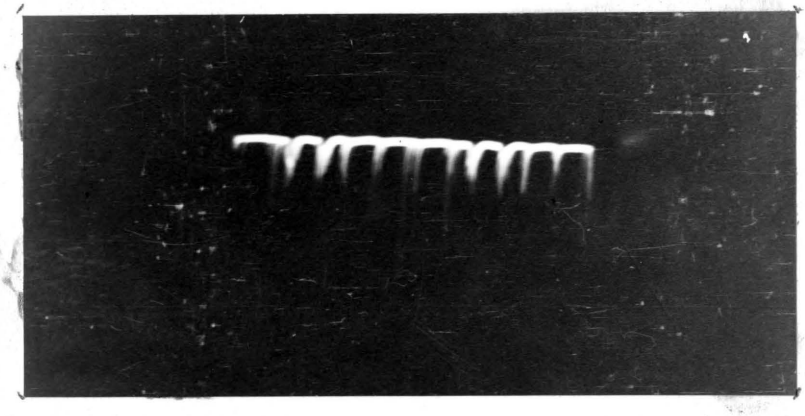

Fig. 64. Light intensity variation of argon discharge (400 cps) at 3.2 mm. Hg. V. A. 45

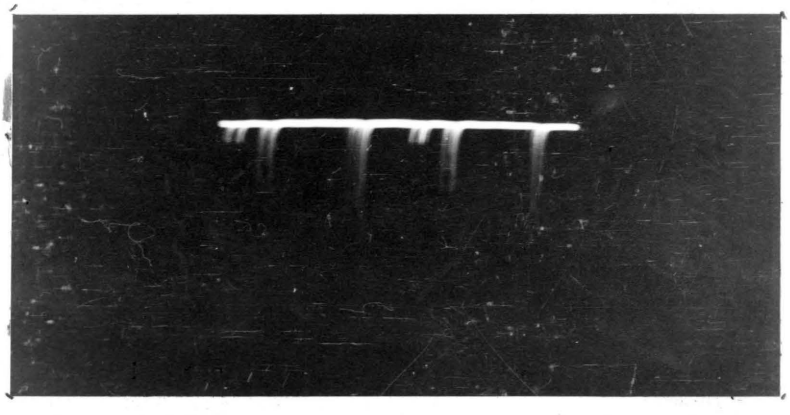

Fig. 65. Light intensity variation of argon discharge (400 cps) at 6.5 mm. Hg. V. A. 20

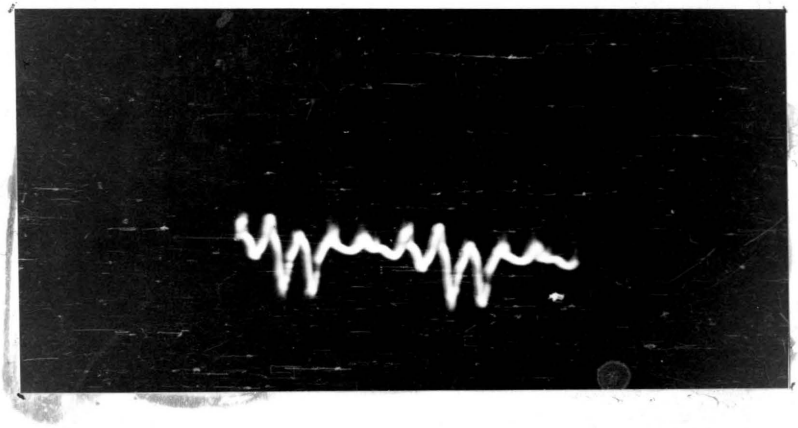

Fig. 66. Load current variation of argon discharge (400 cps) at 14.0 mm. Hg. V. A. 35

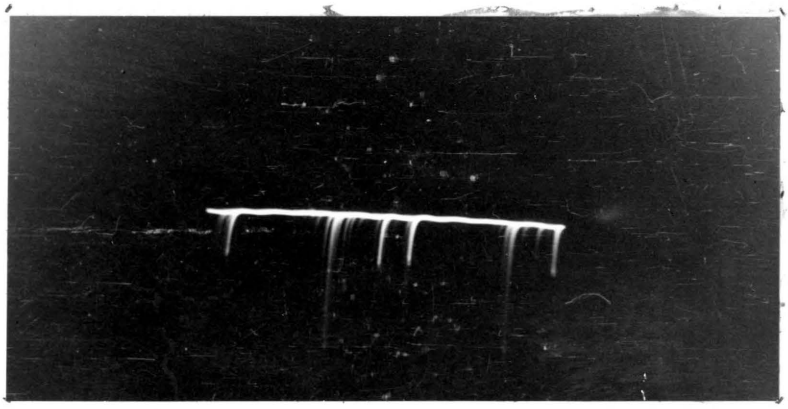

Fig. 67. Light intensity variation of argon discharge (400 cps) at 14.0 mm. Hg. V. A. 12

400 cycles. No peaks were observed under any circumstances, provided that the oscillator was tuned properly. The only variation observed was a random fluctuation resembling disorderly electron oscillations (noise). The level of the observed "noise" with respect to the total intensity could not be determined, because the position of the zero reference line on the oscilloscope screen was shifting. By the amount of the vertical gain used it is believed that the "noise" level was rather small even at high intensities.

The oscillogram shown in fig. 70 is that of the light intensity variation of the mercury discharge when a 634 kc. voltage and current (figures 68 and 69) were produced by the source of r-f.

Results obtained with air and argon discharges at radio frequencies were very similar to those obtained with mercury discharges. Figures 71-76 show oscillograms of terminal voltage, load current, and light intensity variations in air discharges at two different frequencies. As before, applied sine wave voltage produced no regular variation of light intensity, as seen in figures 73 and 76. The above set of pictures was taken at a pressure of 600 microns and a distance of 5 cm. between the terminals. Similar variation was produced at all frequencies within range of the source of r-f, regardless of the pressure.

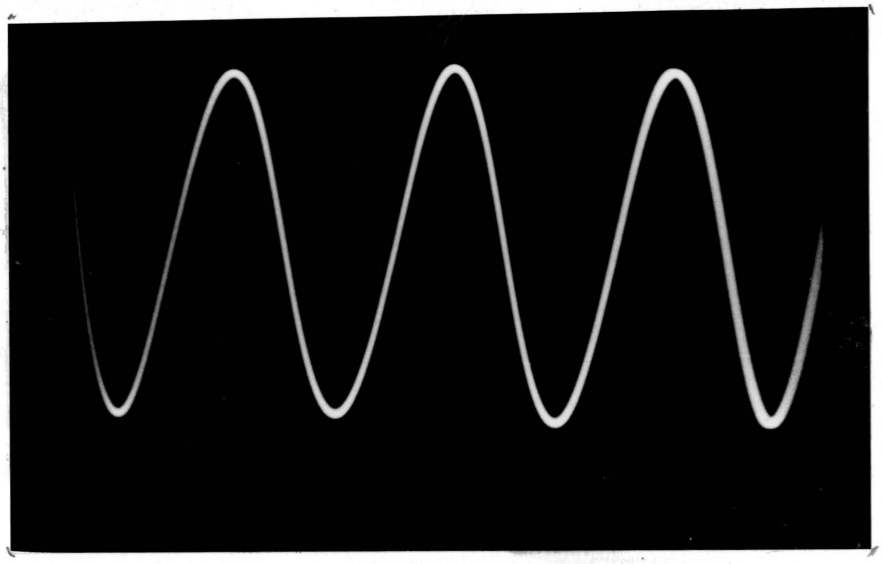

Fig. 68. Terminal voltage variation at 634 kc.

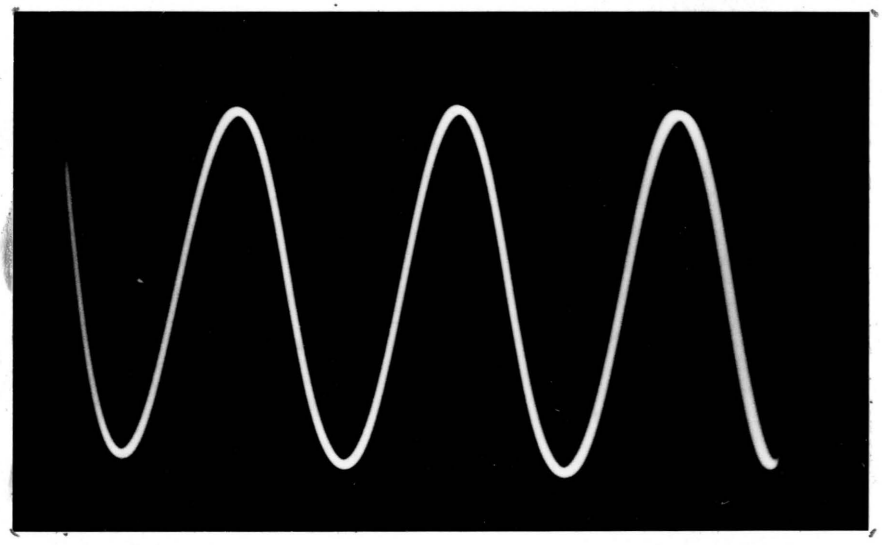

Fig. 69. Load current variation at 634 kc.

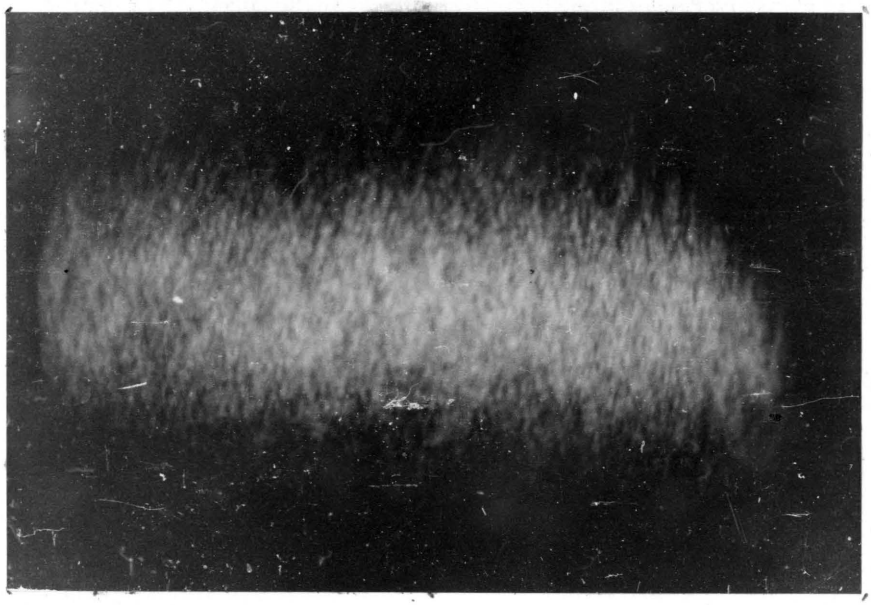

Fig. 70. Light intensity variation of the mercury discharge at 634 kc.

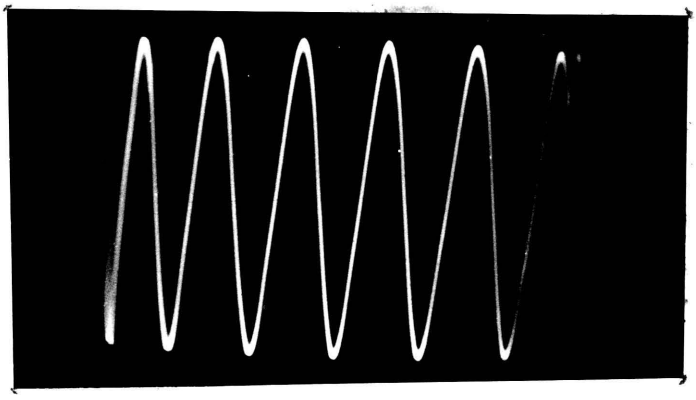

Fig. 71. Terminal voltage variation at 213.4 kc.

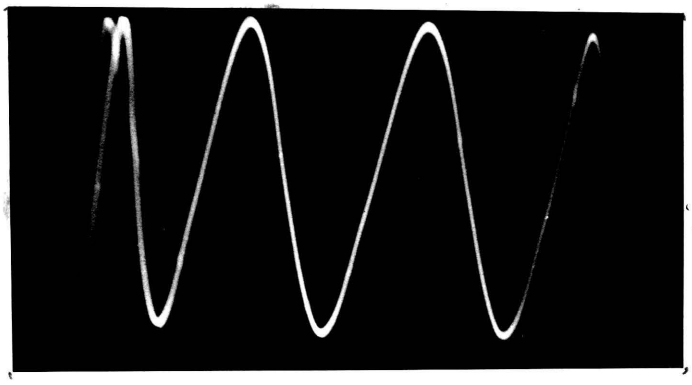

Fig. 72. Load current variation at 213.4 kc.

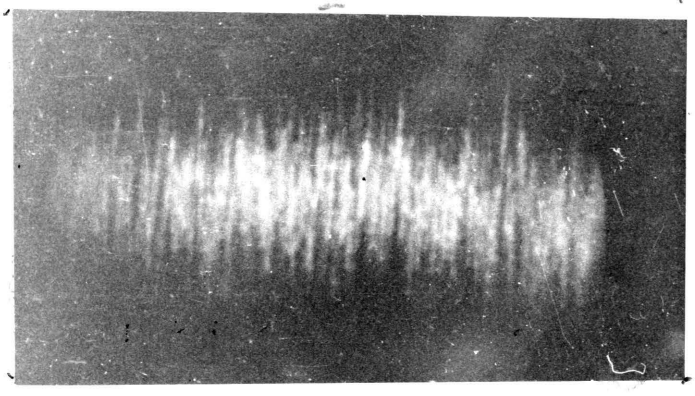

Fig. 73. Light intensity variation of air discharge at 213.4 kc.

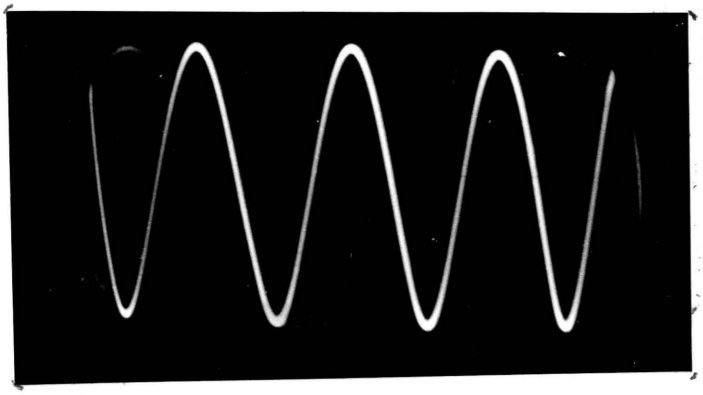

Fig. 74. Terminal voltage variation at 917 kc.

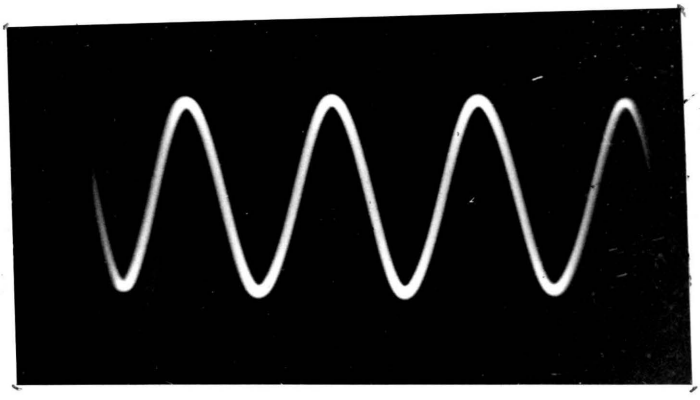

Fig. 75. Load current variation at 917 kc.

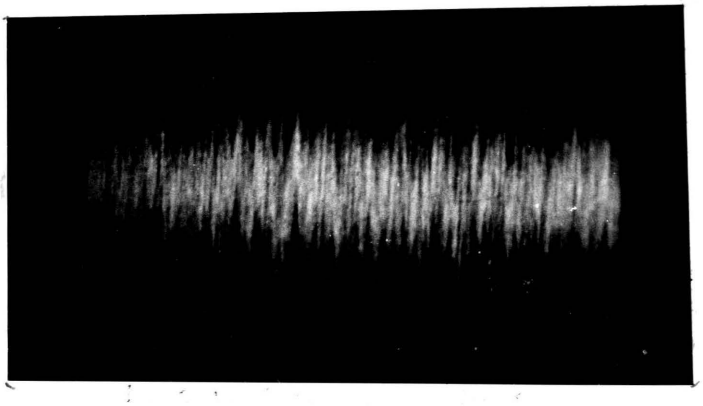

Fig. 76. Light intensity variation of air discharge at 917 kc.

Effects of the parasitic oscillation caused by improper tuning of the 807 plate tank circuit on the light intensity variation studied was rather interesting. When the "modulated" voltage shown in figures 77 and 78 was applied to the terminals of the mercury discharge tube, disorderly wave shape disappeared completely, the new variation produced resembling closely that of a rectified sine wave, as seen in fig. 80. Rectification was produced by the phototube which is capable of conducting current in only one direction.

The condition of "modulated" voltage studied in connection with air and argon discharges produced results similar to those obtained with mercury vapor, as seen in figures 90-94.

The frequency of the light intensity variation produced under conditions described above was equal to that of the parasitic oscillation that caused the modulation envelope.

b. With Applied Terminal Voltage. At a given constant pressure, variation of terminal voltage at 60 cps produced effects very similar to those observed when the pressure was changed. When the terminal voltage was just great enough to start firing of the tube, single peaks of a considerable height appeared, their number per group increasing and their height decreasing as the terminal

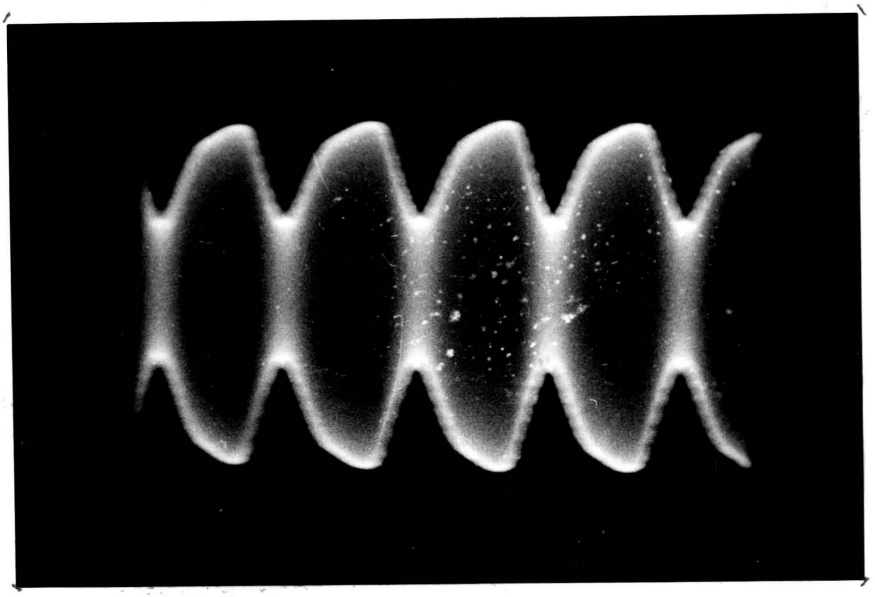

Fig. 77. Terminal voltage modulated by a low-frequency parasitic oscillation, applied to the terminals of the mercury discharge tube.

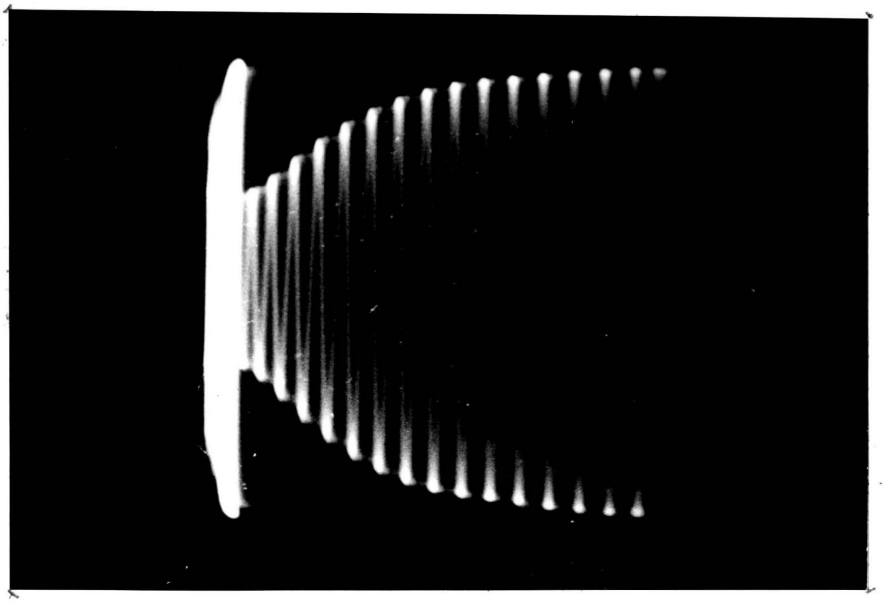

Fig. 78. One cycle of the voltage variation shown in fig. 77.

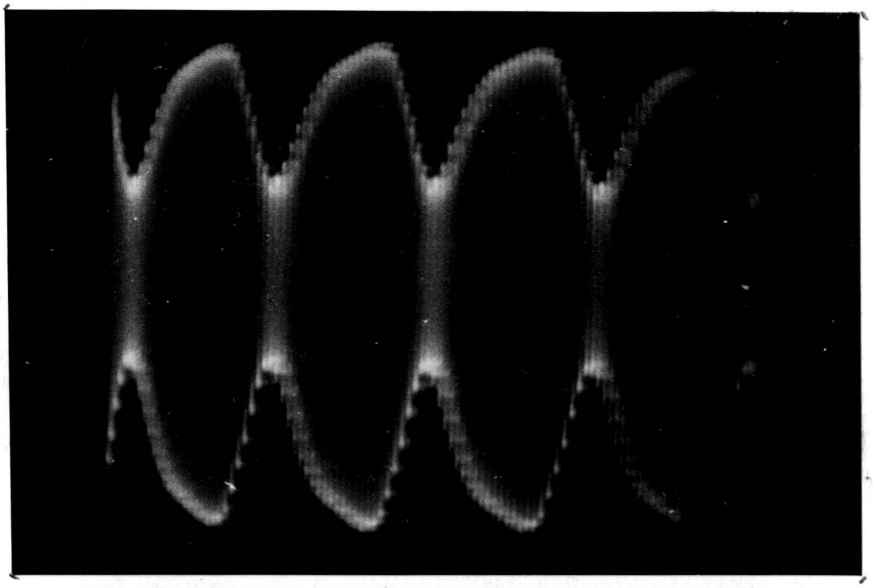

Fig. 79. Load current variation of the mercury discharge produced under conditions of figures 77 and 78.

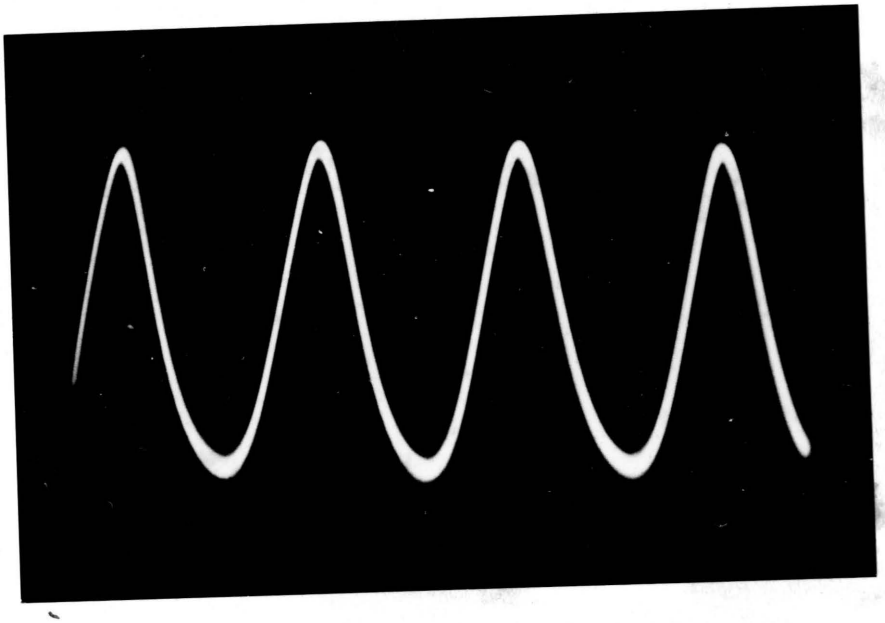

Fig. 80. Typical variation of the light intensity of the mercury discharge excited by "modulated" voltage.

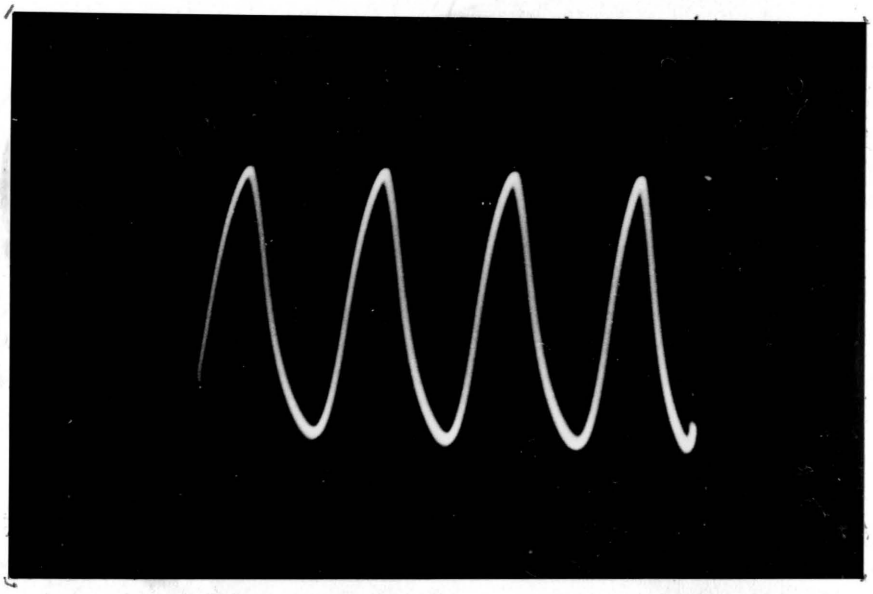

Fig. 81. Light intensity variation of the mercury discharge with drive: lowest drive.

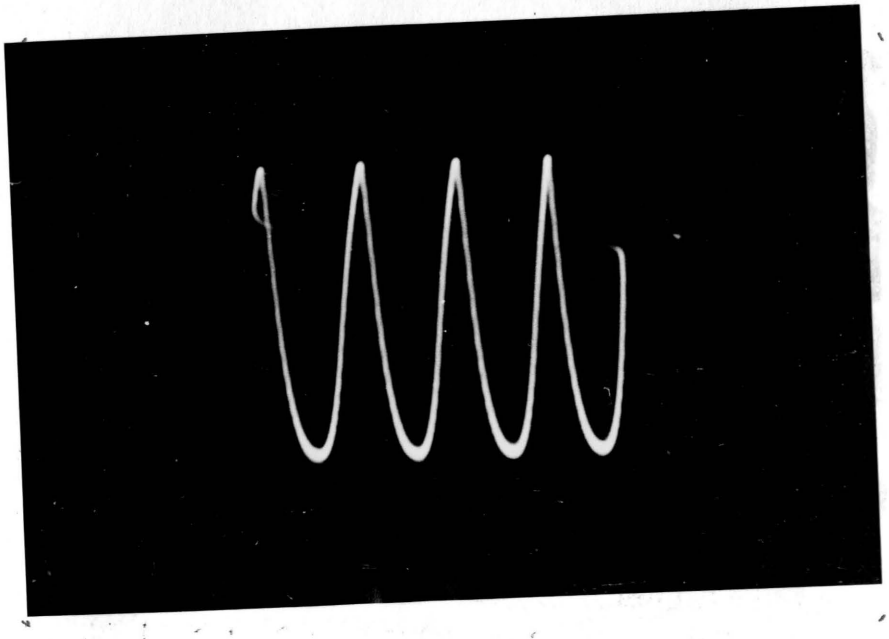

Fig. 82. Light intensity variation of the mercury discharge with drive: low drive.

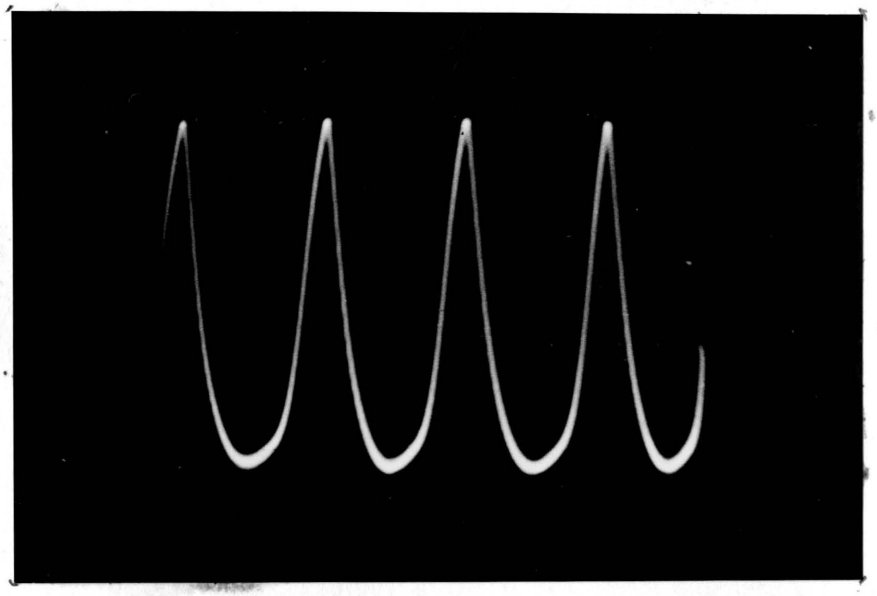

Fig. 83. Light intensity variation of the mercury discharge with drive: moderate drive.

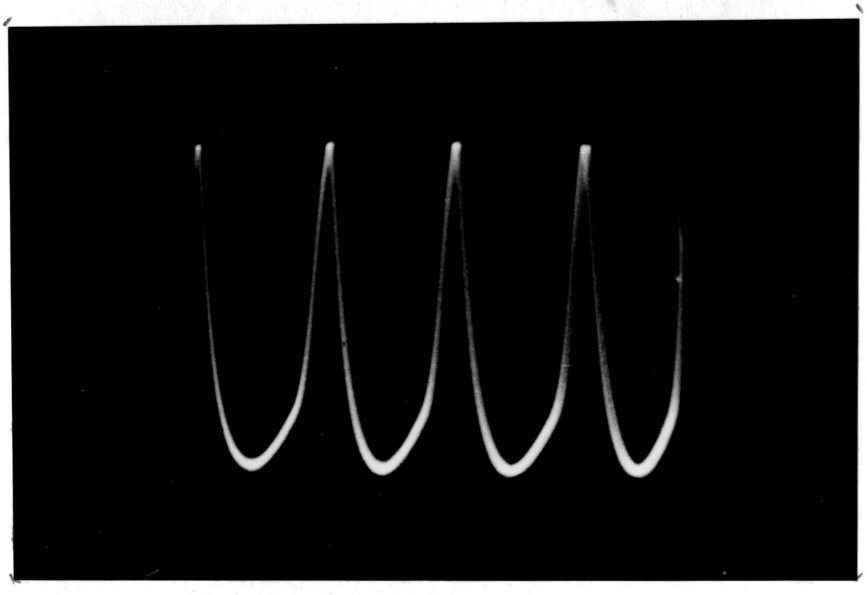

Fig. 84. Light intensity variation of the mercury discharge with drive: low overdrive.

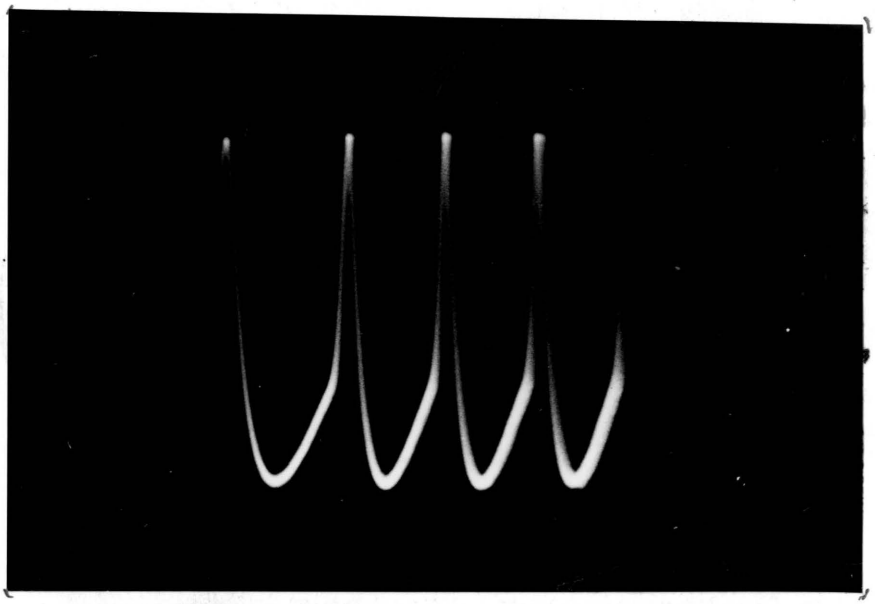

Fig. 85. Light intensity variation of the mercury discharge with drive: moderate overdrive.

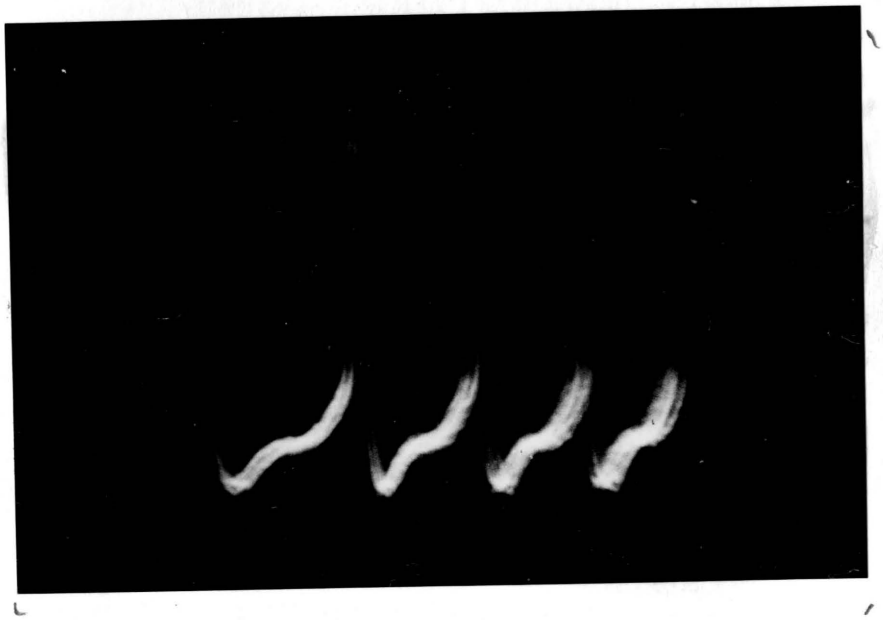

Fig. 86. Light intensity variation of the mercury discharge with drive: high overdrive.

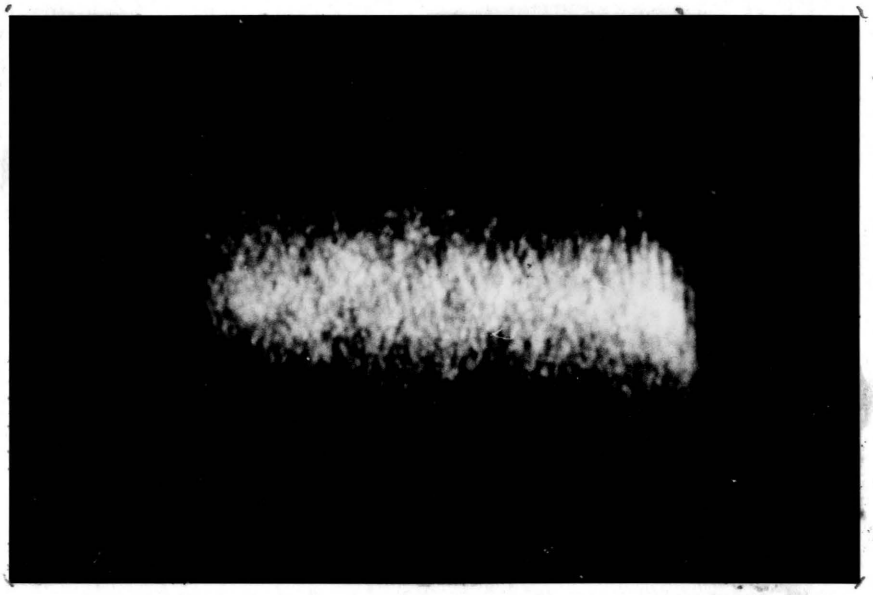

Fig. 87. Light intensity variation of the mercury discharge with drive: maximum drive.

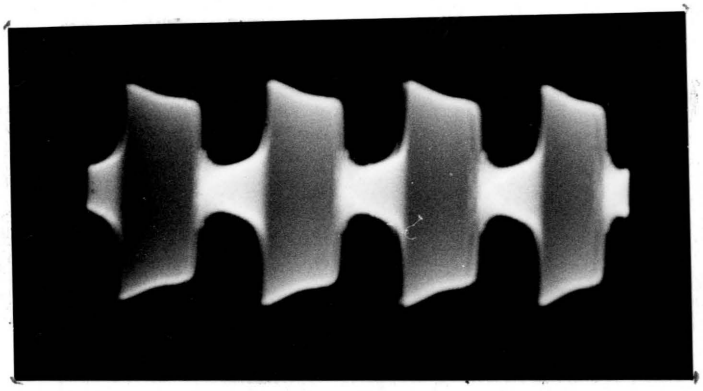

Fig. 88. "Modulated" terminal voltage variation.

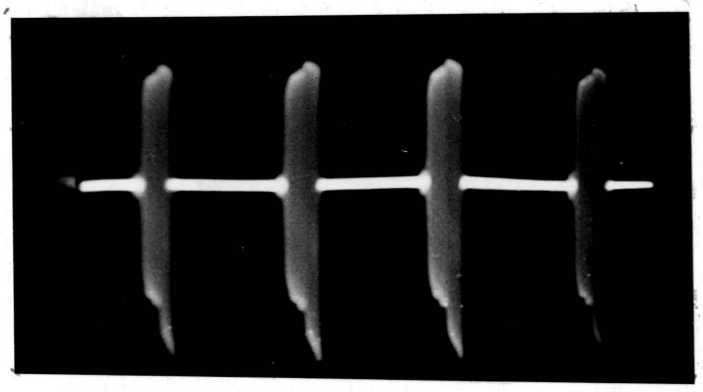

Fig. 89. Load current variation of the air discharge produced under conditions of fig. 88.

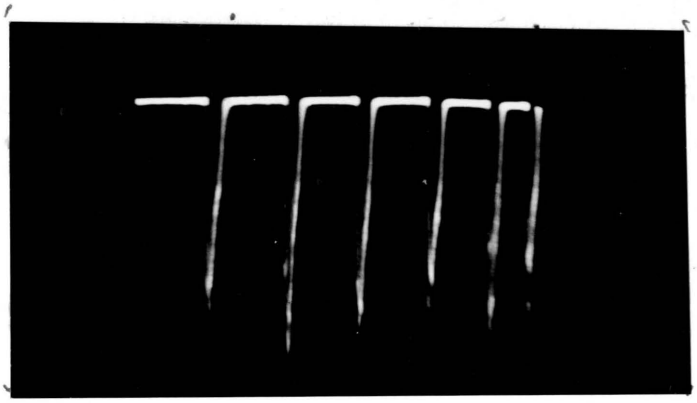

Fig. 90. Light intensity variation of the air discharge under lowest drive conditions.

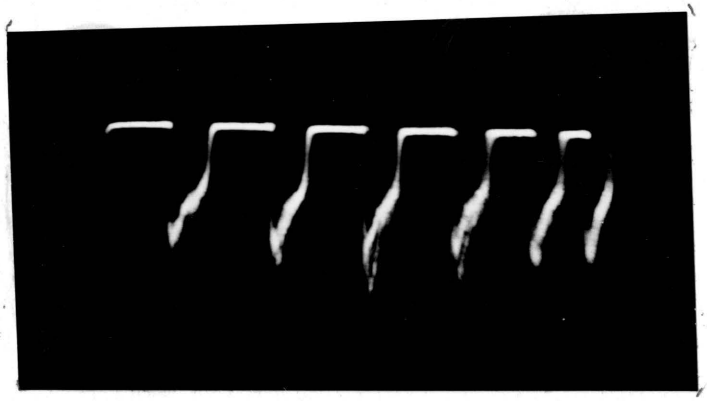

Fig. 91. Light intensity variation of the air discharge under low drive conditions.

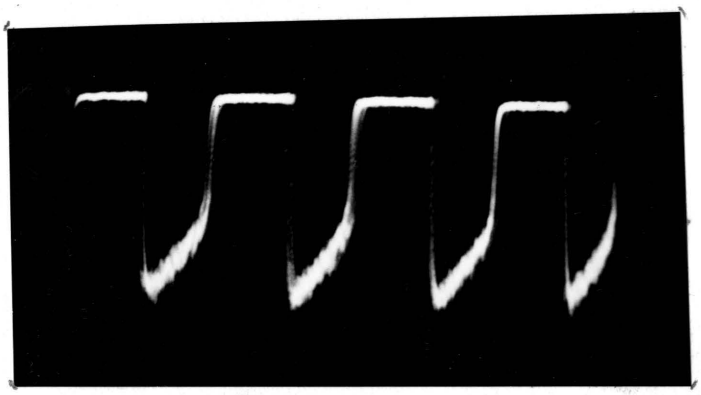

Fig. 92. Light intensity variation of the air discharge under moderate drive conditions.

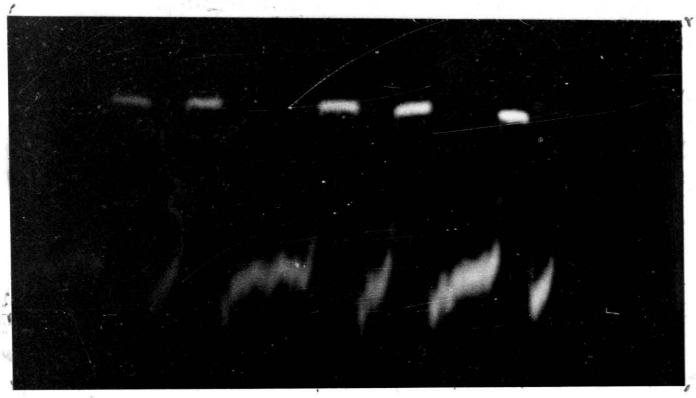

Fig. 93. Light intensity variation of the air discharge under conditions of overdrive.

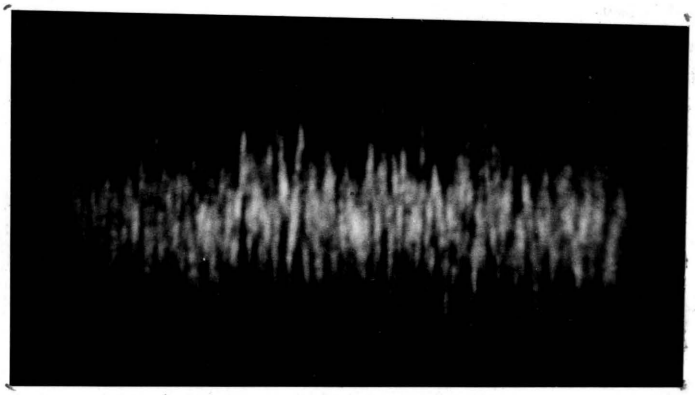

Fig. 94. Light intensity variation of the air discharge under conditions of maximum drive.

voltage was increased.

Instantaneous load current variation was also similar in appearance to that shown in a series of pictures taken in connection with pressure variation in the 60-cycle discharge.

Thus it is seen that decreasing the pressure or increasing the terminal voltage of the 60-cycle discharge studied produced similar variations of the light intensity.

c. With Drive. Variation of the light intensity with drive was studied at radio frequencies.

When sinusoidal voltage was applied to the terminals of the discharge tubes, an increase in drive produced an increase of the amplitude of the light intensity variation observed on the screen of the oscilloscope.

Under conditions of "modulated" voltage, increasing the drive produced results shown in figures 81-87 and 90-94.

In mercury discharge, for a condition of very low drive (fig. 81) the peaks of the waves were sharper and slightly assymmetrical. For moderate drive, the wave shapes produced were very nearly those of a rectified sine wave, as seen in figures 82 and 83. Overdriving the amplifier resulted in distortion and instability of the waves. Figures 84, 85, and 86 show that the amount of distortion produced was proportional to the degree of

overdrive. Maximum drive caused disappearance of the regular wave shape, the irregular variation produced instead resembling that of the familiar "electron noise", as seen in fig. 87.

In the case of air and argon discharges, "modulated" voltage (fig. 88) produced a light intensity variation in the form of thin negative peaks that became wider as the drive was increased, until the regular shape became rather unstable and finally disintegrated into "electron noise". It is seen that the above results parallel those obtained with mercury discharges. Figures 90-94 show light intensity variation in air discharges under different drive conditions.

d. Along the Luminous Column. No variation of the light intensity was observed along the luminous column of the 60-cycle discharge, except that the length of a given group of peaks changed slightly as the phototube was moved along the tube. Typical variation is shown in figures 95 and 96. It will be noticed that every other group is shorter at one point along the tube, while all groups seem to have approximately the same average length at another point.

At radio frequencies, when "modulated" voltage was applied, the light output at different points along the tube did not change except in amplitude, which was lower

Fig. 95. Light intensity variation of air discharge 3.4 cm. from the terminal.

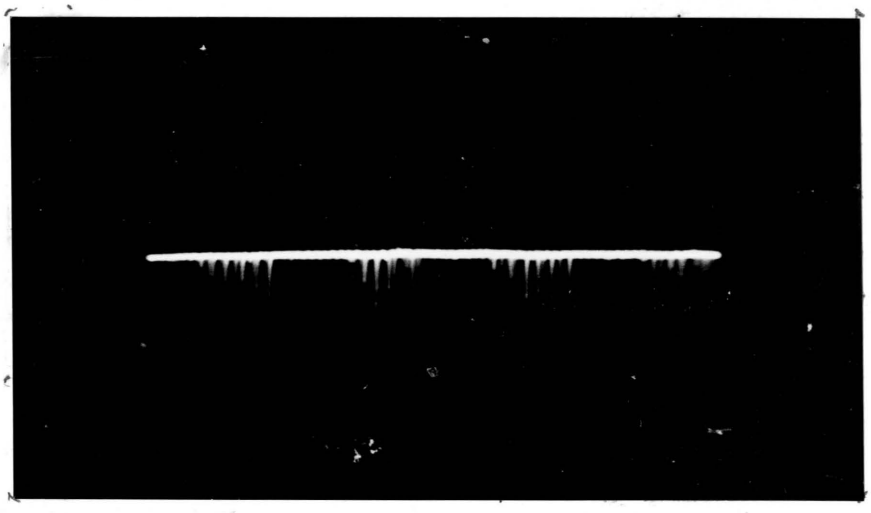

Fig. 96. Light intensity variation of air discharge 3.9 cm. from the terminal.

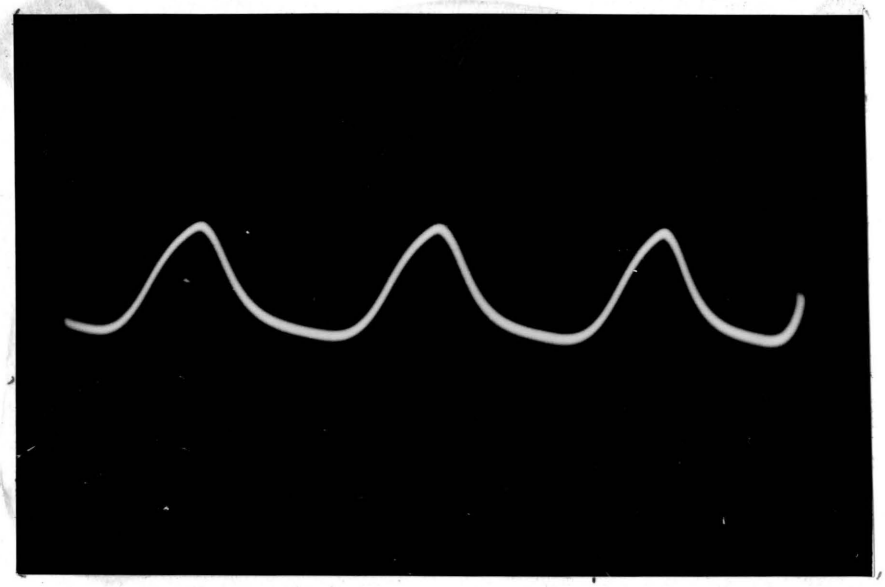

Fig. 97. Light intensity variation of the mercury discharge excited by "modulated" voltage: in the vicinity of the terminals.

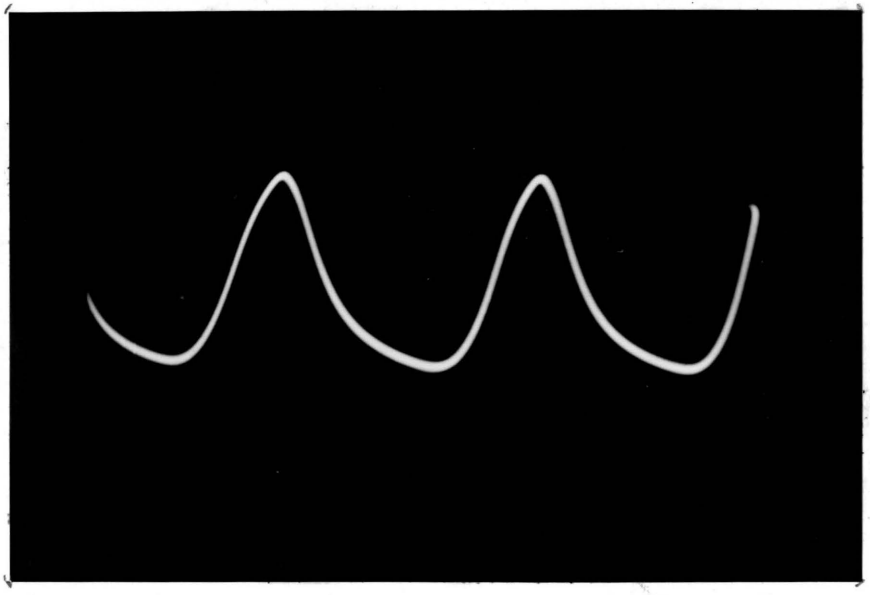

Fig. 98. Light intensity variation of the mercury discharge excited by "modulated" voltage: away from the terminals.

in the vicinity of the terminals (fig. 97), and higher at all other points (fig. 98).

e. With Changing Distance Between the Terminals. While changing the distance between the terminals in air and argon discharges at radio frequencies produced no visible change in the characteristic light output variation, a noticeable change was observed in same at 60 cycles.

At a given terminal voltage and pressure, the number of peaks per group decreased sharply and their height increased as the terminals were pulled further apart, until their number decreased to one per group near the point at which the terminals were too far apart to maintain the discharge. Figures 99-101 show oscillograms of the light intensity variation in argon for various distances between the terminals, other variables remaining the same.

f. With Changing Physical Size of the Terminals. Investigation of the effects of the physical size of the terminals upon the light intensity variation produced at 60 cps involved use of two types of terminals: wire-wound and solid. The former were made by winding a known number of turns of 34-gauge copper wire around the tube.

As the number of turns of wire per terminal was increased, the number of peaks per group decreased and

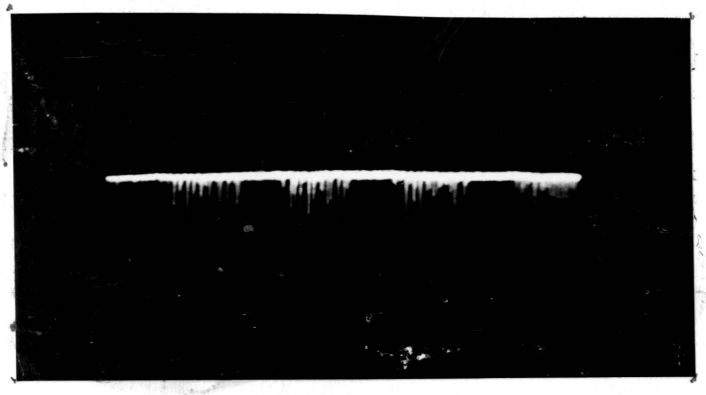

Fig. 99. Light intensity variation of the argon discharge for a distance of 1.9 cm. between the terminals. V. A. 80

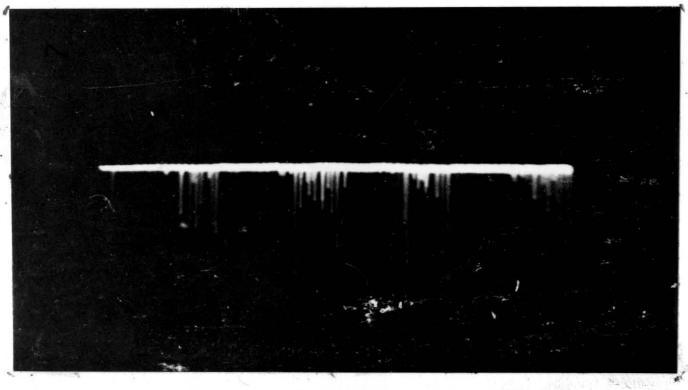

Fig. 100. Light intensity variation of the argon discharge for a distance of 6.45 cm. between the terminals. V. A. 80

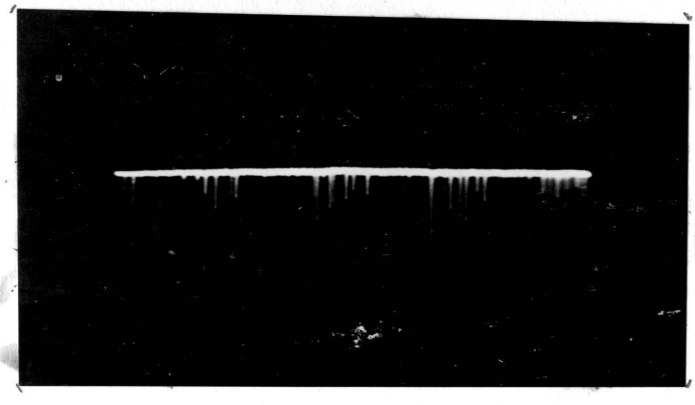

Fig. 101. Light intensity variation of the argon discharge for a distance of 12.9 cm. between the terminals. V. A. 36

remained constant when the number of turns exceeded about thirty per terminal at a pressure of 6 mm. Hg and a terminal voltage of 3730 volts in argon discharge. Oscillograms of the light intensity variation seen in figures 102 and 103 illustrate the effects produced when the number of turns per terminal was changed.

It has been found experimentally that solid terminals made of thin aluminum foil produced the same variation as that already described for wound terminals, if the turns were wound uniformly and close together, and if the overall length per terminal remained the same in both types.

g. Under Different Load Matching Conditions. This part of study was also performed at 60 cycles by using various load matching condensers in the primary circuit of the transformer. The amount of power delivered to the load depended upon the magnitude of their capacitance.

At a pressure of 10 mm. Hg and a terminal voltage of 3730 in air discharges, capacitances of less than .75 mf. or greater than 20 mf. produced a mismatch great enough for the discharge to discontinue. Generally, insertion of a condenser in the primary resulted in a tendency of the peaks in a given group to squeeze closer together, as shown in figures 104 and 105.

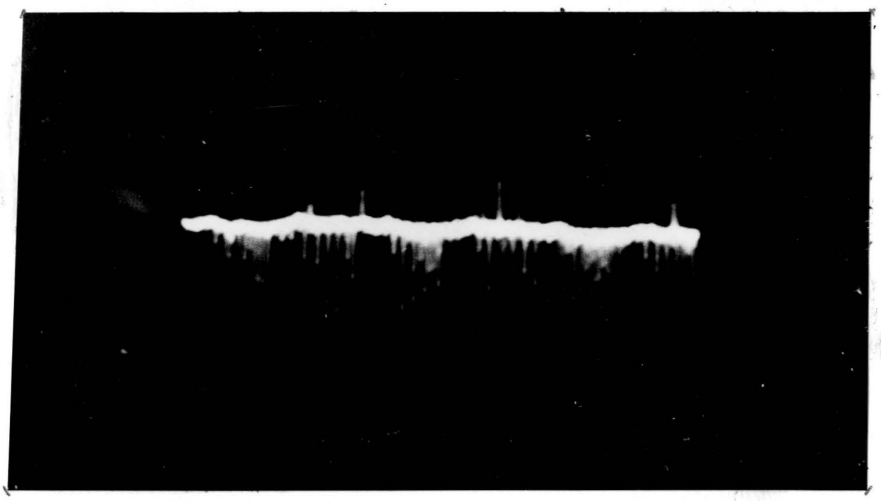

Fig. 102. Light intensity variation of argon discharge produced by 5 turns per terminal.

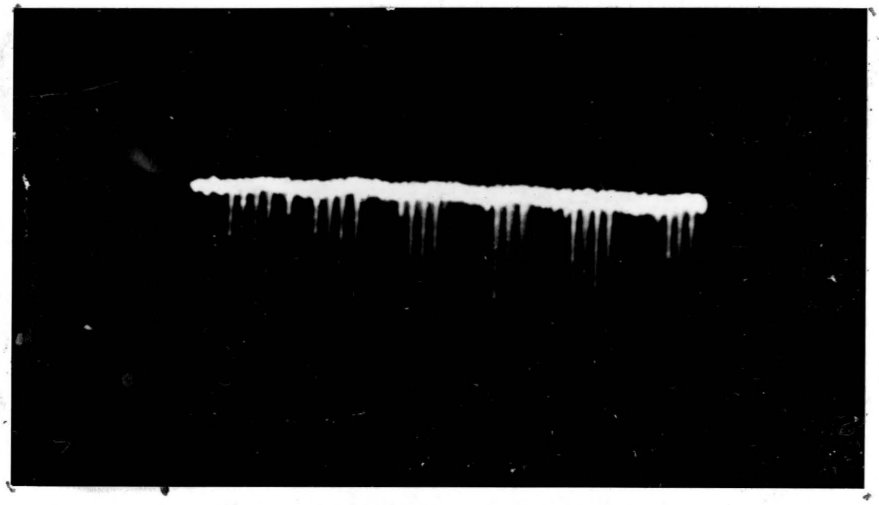

Fig. 103. Light intensity variation of argon discharge produced by 35 turns per terminal.

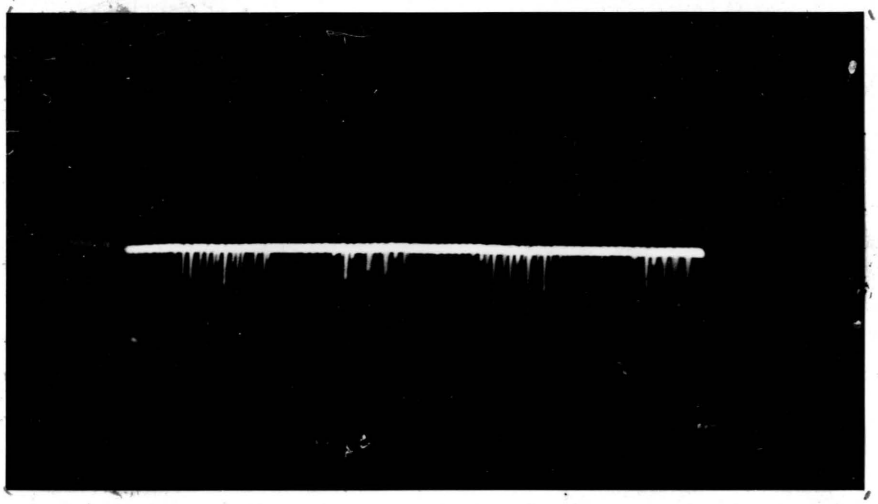

Fig. 104. Light intensity variation of air discharge produced with no provisions made for proper load matching.

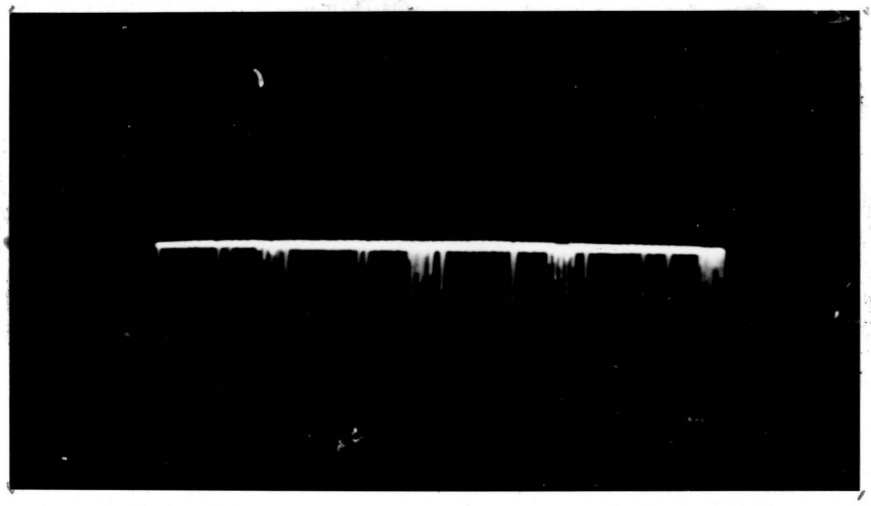

Fig. 105. Light intensity variation of air discharge produced with a 1-mf. condenser in the primary of the transformer.

h. With Changing Diameter of the Tubes. Tubes shown in fig. 21 were employed for this part of the study.

Changing the diameter of the tubes seemed to produce no visible change in either the amplitude or the shape of the instantaneous light intensity variation at all frequencies tested.

Oscillograms shown in figures 106-115 illustrate the above at 60 cps and 434 kc.

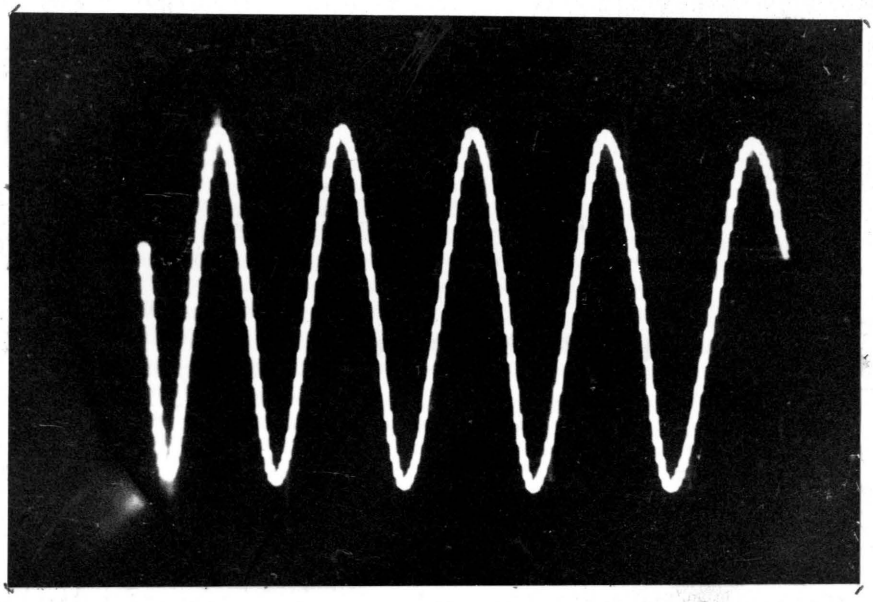

Fig. 106. Terminal voltage variation at 60 cps, applied to the tubes shown in fig. 21.

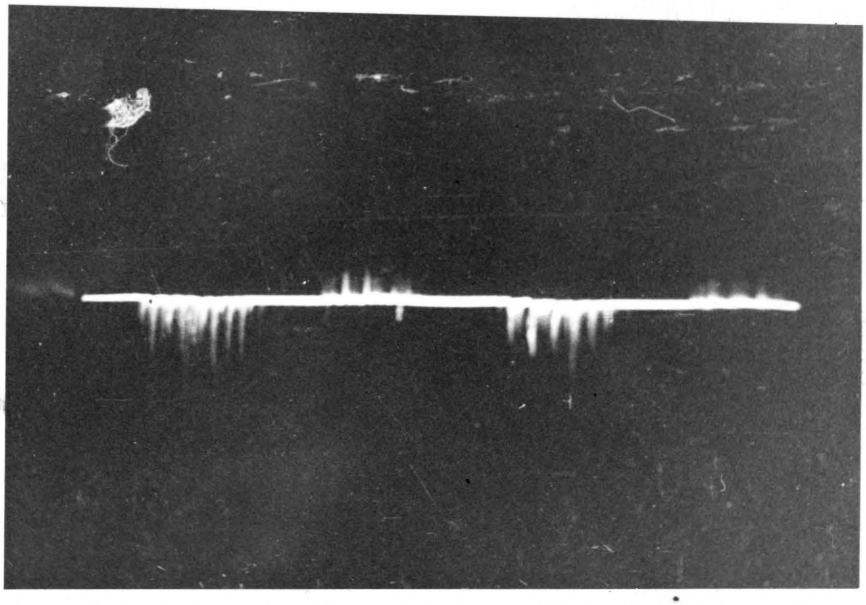

Fig. 107. Load current variation of argon discharge produced by voltage variation shown in fig. 106.

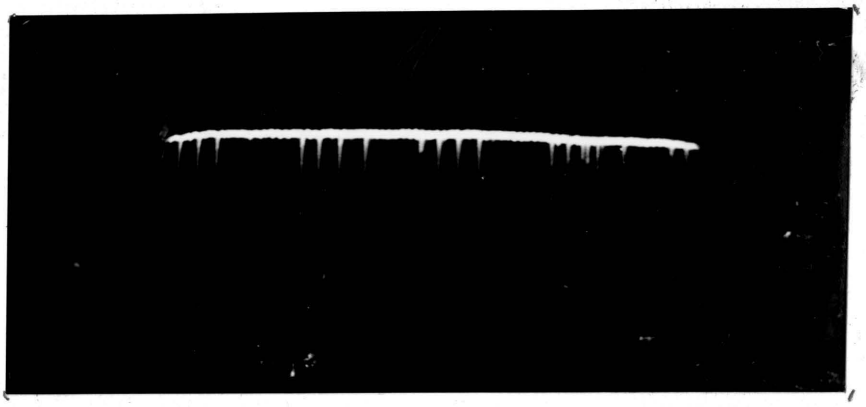

Fig. 108. Light intensity variation of argon discharge in the large tube (60 cps).

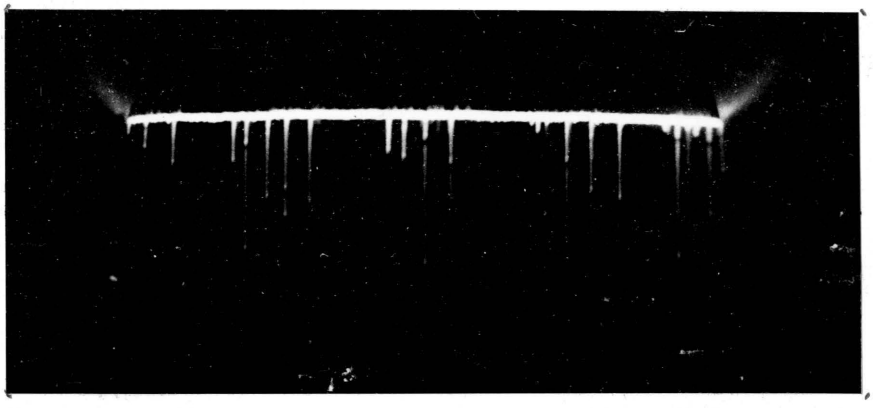

Fig. 109. Light intensity variation of argon discharge in the medium tube (60 cps).

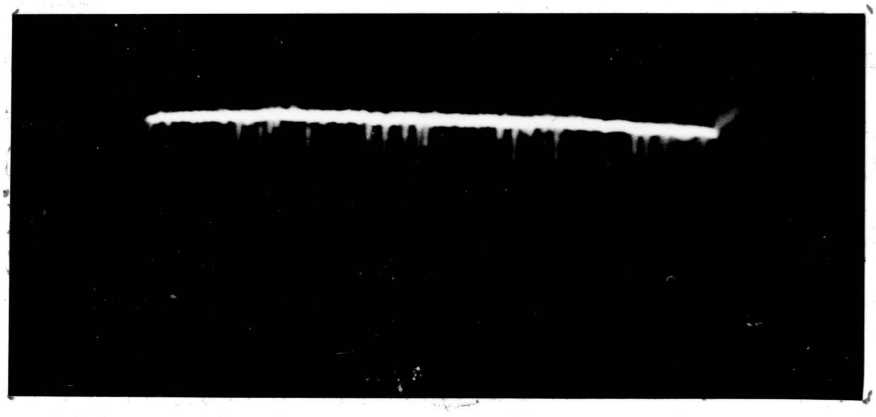

Fig. 110. Light intensity variation of argon discharge in the small tube (60 cps).

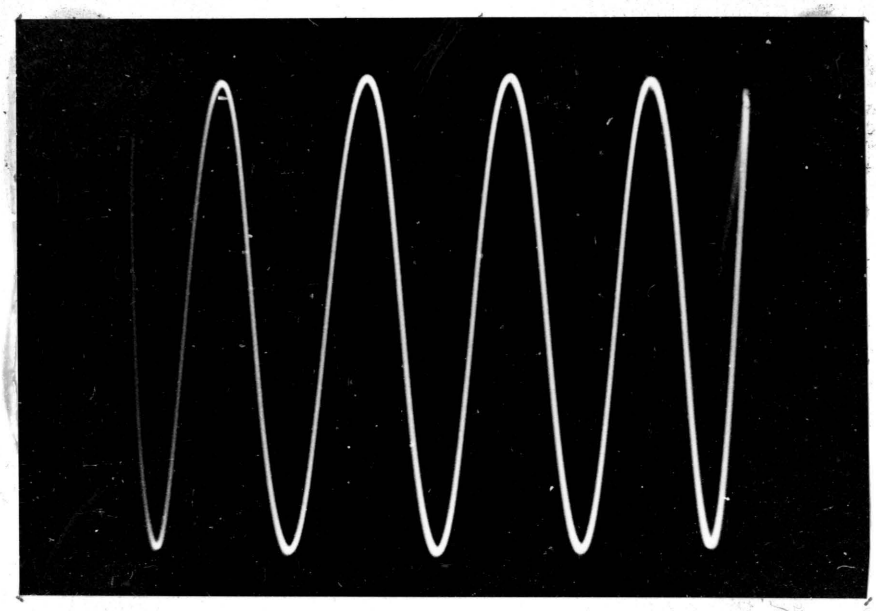

Fig. 111. Terminal voltage variation at 434 kc., applied to the tubes shown in fig. 21.

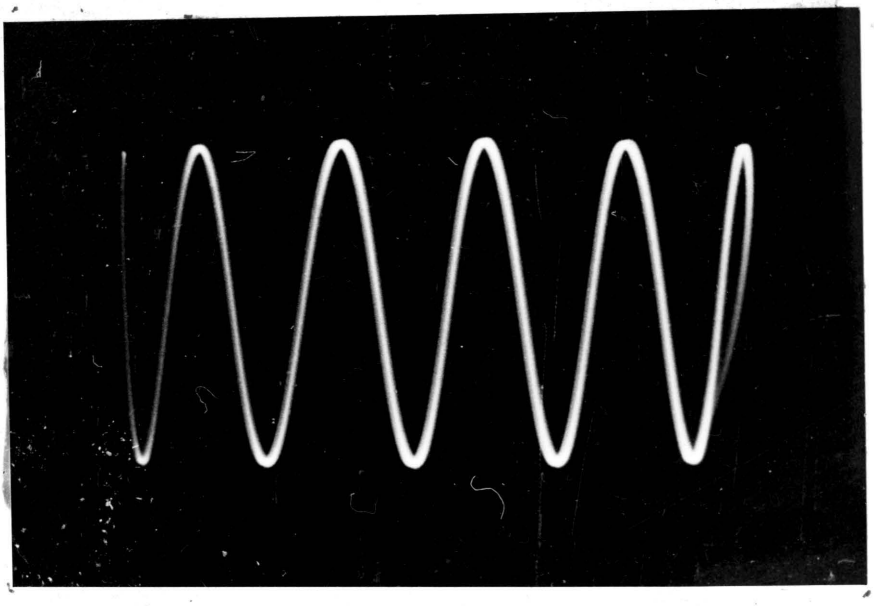

Fig. 112. Load current variation of argon discharge produced by voltage variation shown in fig. 111.

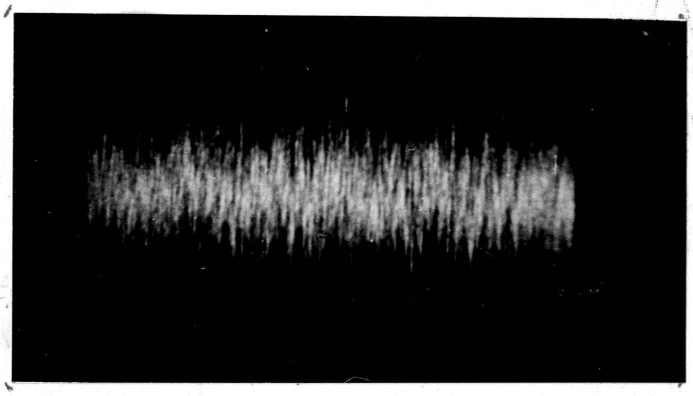

Fig. 113. Light intensity variation of argon discharge in the large tube (434 kc.).

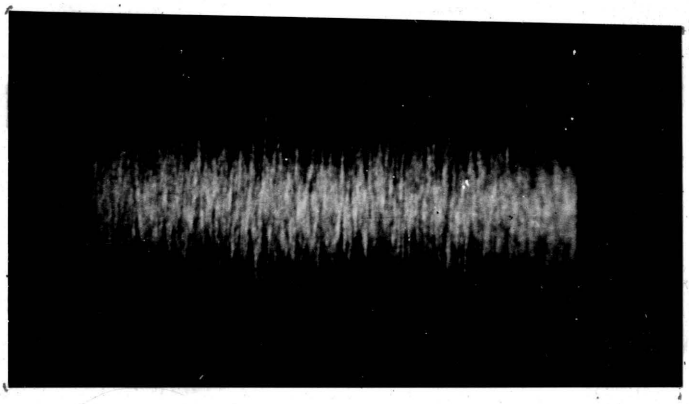

Fig. 114. Light intensity variation of argon discharge in the medium tube (434 kc.).

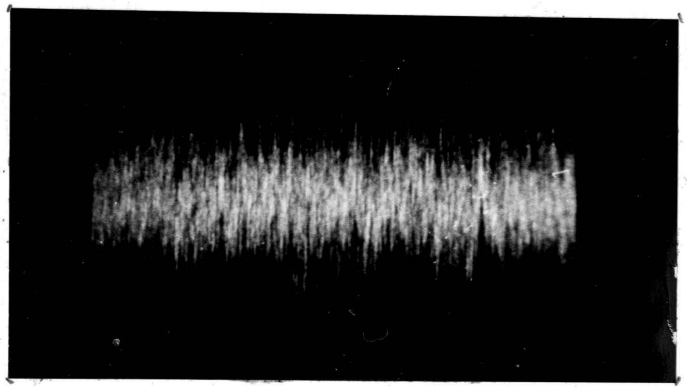

Fig. 115. Light intensity variation of argon discharge in the small tube (434 kc.).

VIII. LIMITATIONS

It was pointed out by McCallum and Klatzow (17) that in order to obtain good results with electrodeless discharges in argon, the latter must be very carefully purified. Whenever argon discharge was desired for the purposes of this study, the electrodeless tube was evacuated to the lowest pressure that could be obtained with the available evacuating system. That pressure was in the neighborhood of 10^{-4} mm. Hg. Then argon was introduced into the tube by opening the valve of the argon tank to which the other end of the tube was connected. The pressure was then again reduced to a desirable value, and read on the McLeod pressure gauges connected to the system. Because of the high sensitivity of the argon discharges to impurities, some unavoidable amount of leakage in the vacuum system, and the fact that the commercially obtained argon was only 99.8% pure, it is not possible to say that pure argon discharges were investigated.

The output voltage of the available source of r-f, although being sufficiently high to initiate and maintain the discharges at radio frequencies, was not much greater than the required minimum. Above limitation did not permit variation of the terminal voltage over any appreciable range.

Another serious limitation was placed by the absence

of a source of frequency continuously variable from the lowest to that corresponding to the maximum response of the available oscilloscope.

Results obtained with mercury discharges could be greatly improved if, for example, a tube equipped with means of precisely measurable temperature variation were available, or if some other provisions were made to vary the vapor pressure in the tube.

IX. CONCLUSIONS

A study made of the general properties of electrodeless discharges revealed that, at all frequencies tested, the best conditions for their initiation and maintenance were attained when the terminal voltage was high, the distance between the terminals was short, the pressure of the gas was low but not lower than approximately one hundred microns, when proper load matching devices were used, and when the diameter of the tubes used was not too large.

Comparing the properties of the discharges through different gases, it was found that argon discharges were easier to initiate and control than air discharges, and that their initiation through mercury vapor generally required less effort as compared to air.

Instantaneous variations of the light intensity of the electrodeless discharges at the lowest frequencies tested (60 and 400 cps) appeared in the form of grouped peaks whose average height increased as the pressure and the distance between the terminals of the electrodeless tube increased, and decreased as the terminal voltage increased. Under any conditions, the number of peaks per group increased as their average height decreased.

Generally, a stable discharge at the two lowest frequencies was characterized by a large number of short

peaks in a given group.

At radio frequencies, the instantaneous light intensity variations produced were entirely different from those discussed above. No definite shapes, or peaks, were observed, except when the r-f was modulated by a lower-frequency modulation envelope.

Although the above experiments helped a great deal to clarify some of the heretofore unknown properties of the electrodeless discharges at frequencies lower than those used by other investigators, no pretense is being made that the same present a complete and exhaustive study of the subject. It was shown, however, that the electrodeless discharges can be easily obtained and controlled by means of a source of sufficient power and a proper frequency range.

Limitations placed by the time and cost of the project did not permit the location of the point of transition from the well-defined wave shapes of the instantaneous light intensity variation to those with no apparent periodicity. It may, however, be assumed that such transition would be a gradual one, and somewhere in the range between 400 cps and the lowest radio frequency used in this study.

All experiments in this study were carried out at sine wave terminal voltage variation, except where a

specific mention was made to the contrary. Sine wave variation is easily reproducible and affords an excellent basis for comparison of various results obtained.

X. SUMMARY

The electrodeless discharges were investigated at the frequencies of 60 cps, 400 cps, and continuously from approximately eighty kilocycles to one megacycle.

A study of the general properties of the discharges, as well as that of the instantaneous variations and fluctuations was made in air, argon, and mercury vapor.

Electrodeless discharges were studied under various conditions of:

a. Pressure of the gas in the tube

b. Terminal voltage

c. Frequency

d. Distance between the terminals

e. Physical size of the tubes

f. Physical size of the terminals

g. Load matching

It is hoped that the comparatively low cost of the required equipment and the usefulness of the electrodeless discharges as spectroscopic light sources will encourage further investigations of the subject.

XI. ACKNOWLEDGMENTS

The writer wishes to take this opportunity to express his great indebtedness to Dr. H. Y. Loh of the Department of Physics for suggesting and supervising this project and for his guidance and assistance throughout the course of the investigation.

It is also desired to express sincere appreciation to Professors R. R. Wright and H. K. Ebert of the Electrical Engineering Department for many helpful suggestions in design and selection of the electronic equipment, to Dr. F. L. Robeson for construction of the McLeod pressure gauges, to Dr. T. M. Hahn for the constructive criticism of the manuscript, to Mr. Howard Halsey for his great interest and invaluable help in design and construction of the radio frequency apparatus, and to other members of the Department of Physics for their help whenever called upon.

Finally, the writer wishes to thank his friends among the students of V. P. I. for their encouragement and help in carrying out some of the routine tasks of this project.

XII. BIBLIOGRAPHY

(1) Banerji, D. and Ganguli, R., Striated and Other Forms of High-Frequency Discharge. Philosophical Magazine and Journal of Science (London, Edinburgh, and Dublin), Vol. 13, pp. 494-501 (1932).

(2) Brasefield, C. J., The Nature of the Electrodeless Ring Discharge. Physical Review, Vol. 34, pp. 1392-1393 (1929).

(3) Braun, M. L., Current, Pressure, and Frequency Relationships for the Initiation and Maintenance of the Electrodeless Glow Discharge. Physical Review, Vol. 36, pp. 1195-1198 (1930).

(4) Cheo, P. K., Some Optical Constants of Thin Metallic Films. M. S. Thesis, Virginia Polytechnic Institute, pp. 13-21 (1952).

(5) Corliss, C. H. and Bozman, W. R., Electrodeless Metal Halide Lamps. Journal of the Optical Society of America, Vol. 43, pp. 398-400 (1953).

(6) Dieke, G. H., Loh, H. Y., and Crosswhite, H. M., Spectral Intensity Measurements with Phototube and the Oscillograph. Journal of the Optical Society of America, Vol. 46, pp. 185-191 (1946).

(7) Engstrom, R. W., Multiplier Phototube Characteristics: Application to Low Light Levels. Journal of the Optical Society of America, Vol. 37, pp. 420-431 (1947).

(8) Francis, G. and Engel, A. V., Development of the Low Pressure Electrodeless Discharge in a High- Frequency Electric Field. Proceedings of the Physical Society (London), Vol. 63, pp. 823-830 (1950).

(9) Gordon, H. T. and Dushman, S., Conditions for Initiation of Electrodeless Discharges in Gases. Physical Review, Vol. 33, pp. 632-637 (1929).

(10) Hilton, A. B., Design and Construction of a High-Frequency Source for the Excitation of Electrodeless Discharge Tubes for Spectrographic Sources. M. S. Thesis, Virginia Polytechnic Institute (1952).

(11) Loeb, L. B., Fundamental Properties of Electrical Discharges in Gases. John Wiley & Sons, Inc., New York, pp. 555-558 (1939).

(12) Loh, H. Y., and Dieke, G. H., Fluctuations in Gas Discharge. Journal of the Optical Society of America, Vol. 37, pp. 837-838 (1947).

(13) Knipp, C. T., Possible Direct Reading Methods for Measuring the Current in Electrodeless Discharge. Physical Review, Vol. 37, pp. 1704-1705 (1931).

(14) Knipp, C. T. and Knipp, J. K., Electrodeless Discharge: Method of Measuring Induced Current, Variation of Current with Pressure for Various Gases. Physical Review, Vol. 38, pp. 948-958 (1931).

(15) Kunz, J., Theory of Electromagnetic and Electrostatic Induction in Electrodeless Discharges. Philosophical

Magazine and Journal of Science (London, Edinburgh, and Dublin), Vol. 13, pp. 964-966 (1932).

(16) MacKinnon, K. A., The Origin of the Electrodeless Discharge. Philosophical Magazine and Journal of Science (London, Edinburgh, and Dublin), Vol. 8, pp. 605-616 (1929).

(17) McCallum, S. P. and Klatzow, L., Electrodeless Discharges in Argon. Philosophical Magazine and Journal of Science (London, Edinburgh, and Dublin), Vol. 15, pp. 829-843 (1933).

(18) M. I. T. Staff, Applied Electronics. John Wiley & Sons, Inc., New York, pp. 101-109 (1949).

(19) Nisewanger, C. R., Holmes, J. R., and Weissler, G. L., Electrodeless Discharges at High Frequency and Low Pressure. Journal of the Optical Society of America, Vol. 36, pp. 581-587 (1946).

(20) Smith, C. G., Study of a Ring Discharge. Physical Review, Vol. 59, pp. 997-1004 (1941).

(21) Smith, H., Lynch, W. A., and Hillberry, N., Electrodeless Discharge in Mercury Vapor. Physical Review, Vol. 37, pp. 1091-1095 (1931).

(22) Terman, F. E., Radio Engineering. McGraw-Hill Book Company, Inc., New York, Third Edition, pp. 545-576, 410-466, and 230-250 (1947).

(23) Thomson, J. J., Mechanism of the Electrodeless Discharge. Philosophical Magazine and Journal of

Science (London, Edinburgh, and Dublin), Vol. 10, pp. 280-290 (1930).

(24) Thomson, J. J., The Electrodeless Discharge through Gases. Philosophical Magazine and Journal of Science (London, Edinburgh, and Dublin), Vol. 4, pp. 1128-1130 (1927).

(25) Townsend, J. S., Electrodeless Discharges. Philosophical Magazine and Journal of Science (London, Edinburgh, and Dublin), Vol. 13, pp. 745-749 (1932).

(26) Townsend, J. S., and Donaldson, R. H., Electrodeless Discharges. Philosophical Magazine and Journal of Science (London, Edinburgh, and Dublin), Vol. 5, pp. 178-182 (1928).

(27) Tykociner, J. T. and Kunz, J., Frequency Variations Due to Electrodeless Discharge. Physical Review, Vol. 37, pp. 100-101 (1931).

(28) Yarnold, G. D., Electrodeless Discharges in Uniform Fields. Philosophical Magazine and Journal of Science (London, Edinburgh, and Dublin), Vol. 15, pp. 294-300 (1933).

The vita has been removed from the scanned document